

Reviewing SDARS Antenna Requirements

Several conflicting requirements, such as achieving two separate high-gain antenna patterns within a single compact module, increase the challenge of designing SDARS antennas.

automotive satellite radios, specifically the Satellite Digital Audio Radio System (SDARS), place stringent requirements on the receiving antenna. SDARS employs a dual-transmitter broadcast format in which signals are sent from both satellite-based and terrestrial transmitters. The satellite transmission cover most areas, but are complemented by terrestrial transmitters when satellite coverage is blocked

(such as by tall buildings in urban areas). Examples of the SDARS include XM Satellite radio and SIRIUS Satellite

Radio in the US, providing customers with as many as 100 channels of MP3-quality digital radio service. Antennas for SDARS must be able to handle both types of transmissions with optimal receive performance.

ARGY PETROS Senior Consultant

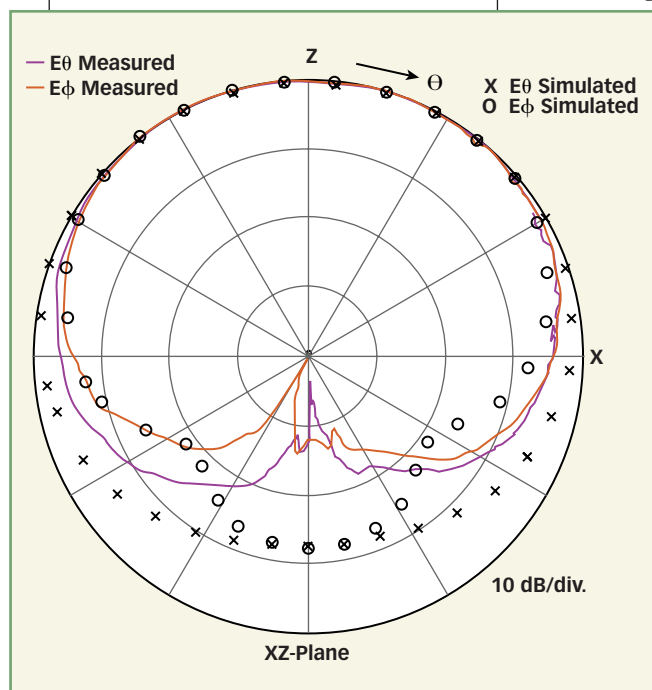
ThinkWireless, Inc., 6208 Grand Cypress Circle, Lake Worth, FL 33463; (561) 543-6197, e-mail: argy@thinkwireless.com, Internet: www.thinkwireless.com.

IMTIAZ (IMI) ZAFAR Product Line Architect—Antenna & RF Technology

Delphi Corp., 5725 Delphi Dr., Troy, MI 48098-2815; (248) 813-2000, FAX: (248) 813-2670, e-mail: imtiaz.zafar@delphi.com, Internet: www.delphi.com.

STANISLAV LICUL Graduate Research Assistant

Virginia Tech Antenna Group, Virginia Polytechnic Institute, and State University, 340 Whittemore Hall, Blacksburg, VA 24060; (540) 239-4607, e-mail: slicul@vt.edu, Internet: http://antenna.ece.vt.edu.



1. This SAT antennas elevation pattern was measured with the antenna on the center of 1-m ground plane.

Antenna modules for SDARS feature low-noise amplifiers (LNAs) and passive elements that receive low-power satellite signals and terrestrial signals. Currently, SDARS antennas are dual-arm antennas, consisting of two separate antennas, one optimized for terrestrial (TER) signal reception and the other optimized for satellite (SAT) signal reception. The TER element is typically a monopole, while the SAT element is a circularly polarized structure. Due to the requirements for extremely low noise figures, the LNAs are located directly below



5114 E. Clinton Way, #101
Fresno, CA 93727
Tel: 559-255-7044
Fax: 559-255-1667
Email: sales@ditom.com
Internet: www.ditom.com

"The Leader in Broadband and High Frequency Isolators and Circulators"



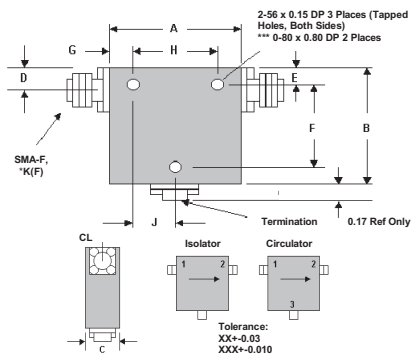
Isolators

Model #	Freq Range GHz	Isol Min	Insertion Loss Max	VSWR Max	Outline #	Price Per Unit
D3I0890	.8-9	20	40	1.25	8	\$235.00
D3I0116	1.4-1.6	20	40	1.25	8	\$235.00
D3I0118	1.6-1.8	20	40	1.25	3	\$210.00
D3I0120	1.7-2.0	20	40	1.25	3	\$210.00
D3I0223	2.0-2.3	20	40	1.25	3	\$210.00
D3I2040	2.0-4.0	18	50	1.30	1	\$215.00
D3I2060	2.0-6.0	14	80	1.50	1	\$250.00
D3I2080	2.0-8.0	10	150	2.00	1	\$395.00
D3I3060	3.0-6.0	19	40	1.30	2	\$195.00
D3I4080	4.0-8.0	20	40	1.25	3	\$185.00
D3I6012	6.0-12.4	17	60	1.35	6	\$195.00
DM6018	6.0-18.0	14	100	1.50	11	\$275.00
D3I7011	7.0-11.0	20	40	1.25	4	\$185.00
D3I7012	7.0-12.0	20	40	1.25	4	\$205.00
D3I7018	7.0-18.0	15	130	1.50	5	\$225.00
D3I8012	8.0-12.4	20	40	1.25	4	\$180.00
D3I8016	8.0-16.0	17	60	1.35	5	\$205.00
D3I8020	8.0-20.0	15	100	1.45	5	\$230.00
D3I1020	10.0-20.0	16	70	1.40	5	\$220.00
D3I1218	12.0-18.0	20	50	1.25	5	\$180.00
D3I1826	18.0-26.5	18	80	1.40	5	\$225.00
D3I1840	18.0-40.0	10	200	2.00	5*	\$1300.00
D3I2004	20.0-40.0	12	150	1.65	5*	\$950.00
D3I2640	26.5-40.0	14	100	1.50	5*	\$700.00

Circulators

Model #	Freq Range GHz	Isol Min	Insertion Loss Max	VSWR Max	Outline #	Price Per Unit
D3C0890	.8-9	20	40	1.25	8	\$235.00
D3C0116	1.4-1.6	20	40	1.25	8	\$235.00
D3C0118	1.6-1.8	20	40	1.25	3	\$210.00
D3C0120	1.7-2.0	20	40	1.25	3	\$210.00
D3C0223	2.0-2.3	20	40	1.25	3	\$210.00
D3C2040	2.0-4.0	18	50	1.30	1	\$215.00
D3C2060	2.0-6.0	14	80	1.50	1	\$250.00
D3C2080	2.0-8.0	10	150	2.00	1	\$395.00
D3C3060	3.0-6.0	19	40	1.30	2	\$195.00
D3C4080	4.0-8.0	20	40	1.25	3	\$185.00
D3C6012	6.0-12.4	17	60	1.35	6	\$195.00
DMC6018	6.0-18.0	14	100	1.50	11	\$275.00
D3C7011	7.0-11.0	20	40	1.25	4	\$185.00
D3C7012	7.0-12.0	15	100	1.50	5	\$225.00
D3C8016	8.0-16.0	17	60	1.35	5	\$205.00
D3C8020	8.0-20.0	15	100	1.45	5	\$230.00
D3C1218	12.0-18.0	20	50	1.25	5	\$180.00
D3C1826	18.0-26.5	18	80	1.40	5	\$225.00
D3C1840	18.0-40.0	10	200	2.00	5*	\$1750.00
D3C2004	20.0-40.0	12	150	1.65	5*	\$1350.00
D3C2640	26.5-40.0	14	100	1.50	5*	\$900.00

Buy Online
—45 products can be bought online with Credit Card.
—Delivery within 24Hrs ARO.
—DITOM stocks over 25 units of each device at all times.
—Units over 26.5 GHz come with K-female



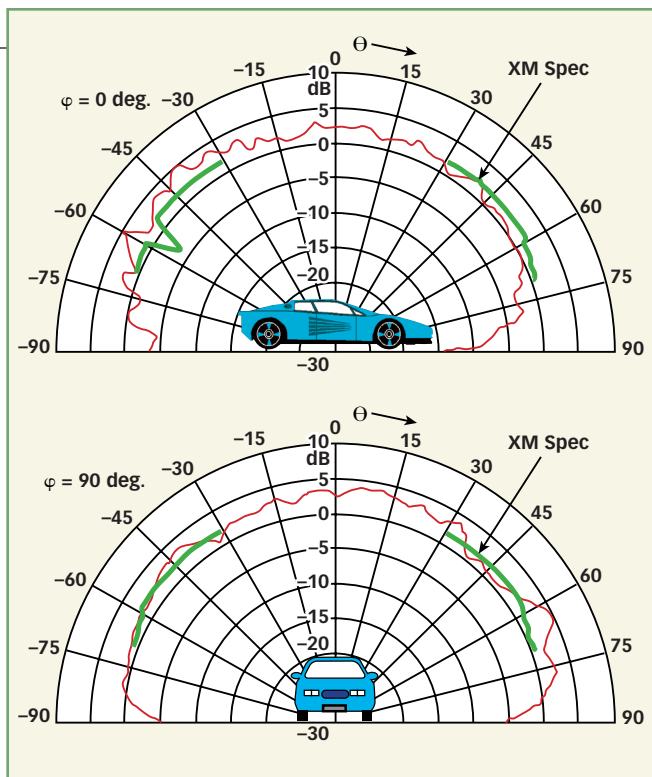
Outline #	A	B	C	D	E	F	G	H	J
1	1.58	1.62	0.70	0.25	0.25	1.265	0.10	1.380	0.690
2	1.25	1.25	0.70	0.25	0.25	0.900	0.10	1.050	0.525
3	1.00	1.00	0.50	0.25	0.25	0.675	0.10	0.800	0.400
4	0.86	0.98	0.50	0.25	0.25	0.625	0.10	0.660	0.330
5	0.50	0.70	0.50	0.25	0.18	0.455	0.08	0.340	0.170
6	0.62	0.78	0.50	0.25	0.25	0.425	0.10	0.420	0.210
8	1.25	1.25	0.72	0.26	0.26	0.900	0.10	1.050	0.525
11***	0.50	0.58	0.38	0.19	0.19	—	0.10	0.300	—

the passive antennas. The separate outputs of the two LNAs is connected to RF cables typically 15 to 20 feet in length; the cables are terminated in SMB connectors to interface with the SDARS radio equipment.

The basic electrical performance of SDARS antenna modules is summarized in the table. The SAT antenna employs left-hand circular polarization while the TER uses linear polarization. Type-approval antenna testing requires that the mobile antenna module be mounted at the center

of a 1.0-m-diameter circular ground plane. Figure 1 shows a typical elevation pattern in two planes of an SAT antenna placed at the center of such a ground plane.¹ Minimum antenna gain of +2 dBic is required for elevation angles between 20 to 60 deg, for XM, while minimum antenna gain of +3 dBic is required for Sirius.² The TER antenna performance should be equivalent to that of a monopole, or -1 dBi antenna gain at an elevation angle of 0 deg. (the horizon).

Figure 2 shows the elevation pattern of a SAT antenna located on a vehicle roof, spaced 15 cm from the back roof



2. This SAT antenna elevation pattern was measured with the antenna located on a vehicle roof, 15 cm from the roof edge.²

edge.² The pattern curves are not as smooth as the ground plane curves of Fig. 1 due to asymmetries. While on a vehicle, ideally the antenna elements must be positioned in a substantially unobstructed view of the satellites. The ideal location of a mobile antenna module is on the vehicle roof. Both SAT and TER elements of roof-mount antennas require a minimum of six inches from sheet metal edge to provide satisfactory antenna performance.³ Other antenna modules such as those for Advanced Mobile Phone Service (AMPS), personal communications services (PCS), and Global Positioning System (GPS), can be incorporated with an SDARS

SDARS antenna-module performance

PARAMETERS	SIRIUS	XM
Frequency band (MHz)	2320 to 2332.5	2332.5 to 2345
SAT antenna polarization	Left-hand circular	Left-hand circular
TER antenna polarization	Linear vertical	Linear vertical
SAT antenna gain (dBic)*	+2 to +4 (25 to 90 deg.)	+2 to +4 (20 to 60 deg.)
TER antenna gain (dBi)*	-1	-1
Current drain (mA)	150	90 to 110
Supply voltage (V)	5 to 8	4 to 5
SAT LNA gain (dB)	36	32
TER LNA gain (dB)	28	30
Max SAT LNA noise figure (dB)	0.7	0.7 to 1.2
Max TER LNA noise figure (dB)	2.0	1.5
Filter attenuation at ±250 MHz	35 dB	25 to 35 dB

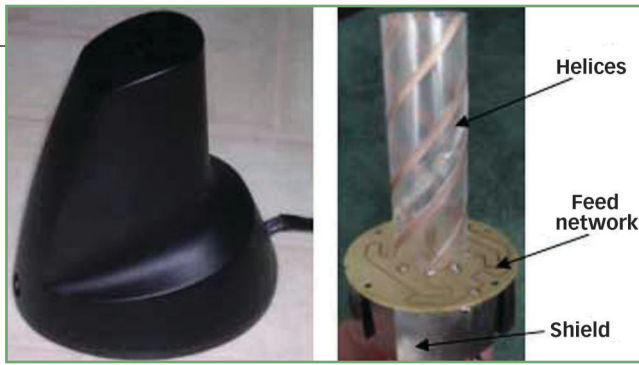
*Note: The antenna was placed on the center of a 1-m-diameter ground plane.

DESIGN

antenna in a common housing as long as the antennas do not interfere with each other. (For example, enough isolation should be provided between the PCS band at 1920

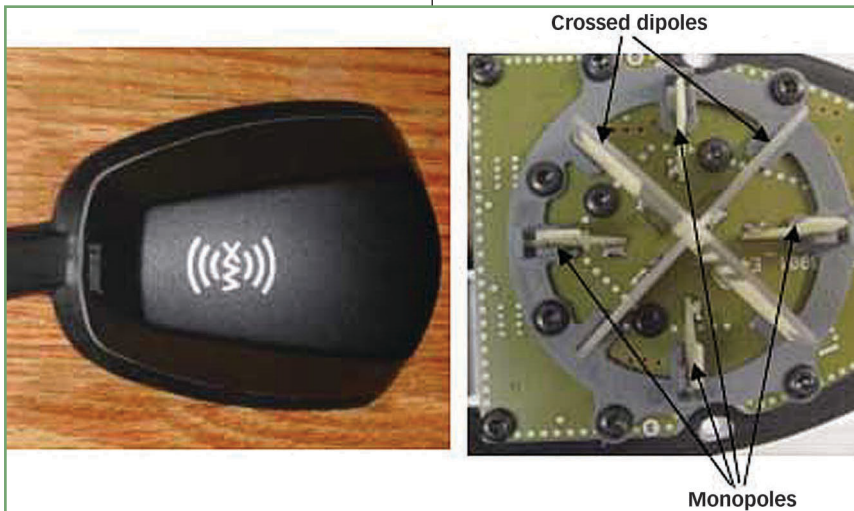
to 1990 MHz and the SDARS band at 2320 to 2345 MHz.)

Figure 3 shows a standard quadrifilar SAT antenna with a helix monopole TER structure located inside the quadrifilar antenna. The quadrifilar helix antenna consists of four helices spaced equally and circumferentially on a cylinder. The four helices are etched on a flexible substrate and wrapped in a cylindrical fashion. From much research,⁴⁻⁸ it is known that quadrifilar antenna performance is unaffected by the presence of the monopole inside. A feed network printed on a low-loss flexible substrate, along with the helix winding direction, helps achieve the left-hand circular polarization. To improve the return loss and radiation characteristics of the monopole antenna, the shield height below the antennas is much higher than that of a standard shield (typically 5 mm). This arrangement yields excellent antenna performance, nearly equal to that of a typical monopole antenna. The height of the antenna including the housing is approximately 95 mm.



3. This design is a combination of a quadrifilar antenna and a monopole structure.

Figure 4 shows a crossed dipole/monopole array combination. The assembly consists of a crossed dipole structure for receiving the circularly polarized satellite signals and an array of four monopoles for receiving linearly polarized terrestrial signals.⁹ The dipoles are etched on a low-loss substrate. While crossed dipoles have been around for several years and used extensively in mobile SAT communications,^{10,11} the novelty of this design is in the way the monopole array is arranged symmetrically about the cross dipoles. This symmetrical configuration yields good performance for both the SAT and TER antennas. Each monopole is positioned within each quadrant of the cross dipole. Each monopole is approximately 0.25 wavelengths in length. The four monopoles are connected to a standard corporate feed network. The two crossed dipoles are connected to a 90-deg. equal-power feed network etched on a low-loss substrate. This configuration yields the circular polarization required for SDARS. The SAT antenna provides



4. This XM antenna features a crossed dipole/monopole array combination.



High Frequency Fundamental Crystal Units

50 MHz
To
250 MHz

For Use In:

- ✓ VCXOs
- ✓ Clocks
- ✓ Discrete Crystal Filters

PO Box 89
Scotch Valley Road
Hollidaysburg, PA 16648
814-695-4428 Phone
814-696-0403 Fax
www.aextal.com
e-mail: sales@aextal.com



5. This antenna design is a combination of quadrifilar and PIFA structures.

excellent performance for elevation angles of 45 deg. or higher. The height of the antenna including the housing is approximately 40 mm.

Figure 5 shows that the SAT element of the quadrifilar/PIFA combination is a “folded” low-profile quadrifilar antenna while the TER element is a planar inverted-F antenna (PIFA).^{12,13} The “folded” quadrifilar antenna is essentially a standard quadrifilar antenna, where the helices in the top section are folded or bent back resulting in a shorter antenna. The helices are etched on a flexible substrate and then wrapped in a cylindrical fashion. The width of each line is 2 mm and each helix is matched to 50 Ω and connected to a miniature surface-mount feed network.¹⁴ The helix antenna height is 6 cm. The SAT antenna provides good performance between elevation angles 20 and 60 deg. However, the TER antenna radiation pattern exhibits a valley due to blockage by the quadrifilar antenna. The height of the antenna including the housing is approximately 70 mm.

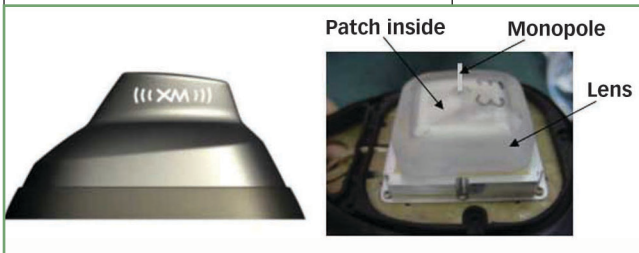
Figure 6 shows this configuration’s lens-loaded ceramic patch SAT antenna. The TER element is a quarter-wave monopole located in the center of the antenna structure and extends from

the base through a hole in the patch. The lens helps increase the patch gain at low elevation angles (20 to 30 deg.) by increasing the antenna beamwidth. However, the antenna gain at high-elevation angles is reduced compared to a patch with no lens. Care must be taken in the placement of the monopole so that it does not interfere with the radiation pattern of the patch antenna, especially when high-dielectric-constant ceramic materials are used. The height of the antenna including the housing is approximately 40 mm.

Of the various antenna SDARS configurations discussed, the coupled loop/monopole combination is the most popular (Fig. 7). It is sold along with the popular XM Delphi SkyFi™ receiver. The SAT element is a coupled-loop antenna with perimeter length of approximately one-half wavelength. The TER element is a helix monopole located inside the SAT antenna without affecting the SAT design’s performance. A feed network printed on a low-loss substrate helps achieve the left-hand circular polarization. It is similar to the feed network used on the quadrifilar/monopole combination design (Fig. 3). This arrangement yields good performance for both SAT and TER antennas in that the TER

radiation pattern presents no asymmetries. The height of the antenna including the housing is approximately 30 mm.

Figure 8 shows an annular microstrip antenna consisting of a full-wavelength loop etched on a low-loss



6. This patch antenna features a lens and monopole structure combination.

Wired?

or Wireless?



Both!

Coming Frequency Control designs and manufactures a complete range of precision crystal, oscillator and filter products to meet the critical timing needs of a broad range of wireless and wire line communications technologies.

Applications include cellular, pcs, test & measurement, military, automotive, avionics, medical, satcom, switching and networking.

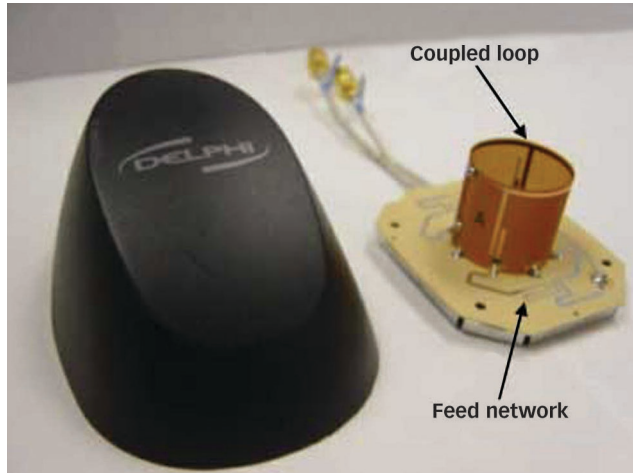


CORNING

The Timing Solutions Leader

www.comingfrequency.com
tel (717)486-3411
fax (717)486-5920

substrate. This type of patch antenna operates in TM_{21} mode and produces a conical radiation pattern. It yields good performance for elevation angles between 20 and 60 deg. but poor performance at higher angles (60 to 90 deg.), with a null at the zenith (90 deg.). For this reason, it is not suitable for Sirius applications. The TER antenna is a top-loaded monopole located at the center of the annular patch and at the same height as the patch. The SAT antenna performance is unaffected by the presence of the monopole.



7. This Delphi antenna is a combination of a coupled loop and monopole structures.

The TER radiation pattern is similar to that of a standard quarter-wave monopole with slightly less gain. The height of the antenna including the housing is approximately 15 mm and it is the lowest-profile XM antenna.

For applications where no ground plane exists, mast or ground-independent antennas are needed. These antennas are mounted on sedan or sport-utility-vehicle (SUV) window glass or on the mirrors of long-haul trucks. A quadrifilar helix antenna is a typical mast-type ground-independent SAT configuration for SDARS. In such a configuration, the four helices and feed network are printed on a low-loss flexible substrate and wrapped around a cylindrical tube (Fig. 9a).

The TER antenna should also be designed to be ground-independent. A natural choice for this element would be a dipole. The first SDARS mast antenna shipped was the TRK SR1 (Fig. 9b).¹⁵ It is a combination SAT and TER antenna comprising a quadrifilar helix antenna and a tubular dipole.¹⁶ The SAT coaxial cable runs substantially concentrically through the dipole without affecting the dipole's radiation characteristics. This arrangement effectively reduces coupling between the two elements and yields good performance for both antennas. The TRK SR1 design is unique in that both dc power and RF energy are transferred from the interior of the vehicle glass to the exterior sur-

face. The coupling scheme utilizes two pairs of RF couplers (SAT and TER), and a pair of large coils which are part of the DC power (bias) circuitry. The LNAs are placed on the exterior glass surface, underneath the antennas, to maintain the low-noise-figure requirements. Technical challenges to this arrangement include oscillation due to the undesired coupling between the antennas, couplers, and LNA outputs, and interference on the AM radio caused by the DC transferring circuitry. These problems are avoided by correct LNA design, filtering, and proper antenna installation.

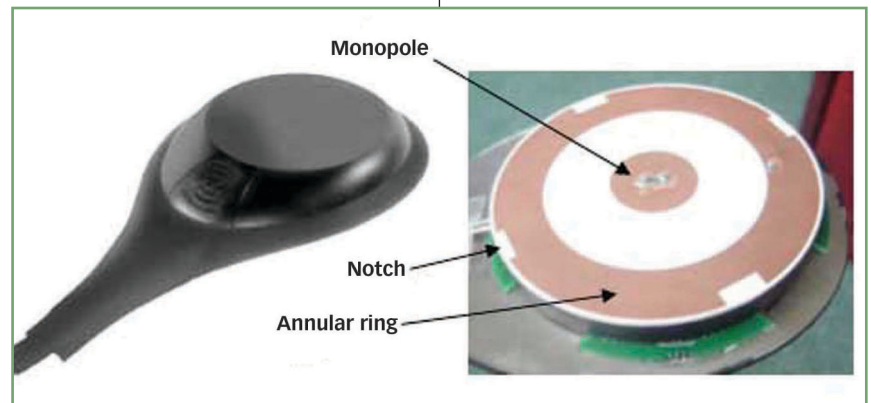
In an alternate implementation from the design of Fig. 9b, the dipole is replaced by a monopole that is printed on the same flexible substrate as the feed network. In this case, the monopole average gain is approximately -1 dBi at the horizon. This antenna element

arrangement yields a shorter combination on-glass mast antenna and is used in both the TRK SR1X (a shorter version of the TRK SR1) and the TRK XM11 antennas (Fig. 9c).¹⁵

More recently, on-glass XM mast antennas have been introduced, incorporating RF coupling only (models XM8000F in Fig. 9d and XM8100F).¹⁵ These configurations utilize low-loss RF couplers for both SAT and TER elements. The SAT coupler loss is 0.5 dB, and this scheme avoids the potential oscillation and AM

interference issues of the TRK SR1 and SR1X models. The trade-off, however, is an increase in noise figure of approximately 0.7 dB for SAT (0.5 dB coupler loss + 0.2 dB cable loss). The TER coupler is physically smaller than the SAT coupler, resulting in a 1 dB loss. The TER antenna for this design is a folded dipole located underneath the SAT antenna. Long-haul truck, recreational vehicle (RV), and marine antennas are mast antennas similar to the quad/dipole or quad/monopole combinations.¹⁵

To reduce the cost of the various antenna modules presented here, there is a need for developing single-arm antennas. These antennas consist of a single passive element and a single LNA configured such that good reception of both TER and SAT signals is achievable. Such modules exhibit vertical polarization properties along the horizon and circular polarization properties at high-



8. This antenna is a combination of a TM_{21} mode annular patch and a monopole.

er elevation angles. Currently, the vast majority of all SDARS receivers have two antenna inputs (TER and SAT). Single-arm antennas can be equipped with an RF splitter in order to be connected to dual-input receivers. A good candidate for single-arm antennas is a microstrip patch antenna etched on a low-loss ceramic or substrate. The right choice of ceramic or substrate can produce acceptable TER and SAT performance. Single-arm SDARS Sirius antennas have been just released into the market. They are patch antennas etched on a low-loss substrate. These antennas yield excellent SAT performance. However, the TER performance is poor, with an average antenna gain of approximately -7 dBi.¹⁷ Single-arm XM antennas are expected to be available by the third quarter of 2003.

The aesthetic limitations of mounting large SDARS antenna structures on vehicles may be in part responsible for the slow customer acceptance of this technology.



9. Examples of mast antennas include the (a) quadrifilar helix, (b) TRK SR1 antenna, (c) TRK XM11, and (d) XM8000F.

For this reason, manufacturers are investigating the use of hidden SDARS antennas, located in the interior of a vehicle. The goal is to match the performance of a single roof or on-glass antenna by using a minimum of two hidden antennas. This is a challenging task, since antennas located inside the vehicle would yield poor performance due to signal blockage from the

roof, pillars, and other vehicle structures. Figure 10 shows two radiation patterns corresponding to an SDARS SAT antenna located inside a sedan (front dash and rear deck lid) for the elevation angle of 25 deg. By itself, neither of the radiation patterns is acceptable. However, when the two patterns are combined through a receiver diversity algorithm, the

Agilis[®]
Connecting Globally

We Connect YOUR Business

- Suitable for MMDS, PDH and SDH applications from 3.5GHz up to 60GHz
- Competitive pricing & performance
- Broad frequency coverage
- Split ODU and IDU construction for quick and easy installation
- Remote monitoring and control

www.agilis.st.com.sg
+65 6567 6791
mktg@agilis.st.com.sg

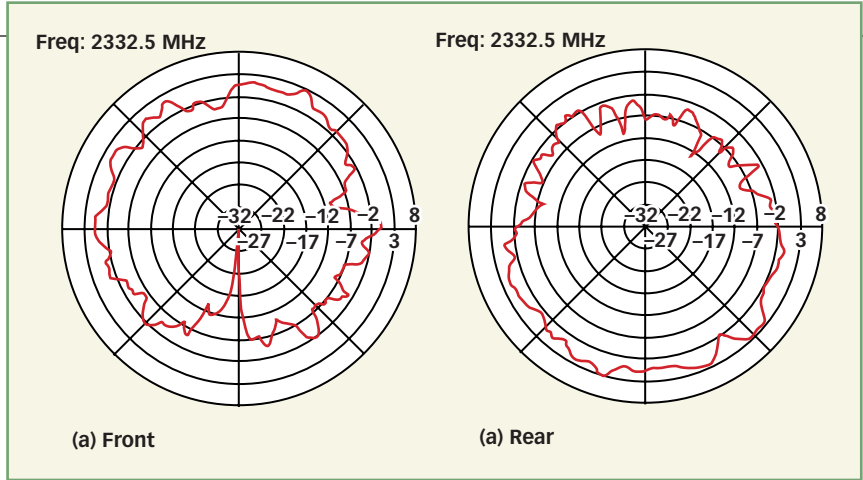
Agilis Communication Technologies Pte Ltd
A company of Singapore Technologies Electronics

Singapore Technologies Electronics
A company of Singapore Technologies Engineering

resulting radiation pattern can be significantly improved. A potential antenna choice for this application is a patch antenna. A pair of patch antennas can be used, one placed in the front and the other in the rear of the vehicle. A perceived disadvantage of implementing hidden antennas is the cost increase associated with each additional antenna module: the antenna element, LNA, cable, and connector. **MRP**

REFERENCES

1. S. Licul, A. Petros, W.A. Davis, and L. Stutzman, "Analysis and Measurements of the Folded and Drooping Quadrifilar Antenna for Land-Mobile Satellite Communications," submitted to IEEE Transactions on Antennas & Propagation, 2003.
2. M. Daginnus, R. Kronberger, A. Stephan, G.H. Hassmann, H. Lindenmeier, J. Hopf, and L. Reiter, "SDARS—Antennas: Environmental Influences, Measurement, Vehicle Application Investigations and Field Experiences," SAE Technical Paper Series, 2002-01-0120, SAE World Congress, Detroit, Michigan, March 4-7, 2002.
3. I. Zafar and B. Pakray, Delphi Corp., SDARS Antenna Report, 2002.
4. C.W. Gerst, "Multifilar Contrawound Helical Antenna Study and Analysis," *Surveillance Technology Study and Analysis*, Vol. I, Tech. Rep. RADC-TR-67-145 May 1967, Vol. II, Final Report, February 1967.
5. C.C. Kilgus, "Resonant Quadrifilar Helix Design," *Microwave Journal*, December, 1970.



10. These radiation patterns were measured for an SAT antenna inside a sedan (elevation angle of 25 deg.): (a) at the front dashboard and (b) at the rear deck lid.

6. T. Adams, R.K. Greenough, R. F. Wallenberg, A. Mendelovitch, and C. Lumjiak, "The Quadrifilar Helix Antenna," *IEEE Transactions on Antennas & Propagation*, Vol. AP-22, pp. 173-178, March 1974.
7. C.C. Kilgus, "Shaped-Conical Radiation Pattern Performance of the Backfire Quadrifilar Helix," *IEEE Transactions on Antennas & Propagation*, May 1975.
8. C.D. McCarrick, "A Combination Monopole / Quadrifilar Helix Antenna for S-Band Terrestrial/Satellite Applications," *Microwave Journal*, May 2001.
9. A.D. Fuchs and R.A. Marino, "Dual-Antenna System for Single-Frequency Band," US Patent No. 6,329,954, (December 11, 2001).
10. A. Kumar, *Fixed and Mobile Terminal Antennas*, Artech House 1991, Norwood, MA, p. 194.
11. D. Allcock, "Crossed-Drooping Dipole Antenna," US Patent No. 4,686,536, (August 11, 1987.)

12. S. Licul and A. Chatzipetros, "Folded Helix Antenna," US Patent No. 6,229,499, (May 8, 2001).
13. A. Petros and S. Licul, "Folded Quadrifilar Helix Antenna," *Antennas & Propagation Society International Symposium Digest*, Vol. 4, (Boston, MA), IEEE, Vol. 4, pp. 569-572, July 2001.
14. Anaren Web Site, http://www.anaren.com/products/product_detail.cfm?prod=1013, Model XQF1306
15. XM Satellite Radio web page on antennas: http://www.xmradio.com/catalog/product_category.jsp?type=Antenna
16. A. Petros, "Combination Linearly Polarized and Quadrifilar Antenna," US Patent No. 6,483,471, (November 19, 2002).
17. Report TW-ANT-KN-01, Antenna Measurements, ThinkWireless Inc., 6/26/2003.

AT GREENRAY, AN ORDER FOR 10 OSCILLATORS HAS ALWAYS BEEN A BIG DEAL.



We call it flexibility.

For over 40 years, customers have relied on Greenray's precision quartz technology for their telecom, military, aerospace and instrumentation applications. Our OXOs, TCXOs and VCXOs are available in a variety of designs and package outlines – any application, any quantity. That's flexibility.

We offer ISO-9001 certification, extensive MIL-spec capabilities, custom build capability, in-house testing and our commitment to the highest standards for performance, reliability and customer service.

So whether you need just ten OXOs or 10,000 – call us at **717-766-0223** or send us an e-mail at sales@greenrayindustries.com.

We're flexible – so you don't have to be.

[[[www.greenrayindustries.com]]]



SDARS – Antennas: Environmental Influences, Measurement, Vehicle Application Investigations and Field Experiences

**Michael Daginnus, Rainer Kronberger,
Axel Stephan and Gerd-Hinrich Hassmann**
Fuba Automotive

Heinz Lindenmeier, Jochen Hopf and Leopold Reiter
University of the Bundeswehr Munich

The appearance of this ISSN code at the bottom of this page indicates SAE's consent that copies of the paper may be made for personal or internal use of specific clients. This consent is given on the condition, however, that the copier pay a per article copy fee through the Copyright Clearance Center, Inc. Operations Center, 222 Rosewood Drive, Danvers, MA 01923 for copying beyond that permitted by Sections 107 or 108 of the U.S. Copyright Law. This consent does not extend to other kinds of copying such as copying for general distribution, for advertising or promotional purposes, for creating new collective works, or for resale.

Quantity reprint rates can be obtained from the Customer Sales and Satisfaction Department.

To request permission to reprint a technical paper or permission to use copyrighted SAE publications in other works, contact the SAE Publications Group.



GLOBAL MOBILITY DATABASE

All SAE papers, standards, and selected books are abstracted and indexed in the Global Mobility Database

No part of this publication may be reproduced in any form, in an electronic retrieval system or otherwise, without the prior written permission of the publisher.

ISSN 0148-7191

Copyright © 2002 Society of Automotive Engineers, Inc.

Positions and opinions advanced in this paper are those of the author(s) and not necessarily those of SAE. The author is solely responsible for the content of the paper. A process is available by which discussions will be printed with the paper if it is published in SAE Transactions. For permission to publish this paper in full or in part, contact the SAE Publications Group.

Persons wishing to submit papers to be considered for presentation or publication through SAE should send the manuscript or a 300 word abstract of a proposed manuscript to: Secretary, Engineering Meetings Board, SAE.

Printed in USA

SDARS – Antennas: Environmental Influences, Measurement, Vehicle Application Investigations and Field Experiences

Michael Daginnus, Rainer Kronberger, Axel Stephan and Gerd-Hinrich Hassmann
Fuba Automotive

Heinz Lindenmeier, Jochen Hopf and Leopold Reiter
University of the Bundeswehr Munich

Copyright © 2002 Society of Automotive Engineers, Inc

ABSTRACT

According to the challenging antenna performance requirements for the reception of the Satellite Digital Audio Radio Services (SDARS), environmental influences are playing an important role for the practical design and application of such an antenna. This paper will report about remarkable influences on the performance of SDARS – Antennas with respect to ground plane conditions for measurements in anechoic chambers, as well as for vehicle mounting conditions. Results of field tests will show, what this means for reception.

1 INTRODUCTION

Almost since the announcement of SDARS-Services there has been a discussion about the challenging performance requirements for the automotive antennas to receive these services.

Regarding design, packaging, integration and other considerations, „non perfect“ antenna mounting locations are playing a decisive role for final, practical vehicle applications of SDARS antennas. The technically optimum antenna mounting location for these satellite based services on a vehicle, at the highest vehicle spot on top and in the center of the roof, is very often not accessible because of other conflicting vehicle design parameters and the existence of other components, which make going by car enjoyable – e.g. like a sliding roof.

This paper will focus on environmental influences on the performance of SDARS – antennas. In section 2, this will be done with respect to the characterization of the antennas itself, independent of vehicle mounting. It will be shown, that – and how much - the 3 dimensional antenna diagrams will vary with respect to the different sizes and different shapes of the applied ground plane in

an antenna measurement setup, even if the same antenna module is used. In the third section, applications and measurement results of SDARS – Antennas in different mounting locations on a vehicle will be shown. The last section presents field test experiences with SDARS Antennas, mounted at different locations on a vehicle.

2 SDARS ANTENNA INVESTIGATIONS ON GROUND PLANES

When the SDARS services were announced, it became quite clear, that a careful antenna design is needed to fulfill the requirements [4,5], especially for the antenna diagram in the satellite path (see Fig. 2.1). An antenna gain of 2 dBic is required for elevation angles between 20°- 60° for the XM service provider, and an antenna gain of 3 dBic is required between 25°-90° elevation for Sirius service provider.

These requirements are already rather close to the optimum of 3 dBic, that could be achieved theoretically for an ideal, three dimensional omnidirectional antenna, mounted on an ideal, infinite ground plane, radiating into the upper hemisphere with the elevation range from 0° to 90°.

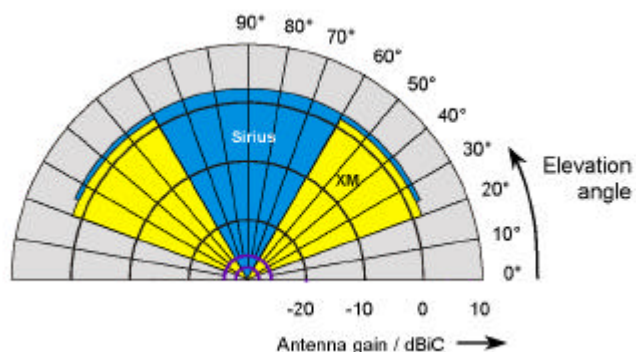


Fig. 2.1: Passive antenna gain requirements for the satellite antennas of the SDARS – services. Polarization is LHCP.

Examples for SDARS - antennas were already proposed on different occasions last year, e.g. in [1] and [2].

Of course, practical antennas cannot be mounted on an infinite ground plane, and also cannot be measured on it. For these reasons, for vehicle independent measurements in an anechoic chamber they have to be mounted on a real ground plane, that should correspond to the environmental mounting conditions on vehicles, e.g. vehicle roofs. Certain time it was not really fixed, how this “real” ground plane should look like. Also, the influence of this ground plane as one important environmental condition for the antenna radiation pattern was underestimated, or could not be systematically investigated.

To get comparable results, a “one meter in diameter” (see Fig. 2.2) specification was set for this ground plane size. Although this was a needed step to integrate the antenna mounting environment into the consideration, this again has its own specialties.

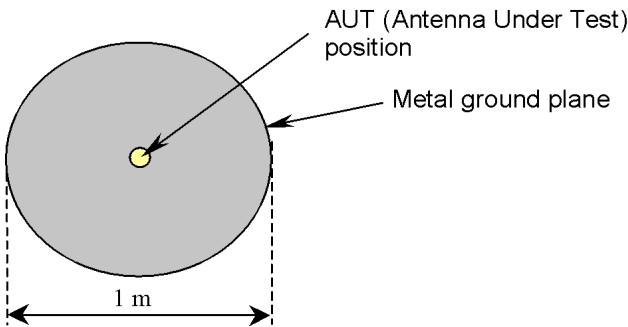


Fig. 2.2: One meter in diameter ground plane, top view sketch

To demonstrate these influences, in this report the effects of varying ground plane conditions were investigated for a quadrifilar helix antenna, which is a typical and often used antenna type for circular polarized antenna requirements.

Fig. 2.3 shows simulated results for the antenna diagrams on an infinite, Perfect Electrical Conductive ground plane (PEC), the “one in meter diameter” ground plane of Fig. 2.2 and the antenna without a ground plane, i.e. in free space. For all simulated curves, the antenna itself remained unchanged.

It can be seen, that the configuration of the ground plane plays a significant role for the 3-dimensional antenna characteristic. Especially for the finite, one meter diameter ground plane, a significant ripple of about ± 1 dB in a wide elevation angle range exists, and an even larger one close to 90° . This would have not been expected from the typically known antenna diagram of helix antennas, which is shown in the curve b.) “without ground plane”. Especially because there is only a small margin compared to the required antenna performance, and because of different ground plane sizes and shapes

for almost each vehicle in an automotive antenna integration these finite ground plane effects have to be further investigated.

This becomes even more important, because these diagrams only show lossless, perfectly omnidirectional antenna simulations. Taking real devices into account, losses will be added. Furthermore, an antenna diagram with a best case deviation of ± 0.5 dB from the perfect round azimuth diagram can be achieved for a stand alone antenna in a perfect environment. If then, additionally an antenna gain measurement uncertainty of only ± 0.5 dB is assumed, the “only small margin” mentioned above is consumed rather quickly, and a proof to meet the antenna requirements gets difficult.

So, it is important to clear up the origin of these ripples. Why do they exist in the antenna diagram? An

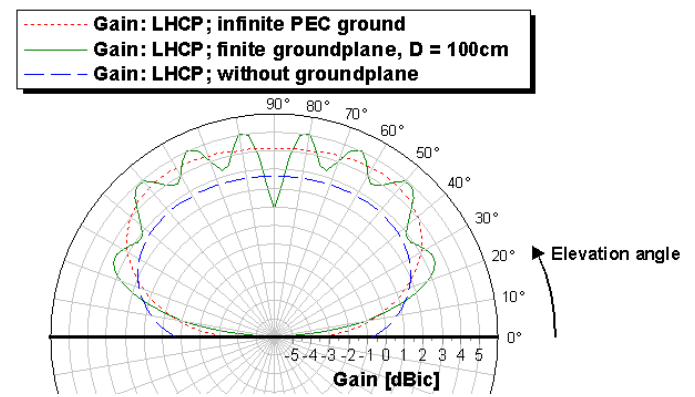


Fig. 2.3: Simulated elevation antenna diagram for a SDARS satellite antenna on
a.) infinite Perfect Electrical Conducting ground plane (PEC ---),
b.) without ground plane in free space (---) and
c.) one meter in diameter ground plane (—).
The antenna itself remained unchanged. Azimuth angle is $\varphi = 0^\circ$.

explanation will be found in Fig. 2.4. There, a simulation of rf (radio frequency) surface current densities for the arrangement of the antenna on the one meter in diameter ground plane, is shown. The more the colors are tending to the red, the higher these densities are, the more tending to the blue, the lower they are. As seen from Fig. 2.4 the main contributions are located close to the center of the ground plane and directly at the antenna itself, of course.

But, walking away from the center, a periodically repeating pattern of rf current density amplitude maxima and minima exists. These rf current densities are a origin of radiation itself, and their effects for the radiation pattern superpose the beam forming rf current densities of the antenna in the center. According to the physical spacing of these spurious rf current densities, the whole arrangement of antenna plus ground plane acts as a kind of unwanted array, causing the maxima and minima pattern of the antenna diagram in Fig. 2.3 as a function of elevation angle.

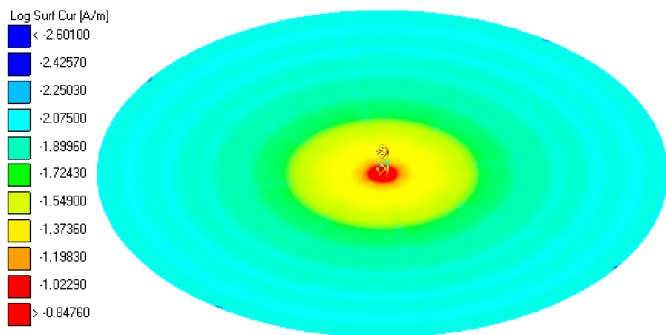


Fig. 2.4: Simulated rf current densities for the SDARS-antenna and the 1m in diameter ground plane arrangement.

With a first step the ground plane size dependence for the SDARS frequency was investigated. A set of simulations with varying diameter was performed. The results are shown in Fig. 2.5 and are compared to the calculated antenna gain on the infinite ground plane, which is set to 0 dB as a reference for this purpose.

It can be seen that the amount and location of the ripples is strongly dependent on the ground plane size. Unfortunately, the 1m size leads to a peak in ripple. So, a first recommendation would lead to a change of the diameter size to overcome the largest deviations in comparison to excluded ground plane effects.

In a second step, measures had to be taken to lower these spurious rf current densities at the ground plane. These can be achieved by changing the abrupt end of the ground plane, which sets a sharp boundary condition to the current densities there, to a rounded structure, like it is shown in Fig. 2.6.

The positive effects with application of bent edges can be

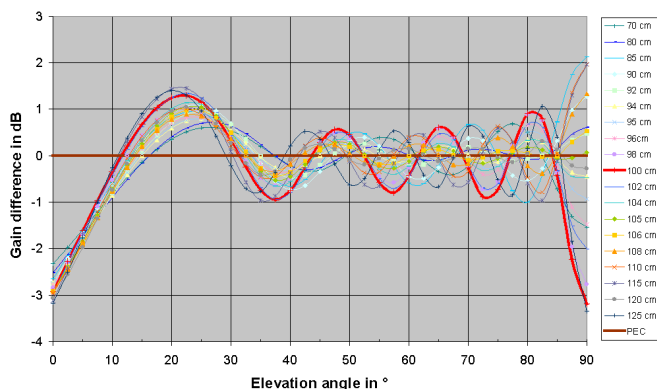


Fig. 2.5: SDARS – Satellite antenna gain differences on different circular ground plane sizes, as a function of elevation angle.

seen in Fig. 2.7. Compared to the results of Fig. 2.5, where no rounding of the ground plain edges was done, a significant reduction of the unwanted ripple is obtained. For elevation angles $> 30^\circ$ and ground plane sizes between diameters $D_{\text{ground plane}}$ of 70 cm and 120 cm the result is a gain uncertainty $\pm 0,5$ dBic, if a bent edge of a diameter of 4 cm according to Fig. 2.6 is applied. Further optimizations are is still possible.

For elevation angles between $\approx 15^\circ$ and 25° these ground plane sizes enhance the gain compared to the antenna arrangement with the infinite ground plane, as could already be seen from Fig. 2.5 . In summary: the ground plane size can tune the circular polarized satellite antenna performance at the low elevation angles, and a bent egde takes care for reducing gain ripples as a function of elevation. Meanwhile, these observations

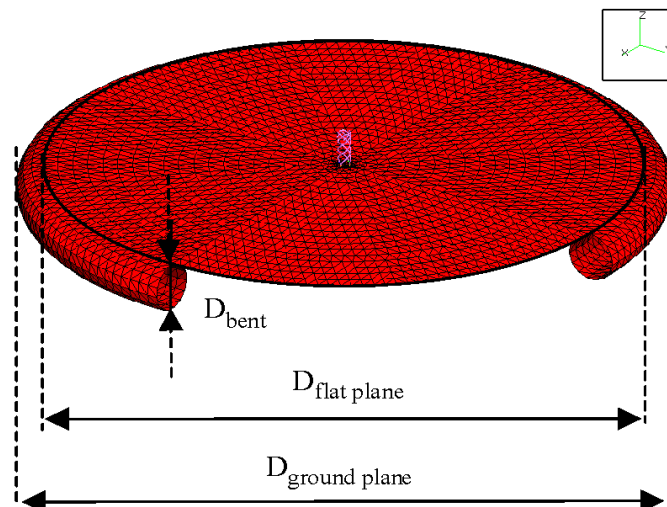


Fig. 2.6: Simulation model of a ground plane with bent edge, with mounted antenna. X and y span the horizontal plane, z refers to the elevation angle = 90° .

have been considered in newly released SDARS specifications.

For the vertical polarized, terrestrial antenna these ground plane dependent calculations are done with a quarter wavelength vertical monopole antenna. In the automotive industry, this antenna type is considered as a reference antenna for services, which are broadcasted with vertical polarization. The circular ground plane size was varied between 90 cm and 110 cm. Very similar to the circular polarized antenna, the antenna diagram changes significantly from the PEC configuration, if a finite ground plane is used. Again, gain enhancement can be noticed between 15° and 25° elevation angle, again ripples in the antenna diagram can be observed as

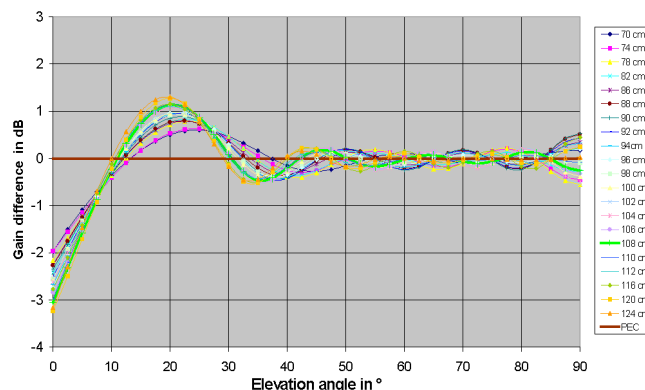


Fig. 2.7: SDARS-Satellite antenna gain differences on different circular ground plane sizes with bent edges, as a function of elev. angle.

a function of the elevation angle.

Having a closer look to the interesting low elevation angle areas for the terrestrial antenna, Fig. 2.8 clearly indicates a significant drop for the max. gain of a monopole antenna with a finite ground plane. Compared to the 5.15 dBi value for a monopole on an infinite ground plane as known from the literature, for the finite ground plane in Fig. 2.8 there is only a gain of about -1 dBi available at 0° elevation - for this ideally simulated,

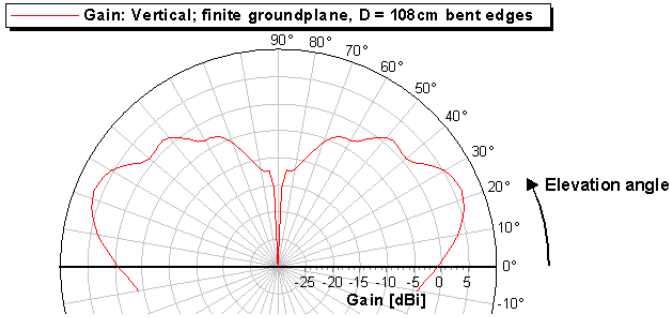


Fig. 2.8: Simulated gain for a monopole antenna on a finite ground plane with a diameter of 108 cm and bent edges.

lossless case in an optimum environment.

The antenna gain is calculated also for negative elevation angles in this example arrangement, which is the monopole on the ground plain of a diameter of 108 cm including bent edges according to Fig. 2.6. Fig. 2.8 shows, that e.g. a gain requirement of -1 dBi cannot be achieved for an elevation angle of -10° for this reference type antenna.

The simulation results on the previous pages correspond very good to measurement results that were performed in Fuba's precision anechoic chamber. The typical ripple pattern could be observed also for other antenna types, e.g. low profile types, and the elevation angles where minima and maxima appear were the same within a few degrees, when the same ground plane was applied.

From experiences of antenna measurements on different antenna measurement sites, the usage of different ground plane configurations is one reason that leads to different measurement results. In the past, these different results lead to difficulties to judge about an antenna performance according to the strict requirements. The additional environmental parameters, when the antenna is mounted on a vehicle, will be discussed in the next chapter.

3 ON VEHICLE ANTENNA APPLICATION

As described in the previous section, antennas for SDARS have to keep the given specifications also on the vehicle. Therefore the main task of antenna designer/manufacture is realizing SDARS vehicle antennas that satisfy the electrical requirements constrained by environmental conditions. In contrast to the simulation results of the antenna on an ideal circular ground plane (see section 2) only measurements of the antenna on the exact mounting location on the vehicle will show up the real antenna performance. Similar to the



Fig. 3.1: Antenna measurement on the vehicle

behavior of cellular phone antennas on the vehicle, an influence on the antenna pattern caused by the metallic vehicle body is expected [6]. Especially at low elevation angles reflections and shadowing effects will significantly

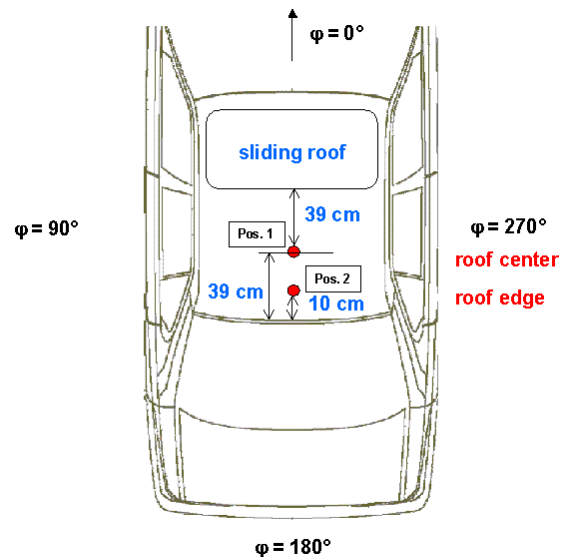


Fig. 3.2: Mounting locations of the antenna on the vehicle

change the antenna pattern. Therefore a variety of measurements was performed to study those effects. Fig. 3.1 shows the vehicle on the turntable in the measurement site [1]. The optimum mounting location for an SDARS antenna on a vehicle is supposed to be in the center of the roof, wavelengths away from all the edges. This also appears to be very close to the metallic plate of approximately 1 m in diameter, as given in the SDARS specifications [4, 5]. Practically, the sliding roof or design restrictions exclude that location. Fig. 3.2 displays two different mounting positions of the antenna on the vehicle on which the antennas were measured. Position 1 is located in the middle between sliding roof and roof edge and must be regarded as reference position only. There, maximum ground extension for the antenna towards all directions is given. A realistic antenna location on the vehicle is position 2, which is located 10 cm in front of the rear edge. The antenna being measured was of low profile structure, as described in [7]. For each position the satellite antenna pattern with left handed circular polarization (LHCP) was fully measured 3 dimensional as well as the terrestrial element with vertical polarization.

Compared to the results on the circular metallic plate (see Fig. 2.2) the patterns of the antenna, even at position 1 on the vehicle, already show the additional environmental influences. The specifications (XM), which are also displayed in Fig. 3.3, cannot be kept for all elevation angles according to a ripple on the pattern, especially for the longitudinal section ($\varphi = 0^\circ$). The ripple for the cross section ($\varphi = 90^\circ$) is slightly lower. Comparing now the pattern of the antenna near the roof edge at position 2 a slightly increased ripple in both patterns is visible (see Fig. 3.4) Additionally, with the

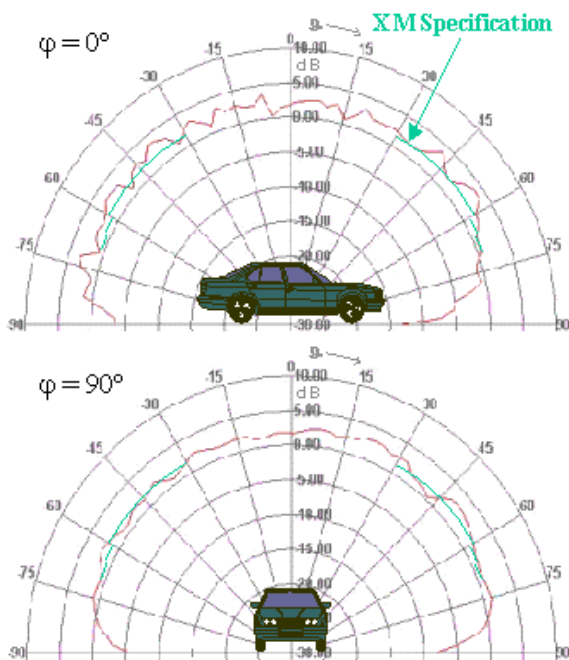


Fig. 3.3: SDARS antenna at position 1 (satellite pattern, LHCP, 2335 MHz)

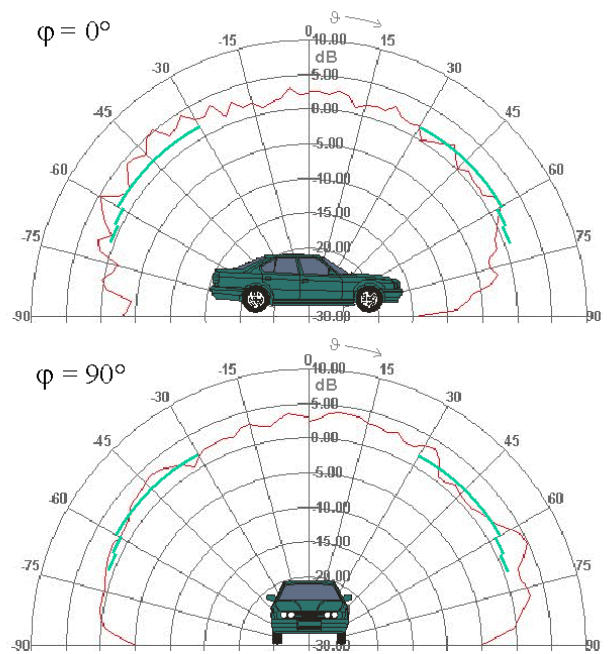


Fig. 3.4: SDARS antenna at position 2 (satellite pattern, LHCP, 2335 MHz)

curvature of the roof a shadowing towards the front direction occurs, which is visible in the pattern as a gain reduction of approximately 2 - 5 dB, compared to the antenna at position 1. To overcome those effects, either an expensive mechanical adaptation of the antenna diecast case to the given mounting situation on the vehicle has to be done (compensation for tilt angle and additional increase of height) or, more elegant, gain compensation with the antenna element must be applied [7].

In Fig. 3.5 the measurement results of the terrestrial SDARS antenna are displayed, compared to a reference quarterwave monopole at the same location on the vehicle. In contrast to the patterns above only azimuth patterns for 0° elevation, respectively $\vartheta = 90^\circ$, are displayed. The gain is normalized to the average azimuth gain of the monopole at position 1. Even that monopole shows a significant degradation of the desired omnidirectional pattern, with a ripple of approximately 13 dB. That deviation from the omnidirectional pattern caused by the environmental influence of the vehicle is well known from cellular phone antennas in the 1900 MHz band. Comparing the terrestrial SDARS antenna the pattern is almost the same, with a slightly reduced average gain of -2.2 dB and a ripple of 12 dB. Regarding the antennas near the roof edge, the average gain of both antennas decreases more than 1 dB. This is also well known from cellular phone antennas [6]. This shows clearly that the final qualification of the antenna performance can only be given by means of vehicle antenna measurements.

On the other hand, antennas which keep the specifications on the circular ground plane may be specifically influenced by the vehicle body which results

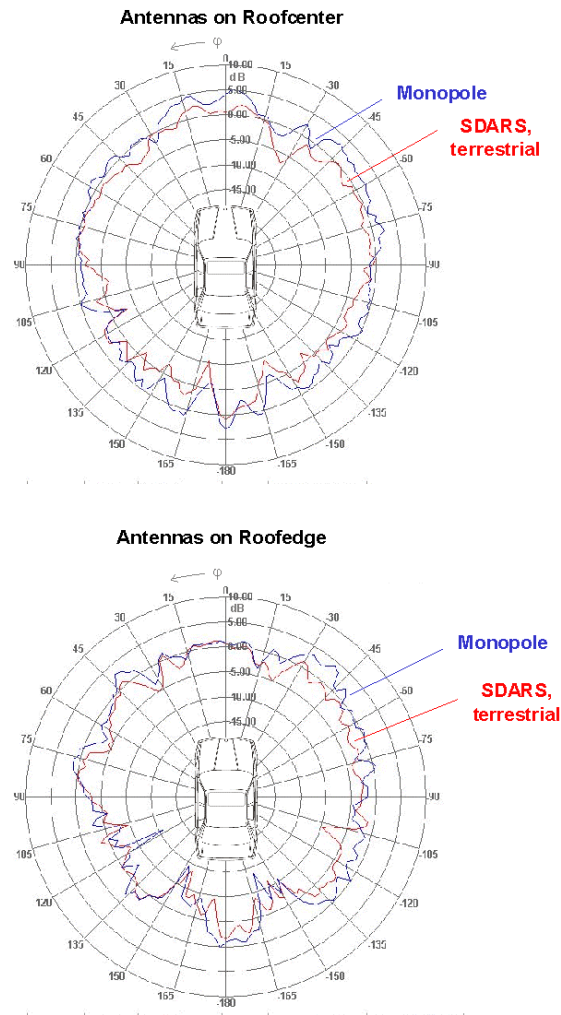


Fig. 3.5: Terrestrial SDARS antenna and reference monopole at position 1 and 2

in severe deviations from the desired patterns (see Fig. 3.3 - 3.6).

Antennas being placed on other locations on the vehicle than on the roof, e.g. on the trunk lid, are blocked by the body and show a significant reduction of gain in a certain direction. Therefore only field testing allows a final judge whether the antenna can be used or not.

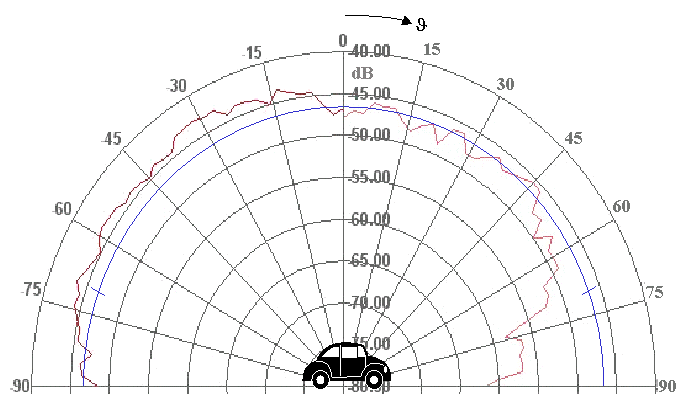


Fig. 3.6: SDARS satellite antenna on the trunk lid of a vehicle

4 FIELD TESTING

The measurements above show that in most cases the specifications cannot be met with the antenna on the vehicle, whereas the same antenna meets the specifications on a ground plane in the anechoic chamber.

During a special test drive antenna performance has been evaluated for different locations on a convertible vehicle. According to the missing metal roof, the recommended roof location for the antenna module was not available. Therefore the antenna was mounted on two different positions: on the windshield cowl and on the metal roof cover near the trunk lid (antenna diagram see Fig. 3.6). With both antennas the satellite signal level was recorded. Table 4.1 shows the satellite signal availability based on a given receiver threshold level within the test setup.

Test condition		Satellite 1 Ensemble A	Satellite 2 Ensemble A
Round trip (all directions), rural	front	99.09 %	97.84 %
	rear	99.22 %	93.48 %
Trip in N-S direction, suburban and rural	front	99.06 %	98.13 %
	rear	98.69 %	98.34 %

Table 4.1: Satellite signal availability with test vehicle, XM - satellite

Despite the different antenna locations and the different antenna radiation patterns almost the same overall satellite availability could be determined. The recorded dropouts showed no significant dependency of the driving direction and occurred almost uniformly distributed, especially in low signal regions. This shows clearly that the reception performance is mainly influenced by shadowing effects due to obstacles in the line of sight (LOS) to the satellite.

In Fig. 4.1 the shadowing and attenuation effect of heavy foliage is shown. One drive was conducted far away of the trees so that a direct signal reception from the satellite was given. The signal level of one satellite varies in a range of typically less than 5 dB. The second drive was performed very close to the trees which led to a significant attenuation of the signal of approximately 10 to 15 dB. Furthermore this signal also shows a typical fading due to multipath propagation through the trees. Thus a continuous and undistorted reception was not possible. Heavy dropouts occurred.

To avoid the described multipath effects and to increase the reception performance in such weak signal regions an antenna diversity system might be the solution.

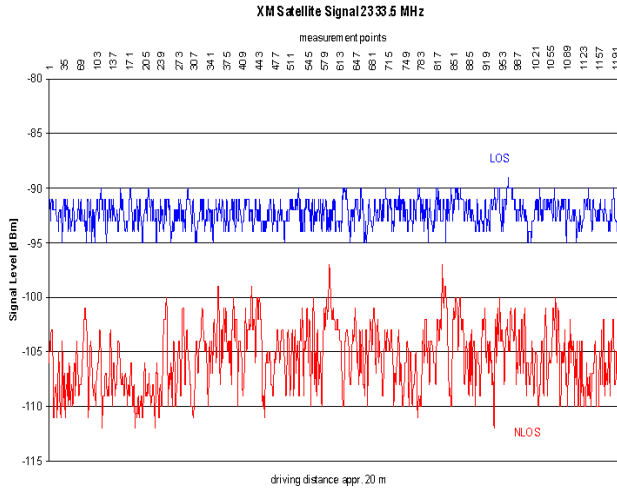
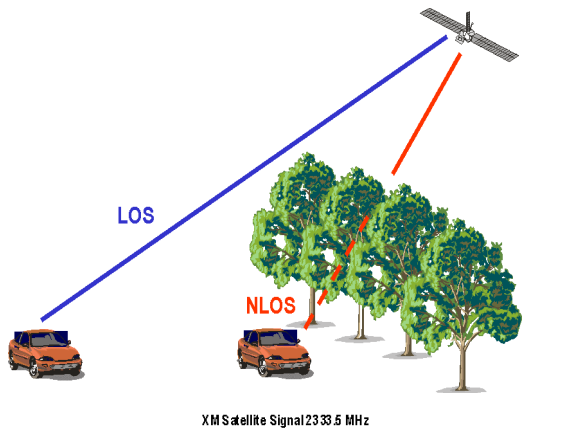


Fig. 4.1: Comparison of direct and shadowed signal reception from a satellite

5 CONCLUSION

In this paper environmental parameters were discussed for the characterization and application of SDARS – Antennas.

It was shown, that a “one meter in diameter” ground plane leads to a significant ripple in antenna directionality over varying elevation angles for Antennas in the SDARS frequency range. Ground plane size and edge shapes are important for the required exact antenna measurement. They cannot be neglected for getting antenna measurement results within comparable tolerances between different antenna measurements.

Practical vehicle mounting conditions have significant influence on the antenna radiation patterns as well. By installing the antenna on a vehicle, respectively integrating it, the antenna radiation pattern could look significantly different compared to that of the vehicle independent measured antenna, if not taken care, and has therefore a rather high probability not to meet the strict requirements. Environmental influences like ground plane conditions, shadowing and antenna tilt play an important role.

This is especially important to consider in a situation, where automotive manufacturers are focussing on an invisible or at least almost invisible antenna integration, which does not affect their vehicles design negatively.

A field test was performed in different areas to get an insight of the rf -signal behaviour and of the subjective SDARS reception. Besides investigating the outcome of two antennas mounted at different vehicle locations., to check a practical antenna integration effort, more significantly it also turned out, that especially for reception situations with a multipath environment there is room for improvement, e.g. by antenna diversity means.

6 REFERENCES

1. M. Daginnus, A. Stephan and R. Kronberger: “Simulation and Measurement Results of Complex Integrated Vehicle Antenna Systems for Premium Audio Reception”, SAE 2001 World Congress, Society of Automotive Engineers, Detroit, March 5-8, 2001, SAE technical paper series 2001-01-0004
2. Argy Petros and Stanislav Licul: “ “Folded” Quadrifilar Helix Antenna” ”, 2001 IEEE Antennas & Propagation Society, International Symposium, Boston, July 8-13, 2001, 2001 Digest, Volume Four, p. 569
3. R. Kronberger, A. Stephan and M. Daginnus: “3 D Antenna Measurement and Electromagnetic Simulation for Advanced Vehicle Antenna Development”, 2001 IEEE Antennas & Propagation Society, International Symposium, Boston, July 8-13, 2001, 2001 Digest, Volume Three, p. 342
4. XM Antenna Specification, by XM Satellite Radio, Boca Raton, 2001
5. Sirius-Antenna Specifications, by Sirius Satellite Radio, New York, 2001
6. R. Kronberger et al.: Design Method for Antenna Arrays on Cars with Electrically Short Elements under Incorporation of the Radiation Properties of the Car Body. Influence of the radiation properties of a car. IEEE Antenna and Propagation Symposium, Montreal, 1997.
7. H. Lindenmeier et al.: A New Design Principle for a Low Profile SDARS-Antenna including the Option for Antenna-Diversity and Multiband Application. Accepted for SAE 2002 World Congress, Society of Automotive Engineers, Detroit, March 2002.

7 CONTACT

Dr.-Ing. Michael Daginnus
 Fuba Automotive GmbH & Co. KG
 Tec Center, D-31162 Bad Salzdetfurth, Germany
 Phone +49-(0)5063-990-728
 email: michael.daginnus@delphiauto.com

A New Antenna Principle for Satellite Radio Reception including the Possibility for Diversity Application

Prof. Dr. J. Hopf, Prof. Dr. H. Lindenmeier, Prof. Dr. L. Reiter, Institute for High Frequency Technology, University of the Bundeswehr Munich, D-85577 Neubiberg, Werner-Heisenberg-Weg 39, Phone: 089-6004-3009; Fax: 089-602594; Email: jochen.hopf@unibw-muenchen.de

Abstract

The new Satellite Digital Audio Radio Service (SDARS) has already started in the USA. The circularly polarized satellite signals are supported by terrestrial transmitters in built-up areas using vertical polarization [1]. This is true with both providers, Sirius and XM. Therefore the receiving antenna has to meet the requirements for terrestrial and satellite reception. Due to automotive aspects low profile antennas are required. In this paper such an antenna is presented which meets both the SDARS-specifications and the requirements for SDARS-antenna diversity application due to multipath reception even with satellite signals. The design principle allows in a further up-grading multi-band application for cellular phone e.g. GSM or UMTS.

1 Introduction

The new radio service SDARS now is in operation at a small frequency band of 25MHz bandwidth at 2.33 GHz. For the first time this service delivers an area wide coverage for the total North American continent. The most challenging task for SDARS-antenna design is to satisfy a variety of combined requirements for OEM-applications. Besides of the different antenna parameters according to the different SDARS-Antenna specification of Sirius and XM [1] to be met there is a great desire for a low profile design according to styling conditions given by the automotive industry. As a result of the multitude of communication services in modern cars, the number of which will even expand in future, there is a great need for an antenna principle that allows a combined application of a variety of communication services in one integrated antenna, for example for SDARS, mobile phone and GPS. This is especially true due to the lack of acceptable

mounting positions on a carefully styled passenger car body.

Both provider delivered specifications for the antenna diagrams to be measured on test plates of for example a diameter of 1m. However, the respective gain values to be met are different. In addition the respective postulated data are on the absolute fringe of the physical possibilities. Fig. 1a gives an impression of the required three dimensional antenna diagram to be achieved for left hand circularly polarized satellite signals (LHCP) with omnidirectional properties in the azimuthal planes and Fig. 1b shows the required basic radiation pattern for the reception of the vertical polarized terrestrial signals.

The present paper will present a new design principle that allows for the conveniently adjustable superposition of the horizontally and vertically polarized components of the circular polarized incident waves of the SDARS-satellite signals by means of reactive components. Thus the antenna diagram can be easily adjusted to the respective specifications.

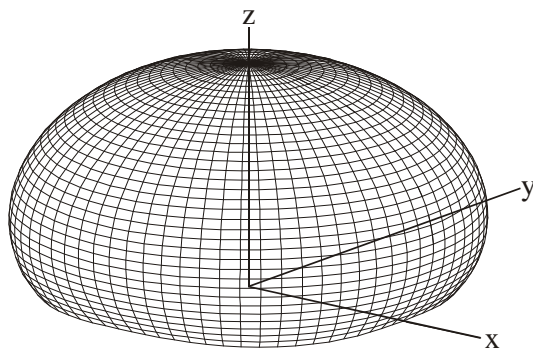


Fig. 1a: Basic radiation pattern for reception of circularly polarized satellite signals

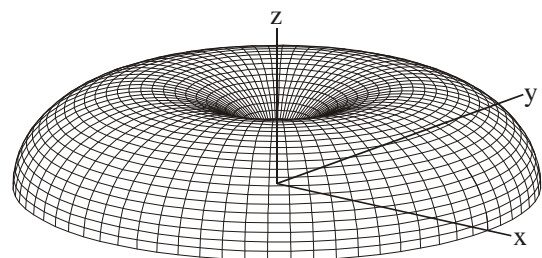


Fig. 1b: Basic radiation pattern for reception of vertically polarized terrestrial radiated signals

2 Design principle for a low profile SDARS-antenna

2.1 SDARS antenna for satellite signals

In order to meet the specifications the radiation must be carefully distributed versus the zenith angle Θ with omnidirectional radiation and the efficiency factor of the antenna must be close to 1. The radiation diagram of the new antenna design presented may be understood as a superposition of a vertical diagram (Fig. 2a) described by a cosine function of Θ and the vertical diagram (Fig. 2b) approximately described by a sine function.

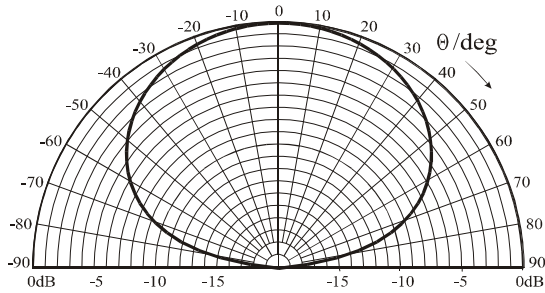


Fig. 2a: Vertical diagram described by a cosine-function of Θ (e.g. horizontal dipole close to ground)

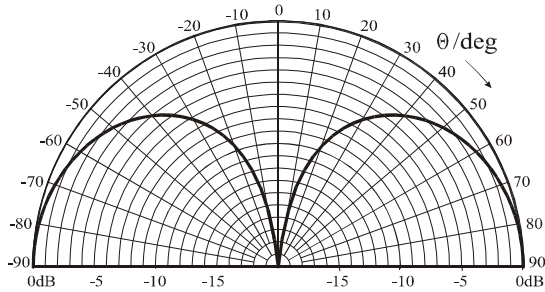


Fig. 2b: Vertical diagram described by a sine-function of Θ (e.g. vertical monopole above ground)

Both diagrams can be superimposed by a weight factor b . This leads to the following function of the vertical pattern $C(\Theta)$ of an antenna over an infinite and perfectly conducting ground:

$$C(\mathbf{q}) = \frac{2 \cdot [\cos^2(\mathbf{q}) + b \cdot \sin^2(\mathbf{q})]}{\int_0^{\pi/2} [\cos^2(\mathbf{q}) + b \cdot \sin^2(\mathbf{q})] \cdot d\mathbf{q}} \quad (1)$$

This function delivers for each value of b the same integral representing the total radiated power. For a better understanding curves of this function are plotted

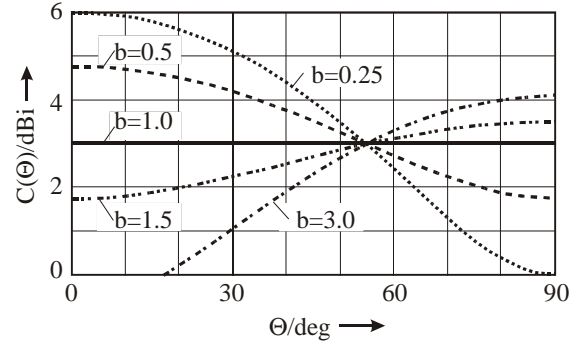


Fig.3: Vertical pattern with different weight factor b

as $20 \cdot \log(C(\Theta))$ in dBi versus the zenith angle Θ for various values of the weight factor b (Fig. 3). These curves show clearly that an accentuation of the radiation towards the high elevation angles reduces the radiation at the lower angles and vice versa. With an equalized superposition of both radiation pattern characterized by $b=1$ the diagram forms an idealized half sphere of 3dBi independent of the radiation angle Θ . The design principle of the presented antenna is based upon this principle of superimposing the diagrams of Fig. 2a and 2b. Substantially the designed antenna forms a rectangular loop with horizontal and vertical conductors by means of implemented reactive elements (Fig. 6). These can be easily adjusted according to a special required curvature of the vertical diagram and can also be adapted empirically to a certain groundplane configuration. The principle of the influence of the reactive element can be seen from the radiation patterns in Fig. 4a and b.

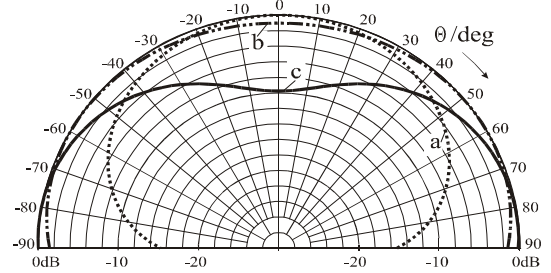


Fig. 4a: Vertical diagram with increasing value "c" to "a" for a capacitive element

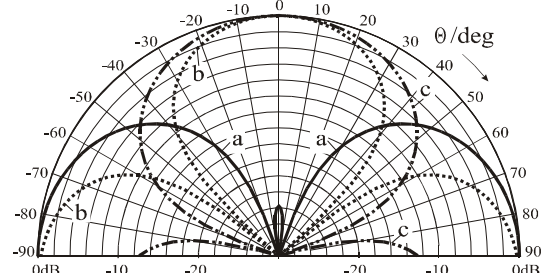


Fig. 4b: Vertical diagram with increasing value "c" to "a" for an inductive element

With a capacitive element there is a tendency to enhance the radiation within the range of $30 \leq \Theta \leq 70$ degrees (Fig. 4a curves “b” and “c”). Curve “a” with a high value of the capacitive element in Fig. 4a is similar to the cosine diagram of Fig. 2a. On the other hand curves “b” and “c” in Fig. 4b are obtained by an inductive element. With a very small value of the inductive element curve “a” in Fig. 4b has the tendency to the sine function of Fig. 2b. Combining 2 rectangular arranged loops by means of a 90 degree phase shift condition by principle a circularly polarized vertical diagram as in Fig. 5 can be adjusted.

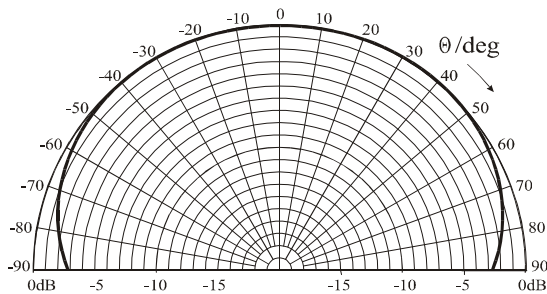


Fig. 5: Computed vertical diagram for LHCP signals over infinite ground

A great advantage of this antenna design is found in the fact that due to this easy to execute adjustment of the antenna pattern a small antenna height can be realized. Fig. 6 shows a photograph of a test sample of the SDARS antenna the footprint of which is only 30mm by 30mm with a total antenna height of 16mm.

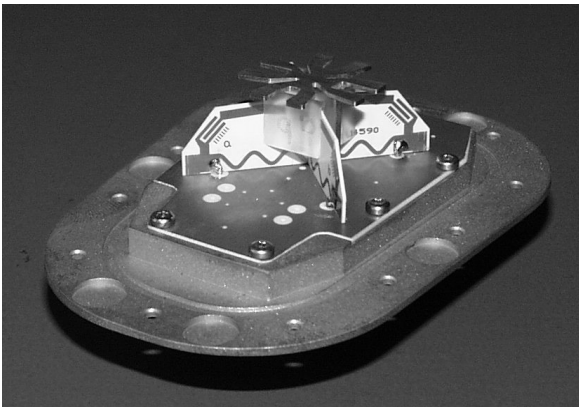


Fig. 6: Test sample of the SDARS-antenna

In Fig. 7 the measured vertical diagrams in 4 different azimuthal planes at the port for circular polarized satellite signal reception are displayed, measured with the antenna being mounted in the center of a circular ground plane. The ripple in the curves result from inevitable standing waves being generated by nature at the edge of the so defined ground plane [2]. In this context it should be mentioned that the inevitable radiation at angles of $\Theta > 90$ degrees at the lower side

of the ground plane reducing the radiation at angles $\Theta < 90$ at the upper side of the groundplane is a further difficulty to satisfy the required specification.

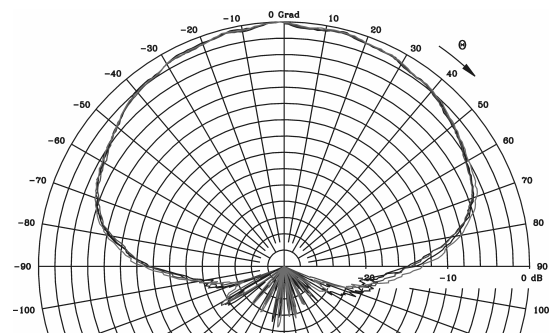


Fig. 7: Measured vertical antenna pattern for LHCP-signals in 4 different azimuthal planes

2.2 SDARS antenna for terrestrial signals

An embedded vertical element (see Fig. 6) within the antenna enables the antenna by symmetry conditions to receive the terrestrial SDARS signals at a second port being decoupled from the SDARS satellite port. In order to satisfy the requirement of an enhanced radiation at low elevation angles it is advisable to use an antenna element of low radiation close to the zenith. This is an element with the character of a vertical monopole the measured vertical diagram of which is displayed in Fig. 8 for vertical polarization in 4 different azimuthal planes. Again the ripple generated by the circular groundplane can be recognized. The effect of the reduced radiation at $\Theta = 90$ degree compared to the sine function as displayed in Fig. 2b results from the limited ground plane. Of course quite different effects on the diagram are found if a SDARS-antenna is mounted on a car roof.

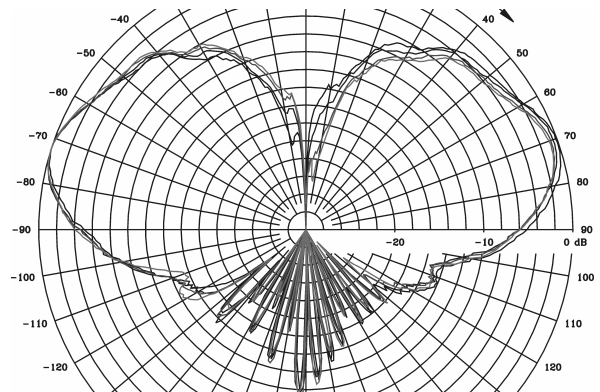


Fig. 8: Measured vertical diagrams in 4 different azimuthal planes of the vertical monopole

3 Diversity antennas for SDARS

Measurements of level distribution versus a driven path have been executed in order to examine if with the reception of terrestrial and even with satellite SDARS-signals as well locations where Rayleigh or Ricean signal level distribution is found in a quite common environment such as houses and trees.



Fig. 9a: Driven path for level measurements

In Fig. 9 a driven path for level measurements is displayed. The transmitting antenna was at the location of the camera simulating a satellite signal incident from appr. 30 degree elevation. Fig. 9b shows the recorded signal level versus time along the driven path at a section next to the building.

Even though in this case the receiving antenna is in direct view of the transmitting antenna strong signal fadings often occur due to the multi-scattered and multi-reflected electromagnetic waves in the displayed environment. Since an environment of this kind is quite normal and moreover in cities the situations where there is neither a direct view to the satellite nor to the terrestrial transmitting station diversity techniques can be usefully applied to improve the reception and reduce the likelihood that the communication link is interrupted.

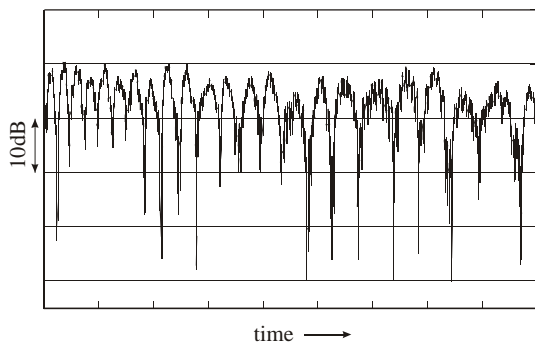


Fig. 9b: Short segment of the measured signal level along the building of Fig. 9a

From an OEM standpoint it is very attractive if the mechanical dimensions of a diversity-antenna providing a multitude of different signals can be designed compatible to the antenna for single signal application. The basic structure of the above described low profile antenna allows the design of up to four different antenna signals which in a Rayleigh field provide excellent values of diversity effectiveness [3].

4 Combination antenna

There is a great need for combination antennas providing several services in one small housing. Such kind of antenna was realized for SDARS, GPS and mobile phone (AMPS and PCS). Especially the phone antenna, mounted at a distance of only 30mm from the center of the SDARS antenna, had to be designed very carefully as it must not change the thoroughly adjusted diagrams of the SDARS antennas at all. For this two stop band filters were inserted in the layout of the phone antenna element being tuned exactly to the center of the SDARS band. Thus the influence of the phone antenna on the SDARS antenna is negligible (Fig. 11a and 11b).

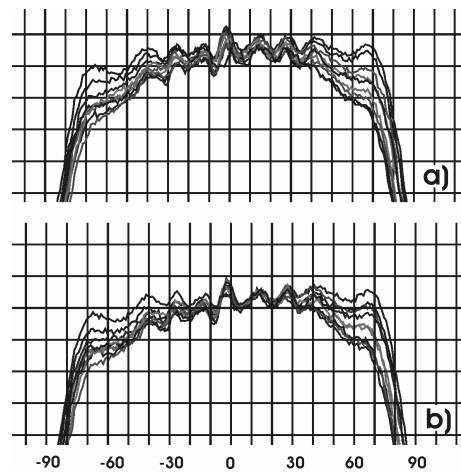


Fig. 11: 8 vertical cut all 22.5 degree of azimuthal angle, vertical axis 1dB per division
a) without phone antennas b) with phone antennas

5 Conclusion

The new design principle for a low profile SDARS antenna allows for a conveniently adjustable superposition of the horizontally and vertically polarized components of the received circularly polarized incident waves of SDARS-satellite signals in order to achieve the required vertical diagram. Making use of receiving signals being available from different parts of this antenna a diversity system can be achieved.

6 References

- [1] Patsiokas, Stellios J.: XM Satellite Radio...; SAE Techn. Paper Series 2001-01-1328; SAE 2001 World Congress, Detroit, Michigan.
- [2] Daginnus M. et al.: SDARS Antennas: Environmental Influences ...; SAE Techn. Paper Series 02AE-143, SAE 2002 World Congress, Detroit, Michigan;
- [3] Lindenmeier, H. et. al. : A New Design Principle SAE Techn. Paper Series 02AE-147, SAE 2002 World Congress, Detroit, Michigan.

Low Profile SDARS–Antenna with Diversity Functionality

*Heinz Lindenmeier, Jochen Hopf, Leopold Reiter

University of the Bundeswehr Munich
Institute for High Frequency Technique, D-85577 Neubiberg, Germany
Heinz.Lindenmeier@UniBw-Muenchen.de

ABSTRACT

The new Satellite Digital Audio Radio Service (SDARS) has already started in USA. The circularly polarized satellite signals are supported by terrestrial transmitters in built-up areas using vertical polarization [1]. Therefore the receiving antenna has to meet both requirements. In this paper such an antenna is presented which meets both the SDARS-specifications and the requirements for SDARS-antenna diversity application due to multipath reception even with satellite signals.

1 INTRODUCTION

The most challenging task for SDARS-antenna design is to satisfy a variety of combined requirements for OEM-applications. Besides of the antenna parameters according to the SDARS-Antenna Specification to be met there is a great desire for a low profile design according to styling conditions given by the automotive industry.

2 DESIGN PRINCIPLE FOR A LOW PROFILE SDARS-ANTENNA

The paper presents and explains a new design principle that allows for the conveniently adjustable superposition of the horizontally and vertically polarized components of the circular polarized incident waves of the SDARS-satellite signals by means of reactive components.

2.1 SDARS ANTENNA FOR SATELLITE SIGNALS

In order to meet the SDARS-specifications the radiation must be carefully distributed versus the zenith angle Θ with omnidirectional radiation and the efficiency factor of the antenna must be close to 1. The radiation diagram of the new antenna design presented may be understood as a superposition of a vertical diagram described by a cosine function of Θ and the vertical diagram approximately described by a sine-function. Both diagrams can be superimposed by a weight factor b . This leads to the following approximated function of the vertical pattern $C(\Theta)$ of an antenna over an infinite and perfectly conducting ground:

$$C(\theta) = \frac{2 \cdot [\cos^2(\theta) + b \cdot \sin^2(\theta)]}{\int_0^{\pi/2} [\cos^2(\theta) + b \cdot \sin^2(\theta)] \cdot d\theta} \quad (1)$$

This function delivers for each value of b the same integral representing the total radiated power. For a better understanding curves of this function are plotted as $20 \cdot \log(C(\Theta))$ in dBi versus the zenith

angle Θ for various values of the weight factor b . These curves show clearly that an

accentuation of the radiation towards the high elevation angles reduces the radiation at the lower angles and vice versa. But there is no way to increase the antenna gain at all angles as sometimes claimed except by active means. With an equalized superposition of both radiation pattern characterized by $b=1$ the diagram forms an idealized half sphere of 3dBi independent of the radiation angle Θ . Substantially the designed antenna forms a rectangular loop with horizontal and vertical conductors combined by means of implemented reactive elements. These can be easily adjusted according to a special required curvature of the vertical diagram and can also be adapted empirically to a certain groundplane configuration. The principle of the influence of the reactive element can be seen from the radiation patterns in Fig. 2a and b. With a reactive (capacitive) element providing positive reactive power there is a tendency to enhance the radiation within the range of $30 \leq \Theta \leq 70$ degrees (Fig. 2a curves "b" and "c"). Curve "a" with a high value of the capacitive element in Fig. 2a is similar to the cosine-diagram. On the other hand curves "b" and "c" in Fig. 2b are obtained by a reactive element of negative reactive power. With a very small value of the inductive element curve a in Fig. 2b has the tendency to the sine-function.

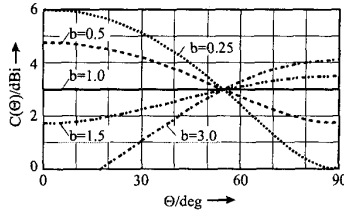


Fig. 1: Vertical pattern with different weight factors b according to equation (1)

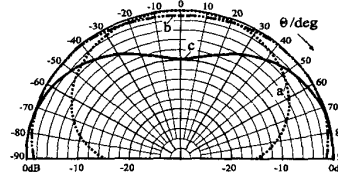


Fig. 2a: Vertical diagram with increasing value "c" to "a" for a capacitive element

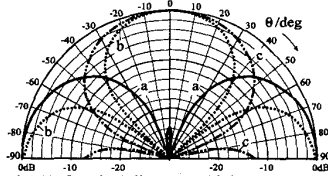


Fig. 2b: Vertical diagram with increasing value "c" to "a" for an inductive element

Combining 2 rectangular arranged loops by means of a 90 degree phase shift condition by principle a circularly polarized vertical diagram can be achieved. Or even a voluntarily slightly asymmetric adjusted diagram can be obtained for the reason of compensating a certain asymmetric influence of a ground plane such as a car body for example.

A great advantage of this antenna design is found in the fact that due to this easy to execute adjustment of the antenna pattern a small antenna height can be realized. With the example of such an antenna with quadratic ground plane the size of which can be seen from Fig.3 (antenna height: 2cm).

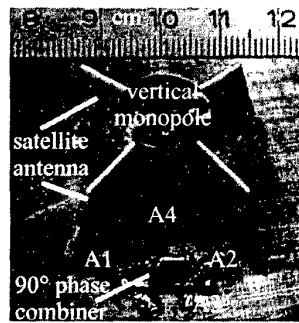


Fig.3: Test sample of realized SDARS-antenna with antenna ports A1 to A4

In Fig. 4 the measured vertical diagrams in 4 different azimuthal planes at the port A3 (see Fig. 3) for circular polarized satellite signal reception are displayed, measured with the antenna being mounted in the center of the obligatory 1m circular ground plane. The ripple in this curve results from inevitable standing waves being generated by nature at the edge of the so defined ground plane. In this context it should be mentioned that the inevitable radiation at angles of $\Theta > 90$ degrees at the lower side of the ground plane reducing the radiation at angles $\Theta < 90$ at the upper side of the groundplane is a further difficulty to satisfy the required specification which is overcome by fine adjustment of the reactive elements.

2.2 SDARS ANTENNA FOR TERRESTRIAL SIGNALS

An embedded vertical capacitive loaded monopole (see Fig. 3) within the antenna enables the antenna by symmetry conditions to receive the terrestrial SDARS-signals at port A4 being decoupled from the SDARS-satellite port A3. In order to satisfy the requirement of an enhanced radiation at low elevation angles it is advisable to use an antenna element of low radiation close to the zenith. This is an element with the character of a vertical monopole the measured vertical diagram of which is displayed in Fig. 5 for vertical polarization in 4 different azimuthal planes. Again the ripple generated by the circular groundplane can be recognized. The effect of the reduced radiation at $\Theta = 90$ degree compared to the sine-function results from the limited ground plane. Quite different effects on the diagram are found if a SDARS-antenna is mounted on a car.

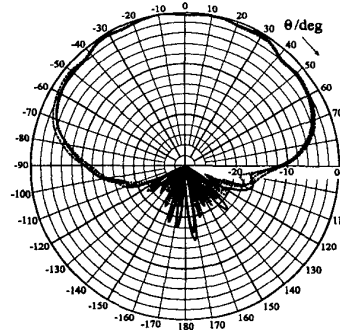


Fig. 4: Measured vertical antenna pattern at antenna port A3 for SDARS satellite signals in 4 different azimuthal planes

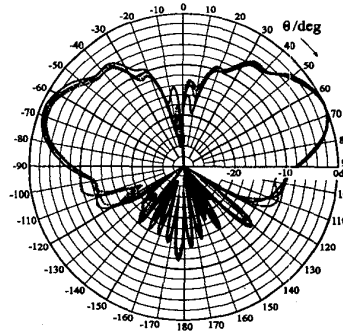


Fig. 5: Measured vertical diagrams in 4 different azimuthal planes at the antenna port A4 of the vertical monopole

3 ANTENNA DIVERSITY FOR TERRESTRIAL AND SATELLITE SDARS-SIGNALS

Measurements have shown that signal fadings can be reduced to a great extent by means of antenna diversity techniques which can be designed for the digital SDARS-signals both for terrestrial reception or for satellite reception.

The improvement depends on the diversity efficiency describing the number n of fictitious decorrelated antenna signals. For such an application the design principle of the antenna further allows for a separate access to different parts of the antenna at different ports (A1 to A4) where different radiation pattern are obtained so that up to $n=3.1$ decorrelated signals are available within one antenna. Therewith in the inevitable signal shadow regions of the SDARS signal a considerable reduction of bit error rate can be expected.

With V representing the effective emf-voltage at the output of a single antenna, and with V_m representing the root mean square value of this voltage over a driven distance in the multipath Rayleigh-field distribution (Fig. 6) the well known likelihood density distribution $p_s(V)$ according to Rayleigh reads as:

$$p_s(V) = \frac{2 \cdot V}{V_m^2} \cdot e^{-\frac{V^2}{V_m^2}} \quad (2)$$

In former papers [2] it has been shown that a diversity-system of diversity-efficiency n representing this number of available decorrelated antenna signals reduces this likelihood by the power n . With this the reduced likelihood p_d of erroneous symbol detection with the diversity system can be estimated as (Fig. 7):

$$p_d = p_s^n = \left(1 - e^{-\frac{V^2}{V_m^2}}\right)^n \quad (3)$$

The reduction of erroneous symbol identifications can as well be expressed by a fictitious enhancement of the mean value of the signal voltage received by a single antenna along the identical distinct drive. With the required minimum voltage V_{min} for erroneous free symbol detection for the receiver being a constant, the fictitious signal to distortion ratio SND can be expressed which for large values of SND_s of the single antenna can be simplified to:

$$SND = n \cdot 20 \cdot \log(V_s / V_{min}) \quad (4)$$

For this reason it seems to be advisable to complete the present SDARS receiving system by an inexpensive add on antenna diversity which might be applied optionally for reception improvement.

4 REFERENCES

- [1] Patsiokas et al.: XM Satellite., SAE 2001-01-1328; ISSN 0148-7191, 3/2001
- [2] Lindenmeier et al.: Diversity-Eff..., SAE 981147, ISSN 0148-7191, 2/1998

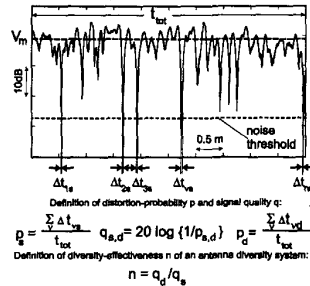


Fig. 6: Measured signal level versus time in the microwave range and explanation of the diversity effectiveness n

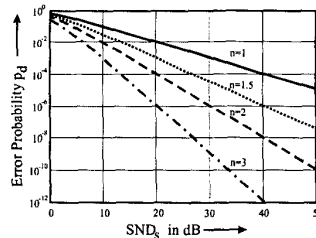


Fig. 7: Error probability with n decorrelated signals as a function of $SND_s = 20 \log(V_m/V_{min})$ with a single antenna



**UNIVERSITY
OF GÄVLE**

FACULTY OF ENGINEERING AND SUSTAINABLE DEVELOPMENT

**NEW INTEGRATED SDARS ANTENNA ELEMENT
FOR AUTOMOTIVE APPLICATIONS**

Muhammad Imtiaz

September 2011

Master's Thesis in Electronics

Master's Program in Electronics/Telecommunications

Examiner: Dr. José Chilo

Supervisors: Dr. Jochen Christ

Dipl.-Ing. Mohammad Bashir

Dedicated To

My beloved parents & family who show me the right path to live successfully

Abstract

In the past few years the demand for light weight compact automotive antennas in the customers desired mounting position has brought a challenge for the automotive antenna developers. Due to the high demands for the accuracy and compactness it became very difficult to develop antenna elements which fulfil all the strict requirements. Integrated SDARS (Satellite Digital Audio Radio Service) antenna element is one of such tasks which require strong gain requirements at particular elevation angles for the best reception of the satellite signals along with the car manufacturer's desired mounting positions.

To achieve the desired objectives for SDARS element, different antenna designs were proposed and tested during the project work. Finally a newly developed two port cylindrical dielectric resonator antenna (DRA) with a parasitic element is presented due to its high performance, simplicity and compactness. The newly developed DRA antenna fulfils the strict SiriusXm gain requirements for the challenging mounting position in the car. The SDARS antenna element is simulated using CST Microwave Studio and verified by prototype measurements. The developed DRA antenna element has a broad beam with a peak gain more than 6dBi at the null position. An axial ratio of less than 3dB is achieved at the peak gain position. Real time 3D far field measurements are taken by using the MiDAS 4.1 system which verifies the simulated results of the developed integrated SDARS antenna. A good agreement is achieved between the simulated and measured results.

Acknowledgements

This thesis presents my research and development in Electronics engineering carried out at the antenna development department of WISI Automotive, Germany, to fulfil the requirement for Master degree in Electronics/Telecommunications at the University of Gävle, Sweden.

First of all I would like to thank Allah Almighty for His blessings and love. I would like to express my sincere gratitude to my supervisors Dr. Jochen Christ and Dipl. –Ing. Mohammad Bashir for all their support, encouragement, valuable guidance, technical training, and inspirations throughout my project at the WISI Automotive. This work would not have been possible without their effort and support.

I would like to thank my academic advisor and examiner, Dr. José Chilo, for his kind guidance and support.

I would like to express my gratitude to all staff members at WISI Automotive for providing me with various supports, valuable talks and nice environments. I would like to express my appreciation to all of my friends for their encouragement, support and prayers.

Last but not least, I would like to express my deepest gratitude to my parents and family for their endless love, support, and encouragement throughout my life.

Table of contents

Abstract	iv
Acknowledgements	v
Table of contents	vi
List of Figures	viii
List of Abbreviations	x
1 Introduction	1
1.1 Background	1
1.2 Objective	2
1.3 Organization of the Report	3
2 Theory	4
2.1 Basic Antenna Theory	4
2.2 Antenna Parameters	4
2.2.1 Antenna Gain	4
2.2.2 Scattering Parameters	5
2.2.3 Polarization	5
2.2.4 Axial Ratio	6
2.2.5 Radiation Pattern	7
2.2.6 Physical Size & Construction	7
2.3 Automotive Antennas	7
2.4 Satellite Radio Services for Automotives	8
2.5 SDARS Antenna	9
3 Design and Results	11
3.1 Numerical Simulations	11
3.2 Measurement Setup	11
3.3 Antenna Mounting Positions in Car	12
3.3.1 Top Roof Position	13
3.3.2 Windscreen Position	13

3.3.3	Spoiler Position	14
3.4	Reference Antennas for the Measurements	14
3.5	Proposed Antenna Elements.....	15
3.5.1	Ring Antenna Design	16
3.5.2	Circular Microstrip Patch Design.....	16
3.5.3	Dielectric Resonator Antenna Design	17
3.6	Comparison & Analysis of Proposed Designs	18
3.7	Results of Dielectric Resonator Antenna	19
3.7.1	Return Loss of DRA.....	19
3.7.2	Axial Ratio of DRA.....	20
3.7.3	Effect of Parasitic Element.....	21
3.7.4	Optimization of the DRA	22
3.8	DRA Simulation Results	23
3.8.1	Roof Top Position	23
3.8.2	Windscreen Position.....	24
3.8.3	Spoiler Position	25
3.9	DRA Measurement Results	26
3.9.1	Roof Top Position	26
3.9.2	Windscreen Position.....	27
3.9.3	Spoiler Position	28
3.10	Discussion	29
4	Conclusions and Future Work.....	31
	References	32
	Appendix A: Measured reference antennas.....	A1
	Appendix B: Measured proposed antennas	B1
	Appendix C: Measure DRA in comparison to reference antenna	C1

List of Figures

- Fig. 1.1: SiriusXM gain requirements for SDARS antenna*
- Fig.1.2: MiDAS 3D far field Test Setup*
- Fig.1.3: Antenna mounting position (a) in car (b) Top roof position*
- Fig.1.4: windscreen position*
- Fig.1.5: Spoiler position.*
- Fig.1.6: Linearly polarized reference antenna*
- Fig.1.7: Circularly polarized reference antenna*
- Fig.1.8: Proposed designs (a) L-shaped patch antenna (b) Z-element (c) Single T-slot*
- Fig.1.9: Ring antenna (a) simulated design in cavity (b) ring element in space*
- Fig.1.10: Circular patch antenna (a) design in space (b) simulated design in cavity (c) feed network*
- Fig.1.11: Dielectric resonator antenna (DRA)*
- Fig.1.12: Simulated return loss of DRA*
- Fig.1.13: Measured return loss of DRA*
- Fig.1.14: Axial ratio of the simulated DRA*
- Fig.1.15: Axial ratio of the measured DRA*
- Fig.1.16: Measured effects of p-element on the DRA*
- Fig.1.17: Simulated design of the DRA in the top roof position*
- Fig.1.18: Simulated co-polarization of the DRA in the top roof position*
- Fig.1.19: Simulated design of the DRA in the windscreen position*
- Fig.1.20: Simulated co-polarization of the DRA in the windscreen position*
- Fig.1.21: Simulated design of the DRA in the spoiler position*
- Fig.1.22: Simulated co-polarization of the DRA in the spoiler position*
- Fig.1.23: Measured design of the DRA in the top roof position*
- Fig.1.24: Measured co-polarization of the DRA in the top roof position*
- Fig.1.25: Measured design of the DRA in the windscreen position*
- Fig.1.26: Measured co-polarization of the DRA in the windscreen position*
- Fig.1.27: Measured design of the DRA in the spoiler position*
- Fig.1.28: Measured co-polarization of the DRA in the spoiler position*
- Fig.1.29: Comparison of the measured co-polarizations of the DRA*

Figures from Appendix A: Measured reference antennas

- Fig.A.1: Measured LHCP for cross dipole at 2320 MHz*
- Fig.A.2: Measured vertical component of quarter wave monopole at 2320 MHz*

Figures from Appendix B: Measured proposed antennas

Fig.B.1: L-shaped patch measured design in windscreen car cavity

Fig.B.2: Measured Z-element design

Fig.B.3: Measured horizontal component of Z-element design

Fig.B.4: Measured T-slot element design

Fig.B.5: Measured vertical component of T-slot element design

Fig.B.6: Measured ring antenna design

Fig.B.7: Measured co-polarization of the ring antenna at 2320MHz

Fig.B.8: Measured circular patch antenna design

Fig.B.9: Measured co-polarization of the circular patch antenna

Figures from Appendix C: Measured DRA in comparison to reference antenna

Fig.C.1 Comparison of the measured reference antenna and DRA at Top roof position

Fig.C.2: Comparison of the measured reference antenna and DRA at windscreen position

Fig.C.3: Comparison of the measured reference antenna and DRA at spoiler position

List of Abbreviations

SDARS	Satellite Digital Audio Radio Service
DRA	Dielectric Resonator Antenna
LHCP	Left Hand Circular Polarized
RHCP	Right Hand Circular Polarized
LP	Linearly Polarized
GEO	Geosynchronous Earth Orbit
LEO	Low Earth Orbit
MEO	Medium Earth Orbit
LTE	Long Term Evolution
UMTS	Universal Mobile Telecommunication System
GSM	Global System of Mobiles
DAB	Digital Audio Broadcast
DVB	Digital Video Broadcast
WLAN	Wireless Local Area Network
GPS	Global Positioning System
FM	Frequency Modulated
AM	Amplitude Modulated
C2C	Car to Car Communication
VICS	Vehicle Information and Communication System

1 Introduction

Due to the increasing demand of infotainment and multimedia services with high performance in the daily life it also became field of interest for the automotive industry to bring the same services available for the car customers while driving on the road. To provide various high performance multimedia and infotainment services such as HD Audio/Video services, GPS, Cellular, SDARS, WLAN and Bluetooth within the car with least effects on the performance, weight, excellence and design of the car it became more challenging and important for the car manufacturers to design such innovative technologies.

Satellite Digital Audio Radio Service (SDARS) is a digital satellite radio service available in the content of USA and Canada provided by the SiriusXm. SDARS uses two GEO and three LEO satellites to provide its digital radio services with both high quality and large quantity. SDARS also provides some video channels along with large choice of audio radio channels. One of the potential customers for the SDARS is the automotive industry as the car customers desire to have high performance infotainment services available in the car.

To provide the satellite radio with in the cars is a big challenge due to the strict conditions for satellite signal availability, car performance issues and car body effects. Considering all these effects the car manufacturer demands for compact, lightweight and high gain SDARS antenna element.

1.1 Background

Automotive vehicles are increasingly being equipped with special electronic modules such as global positioning system, telematics and infotainments devices that require wireless data communications. One such system is SDARS which employs the wireless technology to provide satellite digital audio radio service. Antennas for SDARS should be able to receive an optimal satellite signal at particular elevation angles.

A lot of work is done to improve the performance and compactness of the SDARS antenna elements in past few years. Reference [1] describes an overview of SDARS automotive antennas available in the market. Different types of antenna elements such as microstrip patch, probe feed patch and ceramic patch antennas are in the market for SDARS applications. The different solutions available in literature are the quadrifilar antenna, as in [2], the standard dual polarized antennas, as in [3-7], or the low profile antenna, as in [8]).

Most of the antennas available in the field are complex and expensive which fulfils the version 1 of the SiriusXm gain requirements. However gain requirements are revised by the SiriusXm in version 2 with more strong gain requirements. In version 1 a maximum gain of 3dBi is acceptable but in version 2 it is required to have at least 4dBi gain at the particular elevation angles as shown in fig. 1.1. In this

work a newly developed antenna element is presented which fulfils the strong gain requirements at particular elevation angles according to the version 2 of SiriusXm.

1.2 Objective

There is a great desire for a low profile design or even hidden antenna system due to strict car design and weight limitations by the automotive industry. For the time being there are strong recommendations for a top roof mounting location of a SDARS-antenna in order to meet the required radiation pattern on a vehicle. For many vehicle models this location is considered as inconvenient and there is a strong demand to design more inconspicuous (not clearly visible) antennas.

The objective of this work is to develop a compact new integrated SDARS antenna element which fulfils the new SiriusXm gain requirements for better reception of the satellite signal. Main requirements for the developed SDARS element are

- At least 4dBi gain in the elevation angle of 50 to 70 degrees as shown in the figure 1.1.
- Left hand circularly polarized (LHCP) omni directional radiation pattern in the complete azimuth
- Compact with the maximum dimensions of 40*40*20 mm³, cost effective and easy to design
- Single feed SDARS antenna element
- Typical return loss ≤ -10 dB and axial ratio ≤ 3 dB

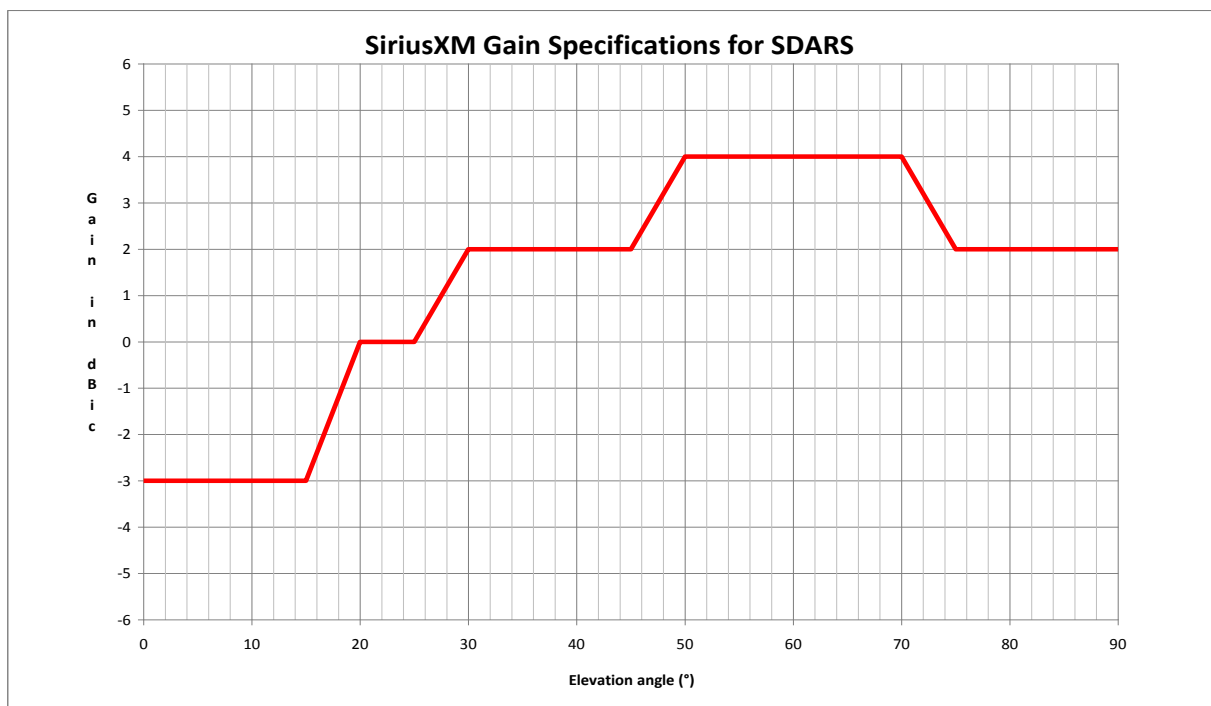


Fig. 1.1: SiriusXm gain requirements for SDARS antenna.

1.3 Organization of the Report

The project report is organized as follows:

Chapter 2: Theory An introduction to the basic antenna theory related to the project work is given in this chapter. A brief description of the automotive and SDARS antenna element and its important requirements mandatory for its application in the automotive industry is given in the chapter.

Chapter 3: Design and Results a detailed description of the different proposed antenna designs is given here including their simulation and measurement results. A comparison with the finally selected SDARS antenna element with a detailed presentation and analysis of the finally developed SDARS antenna element. Finally a brief discussion summarizes the results obtained during the project work for DRA.

Chapter 4: Conclusions and Future Work to summarize the work carried out in this report a conclusion is given here along with some possible future work related to the project.

2 Theory

Selection of a suitable antenna element is the first and most important task for the development of an antenna design. In this chapter the theoretical part of the project is presented in detail which is latter implemented to complete the project.

2.1 Basic Antenna Theory

A device which can transmit and receive electromagnetic waves can be defined as an antenna. In an antenna, the direction of radiated power focuses on itself structure or shape. Like a dipole antenna has the properties of omni directional antenna in the azimuth. However, a horn antenna only has a dominated directional radiated power when it is working [9].

Antennas are widely used in radio frequency range as a key component of radio communication system. There many different types of antennas depending on their electrical characteristics, shape, size such as monopole, dipole, parabolic, micro strip , dielectric resonators, PIFA, yagi etc.

2.2 Antenna Parameters

Antenna performance varies depending on the geometry, physical size, environment and electrical characteristics of the antenna. Some important antenna parameters, which define the electrical characteristics of the antenna, such as antenna gain, s-parameters, polarization and radiation pattern are discussed below.

2.2.1 Antenna Gain

The gain of the antenna can be defined as “the ratio of the radiation intensity in a given direction to the accepted radiation intensity being radiated from the source in homogenously in all directions”. Gain can be calculated by the following equation

$$G(\theta, \Phi) = 4\pi \frac{U(\theta, \Phi)}{P_{in}} \quad (\text{dimensionless}) \quad (1)$$

Here $G(\theta, \Phi)$ = Gain in θ and Φ directions

$U(\theta, \Phi)$ = Radiation intensity in θ and Φ directions

P_{in} = Total input (accepted) power

Antenna gain can also be defined in terms of directivity and the antenna efficiency.

$$G(\theta, \Phi) = k \cdot D(\theta, \Phi) \text{ (dimensionless)} \quad (2)$$

Here $D(\theta, \Phi)$ is the directivity, a measure of radiation intensity in a particular direction, and k ($0 \leq k \leq 1$) is the efficiency factor of the antenna. If the antenna efficiency is less than 100 percent, the gain is less than the directivity. The antenna efficiency depends on the ohmic losses of the antenna, which are due to the non-radiated power of the antenna causing increase in temperature of the antenna structure [10].

2.2.2 Scattering Parameters

For every antenna design scattering parameter is the most important parameter to analyse and compare the performance of the designed antenna. Scattering parameters provides the information for the resonating frequency, bandwidth, impedance match, power transmitted & reflected and coupling effects between the ports. In the thesis work most important S-parameter is S_{11} also called return loss. The return loss of antenna gives the information that how much of the incident power is reflected instead of being transmitted [11]. In the presented work S_{11} is measured in dB. A lower value of S_{11} means most of the input power is transmitted through the network that is antenna and the feed network is well matched. For example if $S_{11} = -10\text{dB}$, it means that 90 percent of the incident power will be transmitted through the network. It is defined as

$$|S_{11}|_{\text{dB}} = 20\log|\Gamma| \quad (3)$$

Where
$$|\Gamma| = \frac{SWR - 1}{SWR + 1} \quad (4)$$

Here Γ = reflection coefficient

S_{11} = return loss

SWR = standing wave ratio

In this project a typical value of the return loss (S_{11}) of -10dB needs to be maintained for the whole operating frequency band of 25MHz.

2.2.3 Polarization

Polarization of the plane wave refers to the orientation of the electric field vector, which may be in a fixed direction or may change with time [12]. The polarization of an antenna is defined as the polarization of the wave radiated when the antenna is excited, or the polarization of an incident wave

which results in maximum available power at the antenna. Polarization of a wave can be classified into linear, circular and elliptically polarized waves.

Linear polarization is obtained if the field vector (electric or magnetic) possesses only one component or two orthogonal linear components that are out of phase by 180° . Linearly polarized wave has either vertical (E_θ) or horizontal (E_ϕ) component of the field vector [12].

Circular polarization occurs when the two linear orthogonal components have equal magnitude and the time-phase difference between them is odd multiples of $\pi/2$. If the magnitudes are different, elliptical polarization is obtained. Clock wise rotation of the field vector is designated as the right hand circularly polarized (RHCP) wave and counter clock wise rotation of the field vector as left hand circularly polarized wave (LHCP). Left and right hand field components can be calculated from the tangential components as follows [13]

$$E_{\text{left}} = \frac{1}{\sqrt{2}} (E_\theta - i E_\phi) \quad (5)$$

$$E_{\text{right}} = \frac{1}{\sqrt{2}} (E_\theta + i E_\phi) \quad (6)$$

Here

E_{left} = Left hand circularly polarized field component

E_{right} = Right hand circularly polarized field component

E_θ = Vertical field component

E_ϕ = Horizontal field component

2.2.4 Axial Ratio

The axial ratio is the ratio of orthogonal components (horizontal and vertical) of an E-field. The axial ratio for an ellipse is larger than 1 (>0 dB). The axial ratio for pure linear polarization is infinite, because the orthogonal components of the field are zero.

An ideal circularly polarized antenna means equal magnitude of the orthogonal horizontal and vertical components and so the axial ratio is 1 (or 0 dB). In addition, the axial ratio tends to degrade away from the main beam of an antenna. As the designed antenna is circularly polarized so axial ratio is an important parameter to measure the circularity of the antenna. An axial ratio of at least 3dB is desired in the main beam direction of the designed SDARS antenna. Axial ratio can be calculated by the following formula

$$\text{XPD} = 20 \log \left(\frac{A.R+1}{A.R-1} \right) \text{ dB} \quad (7)$$

Where

A.R= axial ratio (linear)

XPD= cross polarization discrimination

2.2.5 Radiation Pattern

The radiation pattern of an antenna is a plot of the magnitude of the far-zone field strength versus position around the antenna, at a fixed distance from the antenna [14].

The antenna radiation patterns can be either plotted for the elevation plane ' θ ' or for the azimuth plane ' Φ '. Typically radiation patterns are measured in two dimensional and three dimensional graphs which show the generated field strengths away from antenna at a certain distance. Spherical (r, θ, Φ), polar (r, Φ) or (r, θ) and rectilinear (x, y) coordinate system are used to represent radiation pattern of the antennas. Radiation patterns generated by the antenna mainly depends on the geometry, material, physical size and its electrical characteristics. Antennas have isotropic, directional, omnidirectional radiation patterns.

2.2.6 Physical Size & Construction

Physical size and the construction of the antenna is one of the important parameters which effects the electrical characteristics and performance of the antenna. Size of the antenna mainly depends on the operating frequency. Normally at higher frequencies due to small wavelength size of the antenna decreases and vice versa. Antennas can be constructed in many different ways e.g. simple wire antennas, patch antennas, micro strip antennas, reflector antennas, aperture antennas, horn antennas etc. When considering antennas suitable at 2.320 GHz ($\lambda \approx 129\text{mm}$) frequency for the SDARS application a compact and light weight antenna is desired with high gain.

2.3 Automotive Antennas

The mobility by vehicles is indispensable for our personal lives as well as business activities. There have been strong requirements of safety, comfortable time & space, and convenience for the mobility by vehicles.

Initially AM radio reception was only available in vehicles. Several systems for these requirements have been gradually installed into vehicles with the growth of wireless technologies [15], [16]. FM radio and television (TV) programs can be currently received in vehicles by FM/AM, SDARS, DAB, DVB etc. Drivers can achieve information of own positions by Global Positioning Systems (GPS) and congestion information by Vehicle Information and Communication systems (VICS). Telephone can be used in vehicle and Bluetooth helps links between mobile terminals of driver and vehicle terminals. Laser radars and millimeter-wave radars have been installed as forward looking sensors [17].

Automotive antenna design technique is one of the key techniques to contribute the system realization very much. Automotive antennas generally need simple architectures and low cost due to consumer products, and compactness or low profile due to limited installation spaces of vehicle. Also, inclusion

of the vehicle body into the antenna design is needed, when antenna performance is strongly affected by the vehicle body.

The frequency bands used in automotive wireless systems range widely from AM band to the millimetre-wave band. The different frequency bands result in the different problems and difficulties of the development of antennas. The establishment of automotive antenna design techniques is needed in wide frequency range.

2.4 Satellite Radio Services for Automotives

With the increasing demand for connectivity anywhere and anytime, the satellite services market is contributing to improve the available services to the automotive market. The main automotive and mobile technologies today available, or under development, through the satellite providers are using L and S band, and are able to provide satellite internet access, satellite phone, satellite radio, satellite television and satellite navigation.

While different satellite services are used to deliver the mentioned technologies to end users, the following table 1 depicts some of the main services used for automotive, nautical or air markets in L/S band [18].

Table 1: satellite technologies used in the automotive market [18]

Service	Operating frequency	Polarization	Orbit
Thuraya or Inmarsat BGAN	Downlink: 1525 to 1560 MHz; Uplink: 1625 to 1660 MHz	Dual switchable SAT (LHCP or RHCP)	GEO (Geosynchronous orbit)
Global Navigation Satellite Systems (i.e. GPS and Galileo)	Downlink: 1575 MHz	RHCP	MEO (Medium earth orbit)
Iridium	Uplink /Downlink: 1610 to 1626 MHz	RHCP	LEO (Low earth orbit)
Globalstar	Downlink: 1610 to 1626 MHz. Downlink: 2484 to 2499 MHz	LHCP	LEO
DVB-SH	Downlink: 2170 to 2200	Dual switchable SAT	GEO

	MHz; Uplink: 1980 to 2010 MHz	(LHCP or RHCP) and TER (LP)	
SDARS	Downlink:2320 to 2345 MHz	Dual SAT (LHCP) and TER (LP)	GEO, LEO

The data in the table show the frequencies used for each service, specifying the transmission from earth to satellite (uplink) and the transmission from satellite to earth (downlink) bands. For each service the polarizations required by the antenna specifications is specified, discriminating between the LHCP (Left Hand Circular Polarization), the RHCP (Right Hand Circular Polarization) and the LP (Linear Polarization).

2.5 SDARS Antenna

SDARS (satellite digital audio radio service) is a satellite service used to provide digital radio to end users. Starting from its first requirements release ([19] [20]), it was underlined that the circularly polarized satellite signal should reach the users in the open areas, being further supported by terrestrial transmitters providing the necessary coverage especially in the urban environment, where the satellite signal could be obstructed by buildings or other constructions.

Since several years, SDARS is available in USA and Canada [21], and the service is in operation in the S-band (from 2320 to 2345 MHz), employing dual transmission broadcast format: LHCP signals provided by satellites and LP signals radiated by terrestrial stations. Currently SiriusXm is using a network of five satellites including two GEO and three LEO satellites. GEO is a very common Geosynchronous orbit at the altitude of 35,786km from the Earth whereas LEO is a small low earth orbit with an altitude less than 2000km above the Earth [14]. The network of the satellites operates in such a way that for complete 24 hours of the day, at least one satellite is visible to the SDARS receiver antennas. Unlike global positioning system (GPS) which has a large network of satellites with at least satellite availability of 5 to 6 at a time for its customers. SDARS network of satellite can provide about 2 to 3 satellites in most of the time in a day except a small interval of time when only one satellite is visible to the SDARS receivers. This is why SDARS antenna needs strict gain requirements for high performance and to provide the satellite digital radio service available every time for the users.

Operating satellite system by SiriusXm, for SDARS, uses right hand circularly polarized (RHCP) antenna for the uplink communications whereas for the downlink communications SDARS antenna element uses left hand circularly polarized (LHCP) radiation pattern. To enhance the reliability, overall throughput of the system and performance circularly polarized antennas are required.

The automotive SDARS antennas implement such as dual polarized system either with two separate antennas (dual–arm solution), one optimized for the LP terrestrial reception and the other for the LHCP satellite one; or with a single antenna (single-arm solution) receiving both signals. However now a days antenna element for satellite communication is main topic of interest in SDARS application due to its high performance, quality and complexity instead of terrestrial antenna.

3 Design and Results

An overview of the measurement and simulation tools is given in the beginning in the chapter. Some important proposed antenna elements and their performance issues are discussed in detail here. A comparison of the proposed designs is given and finally the simulation and measurement results for the best selected design are analysed and discussed in detail.

3.1 Numerical Simulations

Computer simulation technology (CST) provides the 3D electromagnetic field simulation tool CST Microwave Studio (MWS). A full-wave electromagnetic field simulator such as CST models and computes the interaction of electromagnetic fields with the physical object and environment. The software efficiently uses Maxwell's equations to calculate antenna performance, electromagnetic compatibility, radar cross section and electromagnetic wave propagation, etc. [13]. It offers the different solvers such as Time and Frequency domain solvers.

In the presented work CST MWS is used for the numerical simulations of the designed antenna elements. Broadband calculations for operating frequency, S-parameters and the radiation patterns were analysed and optimized by CST MWS. CST MWS gives the possibility to optimize the design for the defined goals or optimize and analyse the individual design parameter by setting parameter sweep. Both tools parameter sweep and optimization tool, in CST MWS, are efficiently used throughout the project work for the in depth analysis of the designed antenna models. All simulated results were well verified by the real time measurements of the prototypes.

3.2 Measurement Setup

MiDAS 4.1 system by Orbit/FR is used for the real time 3D far field radiation pattern measurements of the designed antennas. MiDAS system has the capability to measure real time 3D, 2D and 1D far field radiation patterns for the antenna elements. It has the capability to measure vertical, horizontal and circularly polarized (LHCP, RHCP) antenna elements. By control module of the MiDAS system the test antenna can be rotated in the six different axes. In the measurement scenario test antenna is placed about 20m away and 7m high from the transmit antenna as shown in fig. 1.2. Transmit antenna has the capability to transmit circular (LHCP, RHCP) and linearly (Horizontal, Vertical) polarized waves within a frequency range of 1 to 18 GHz [17]. Transmit antenna throughout the measurements, remain fixed at the lower end directed towards the receiver. Before the measurement starts transmit and receive antennas are aligned in their LOS and then control

module automatically adjusts the position of the test antenna to -90 degrees. It is possible to control the rotation and movement of the axes either manually or automatically.

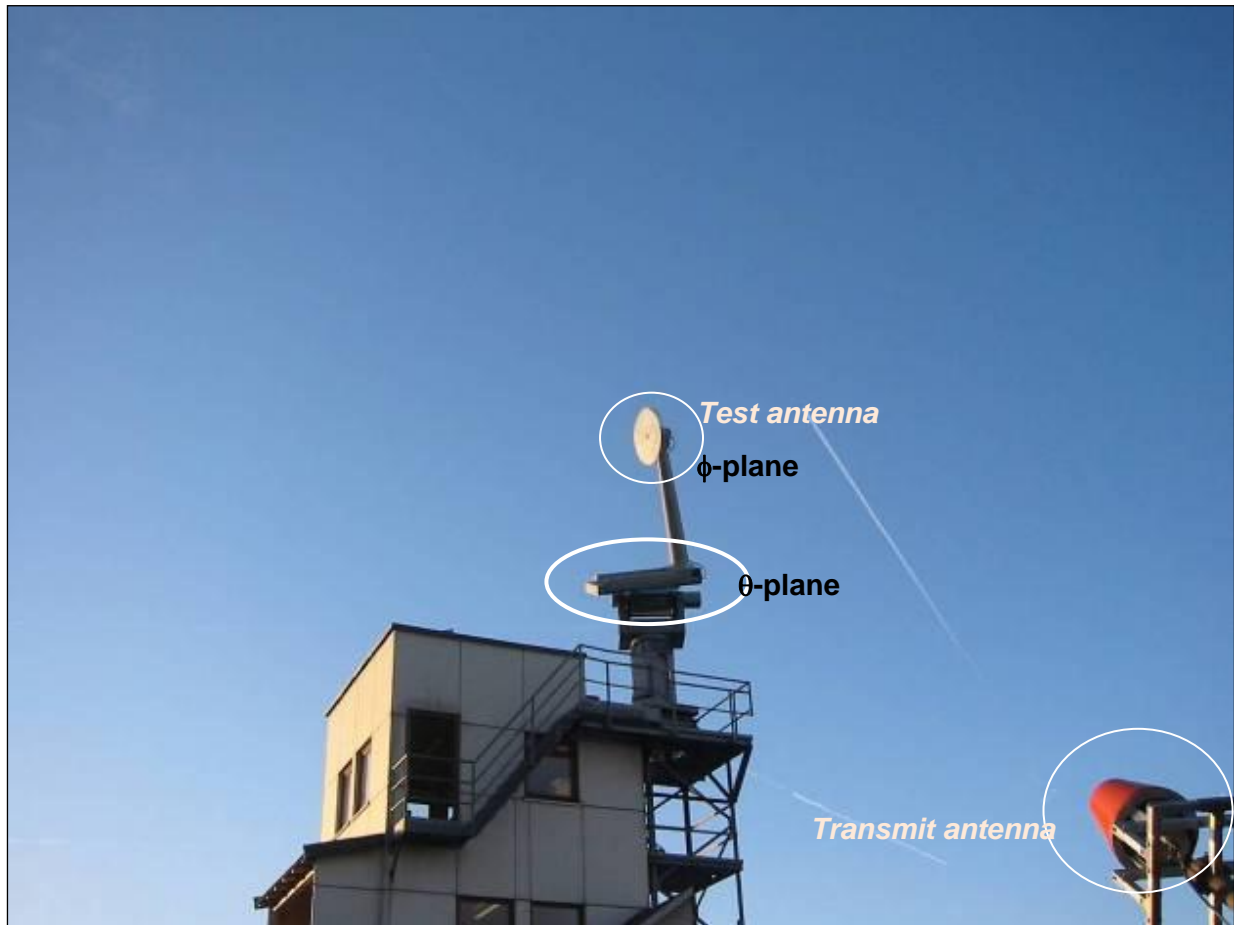


Fig.1.2: MiDAS 3D far field test setup

MiDAS system calculates the receive power (dBm) by rotating the test antenna from -90 degrees to +90 degrees with the step of 5 degrees on axis 3 (elevation plane). On each 5 degree step the test antenna is rotated about its axis 4 (phi-plane) by 360 degrees. To measure more accurate and detailed radiation patterns, the step on the elevation plane can be reduced to 1 degree. In these measurements hemispherical 3D radiation pattern is obtained for the test antenna which gives the information for the received signal power at the test antenna.

3.3 Antenna Mounting Positions in Car

Most challenging task of this project is to make a compact SDARS antenna element which fits well into the small space of the car mounting position. There are many different antenna mounting positions in the car for different antenna services as shown in fig. 1.3(a). However for the SDARS element the desired mounting positions are 7, 4 and 3 as shown in fig. 1.3(a).

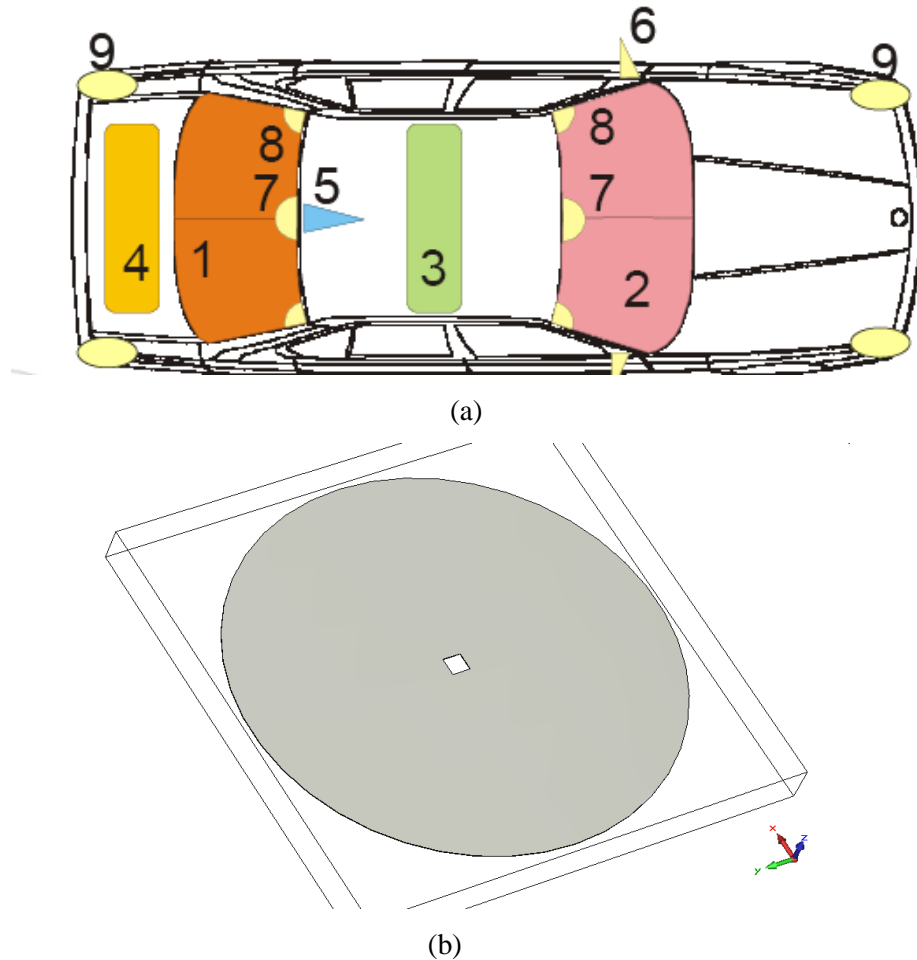


Fig.1.3: Antenna mounting position (a) in car (b) Top roof position.

3.3.1 Top Roof Position

Third possible position for mounting the SDARS antenna element in the car is at top roof as shown in figure 1.3(b). This position is the most suitable place for mounting the antenna element on the car to get best possible quality of receive signal. It is because at the top roof, antenna element has no cavity and no edges near to it also a big ground plane is available around the antenna by the metal roof of the car. In this position the available cavity dimension is $50*50*20 \text{ mm}^3$.

3.3.2 Windscreen Position

The most desired mounting position was just below the wind screen, inside the car. At this position maximum possible space for the complete SDARS antenna element is $41*42*20 \text{ mm}^3$ with a tilt of 10 degree towards the driving direction. In this position distance between the wind screen glass and the antenna mounting position is only 5.6mm. To avoid wind screen glass of the car and its effects on the antenna performance, at maximum the antenna element is allowed to have only 2.5mm space out of the cavity. The car cavity for this position is shown in figure 1.4. In this project work windscreen position is considered initially for the antenna measurements due to its strong requirement and effects

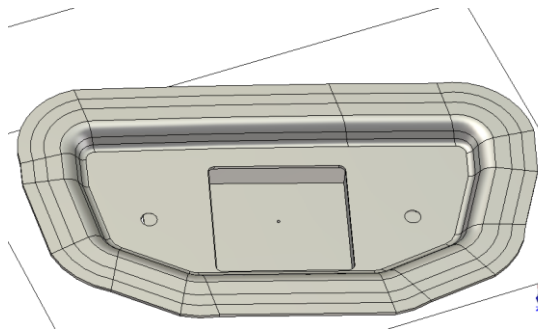


Fig.1.4: windscreen position

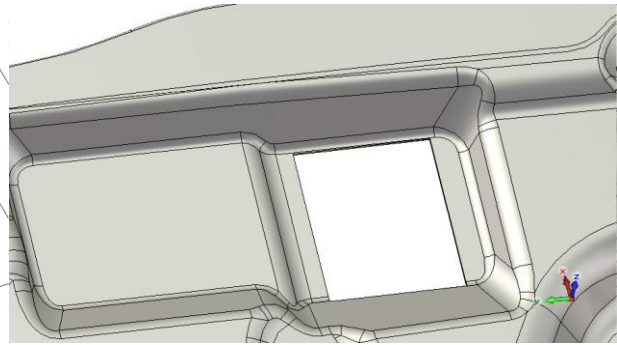


Fig.1.5: Spoiler position.

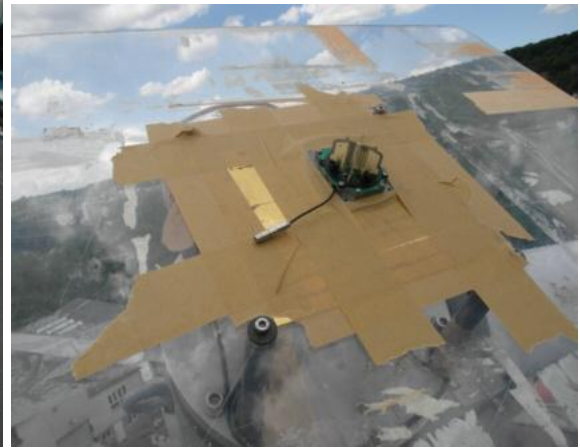
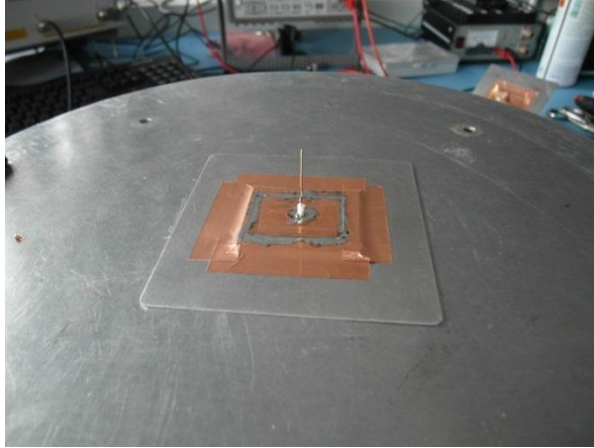


Fig.1.6: Linearly polarized reference antenna Fig.1.7: Circularly polarized reference antenna
on the antenna performance.

3.3.3 Spoiler Position

Second position for the antenna mounting is in the spoiler of the car as shown in the figure 1.5. The spoiler has no cavity but there are high edges of about 7mm quite near to the antenna element which can affect the performance of the element. As compare to the wind screen position, spoiler position has no deep cavity however the surface around the antenna is not smooth, unparallelled with edges and holes near to antenna element which affects a lot the performance of the antenna. The available space for antenna element in the spoiler is limited to $55*60*20 \text{ mm}^3$.

3.4 Reference Antennas for the Measurements

All proposed antennas were manufactured and measured antennas and compared with the reference antenna to analyse and optimize the performance of the antenna. It is required to make a left hand circularly polarized antenna element. So a LHCP cross dipole reference antenna, see fig. 1.7, is used during the measurements of all circularly polarized antennas. However for the linearly polarized antenna elements a primitive quarter wave monopole is used as shown in figure 1.6.

During all measurements the reference antenna is placed on a 1m circular ground plane without car cavity. However the test antennas are measured in the three different car positions. As all measurements during this project were done in an open air environment so for each test antenna measurement, reference antenna is measured in the same weather environment to make exact comparison. At 2320MHz 3D far field radiation patterns for the reference antennas were measured, see Appendix A.

3.5 Proposed Antenna Elements

During the project work different antenna elements such as cross dipole, PIFA, patch antennas, ring antenna, dielectric resonator antennas etc. were designed for the required objectives. Few important designs are discussed in this report. Following designs were simulated and measured with the prototype design. Finally by comparison the best suitable design was selected. Mainly radiation pattern, circularity and gain of the proposed designs were focused for the initial results which are presented here. Manufactured prototypes of the proposed designs and their measured results with SDARS gain specifications are shown in Appendix B.

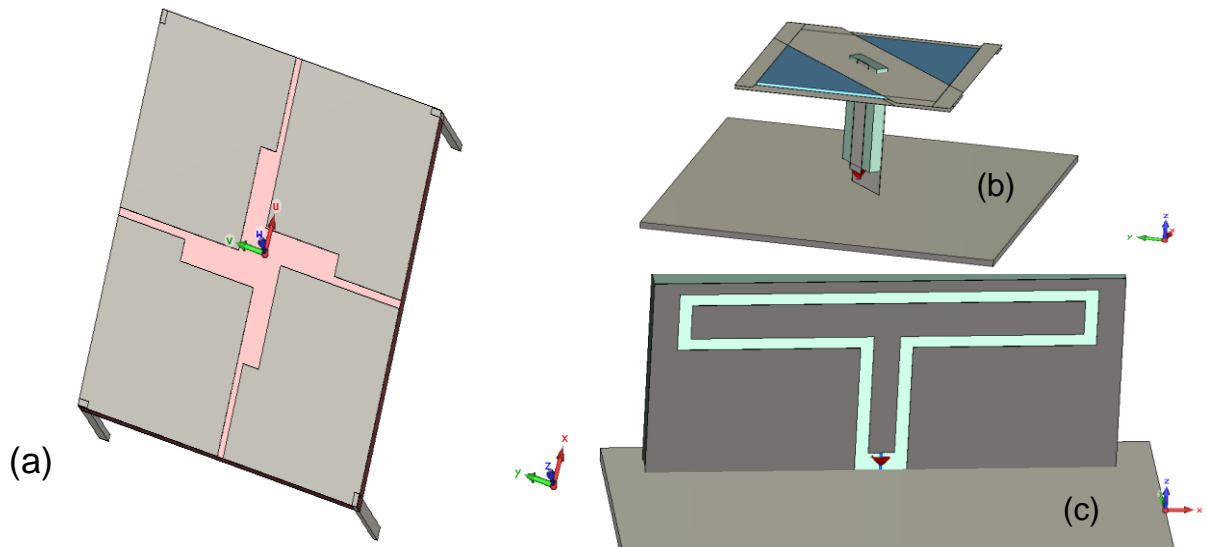


Fig.1.8: Proposed designs (a) L-shaped patch antenna (b) Z-element (c) single T-slot

Initially L-shaped patch design shown in fig. 1.8 (a) is tested and verified by the MiDAS system.

However the simulated and measured results for L-shape patch design has shown that the design does not fulfil the SiriusXm gain requirements.

Another design with a Z-element surrounded by four T-slots is simulated and tested. The simulation results fulfils the requirement however the measured design for the T-slot has less as compare to the simulated result. Also the complete design is complex to manufacture with five ports which also makes this design expensive.

3.5.1 Ring Antenna Design

The proposed design is a primitive circularly polarized ring antenna element as shown in fig. 1.9. The designed ring element has 19mm of outer radius with 2mm height from the ground plane. The ring element is 5mm high and 1mm thick. It has two ports at an angular distance of 90 degrees. All the simulated and measured results presented for the DRA element are at 2320MHz.

The designed ring gives a good circular polarized radiation with good impedance match. The radiation pattern has maxima at null position with a gain of 7dBi in the simulated design. However the measured ring element has good gain but the beam width is not wide as in the simulated results. It is possible to obtain right hand circular polarized or left hand circular polarized just by changing the order in the phase shift of the ports.

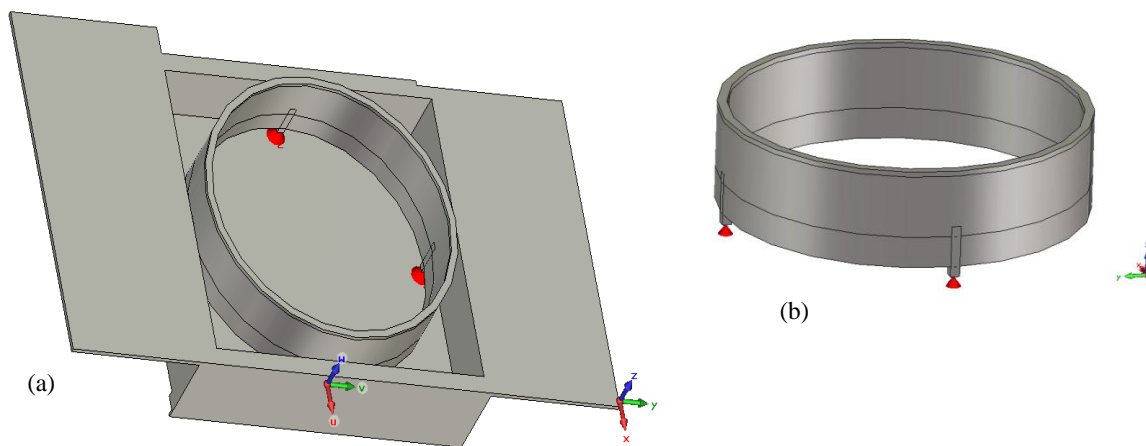


Fig.1.9: Ring antenna (a) simulated design in cavity (b) ring element in space

3.5.2 Circular Microstrip Patch Design

The four-port circular micro strip patch antenna is a simple patch antenna with compact dimensions as shown in fig. 1.10. The designed antenna has a circular patch on FR4 substrate of $\epsilon_r = 4.5$. The outer radius of the circular patch is 17mm whereas the inner radius is 12mm. The structure of the antenna is made on the substrate of the AD1000 Arlon which has the $\epsilon_r = 10$.

The overall thickness of the antenna is about 4mm. A feeding network for four ports is designed using CST Design Studio and Ansoft Designer which is manufactured on FR4 as shown in Appendix B. The benefit of this design is its compact thickness of 4mm. The antenna element can be placed out of the cavity when mounting in wind screen position of the car where 2.5mm space is available out of cavity. In this situation the antenna has a good performance with a ground plane of 1m².

The designed antenna has a gain of more than 5dBi with a good impedance match in the simulated design. The designed antenna becomes non-symmetric with a small ground plan along with cavity. It is because of the high edges near the antenna. Measured results of the circular patch

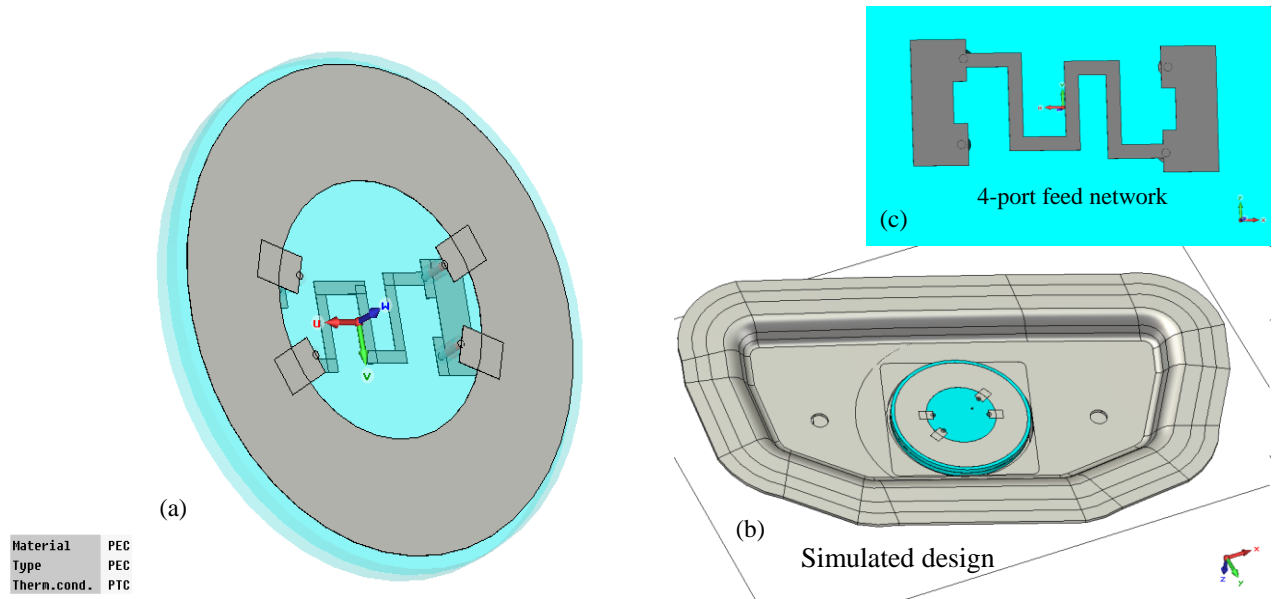


Fig.1.10: Circular patch antenna (a) design in space (b) simulated design in cavity (c) feed network element are not good. It has low gain with high axial ratio. However the antenna element can be improved by the further optimization of the antenna parameters and the feeding network.

3.5.3 Dielectric Resonator Antenna Design

Dielectric resonator antenna (DRA) is a two port cylindrical element with a radius of 13mm and height of 10mm. Two metal strips are used with the width of 1mm and height of 9mm spaced with 90 degree angular distance around the DRA as shown in the fig. 1.11. DRA element has broad beam and strong circularity with a gain more than 6dBi. Due to cavity walls in the mounting position the DRA had reduced a little its performance. To remove the wall effects a parasitic element 1mm above the DRA is used which improves the radiation pattern. Detailed result and analysis for the DRA element are presented later in the chapter.

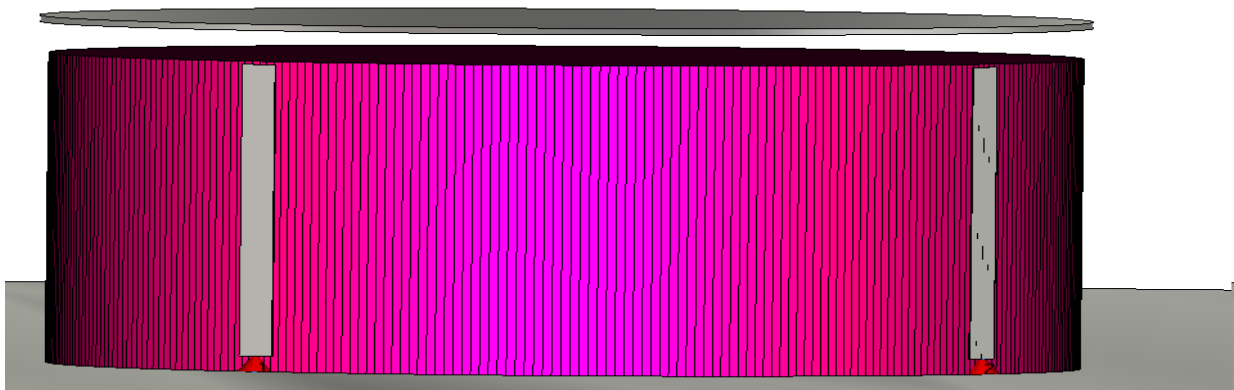


Fig.1.11: Dielectric resonator antenna (DRA)

3.6 Comparison & Analysis of Proposed Designs

The proposed antenna elements were finally analysed & discussed to select the best possible solution considering the performance, compactness, ease of manufacturing and cost effectiveness of the design. As discussed before L-shaped patch element is not a good solution because it is much sensitive to the walls of the car cavity. Also the design does not fulfil the gain requirements in all directions of the azimuth both in simulation and measured results.

The second design consisting of separate horizontal and vertical components performs quite good in the simulations and full fills the requirements. However the measured design is not satisfying the simulated results. Measured z-element has quite good resemblance to the simulated results but the measured T-slots element has about 2dB less gain than the simulated design. With some optimization the performance of the T-slot element can be improved but on the other hand the proposed design is non-compact, difficult to manufacture and also expensive.

Another design was a primitive ring element which is circularly polarized with a peak gain of 7Bi at the null position. The ring element fulfils the requirements in the simulated design but the manufactured design has less broad beam radiation pattern.

A compact design of four port circular patch element is tested which fulfils the requirements on the big ground plane. However the design does not give good performance with the decreased ground plane. Another disadvantage of the design is four ports and the design does not perform well with the four port network. However with optimization the design can be improved.

Dielectric resonator antenna (DRA) which is quite simple to manufacture and also has quite broad beam radiation pattern is a good solution to the SDARS applications. The measured DRA element has shown the similar results as obtained in the simulated design. Latter a parasitic element is introduced which helps to keep the radiation pattern of DRA symmetric within the car cavity. The parasitic element is also helpful to improve the broadness of the beam and the resonant frequency of the DRA can also be adjusted up to 350MHz by changing the size, thickness and height of the parasitic element. It is observed from the results the measured DRA element fulfils the SiriusXm gain requirements.

So finally the dielectric resonator antenna (DRA) element with the parasitic element is selected due to its high sustained performance within the car, simplicity and compactness. The DRA fulfils the gain requirements of the SiriusXm in the car cavity.

Table 2: A comparison of the proposed antenna designs

Proposed Antenna	Gain [dBi]	Return loss [dB]	Axial Ratio [dB]	Physical Size [mm]
L-shaped patch	3.5	-12	7	39*39*11(l*w*h)
Z-element with T-slots	4.67	-10	6	20*20*20(l*w*h)

Ring	7	-14	4	36*9 (diameter*height)
Circular patch	5.53	-5	6	40*3.5(diameter*height)
DRA	6.8	-33	Less than 3	26*10(diameter*height)

3.7 Results of Dielectric Resonator Antenna

The designed and measured results for the dielectric resonator antenna are presented in the following subsections. Effect of the different parameters of DRA on the performance of DRA are presented and discussed in detail here.

3.7.1 Return Loss of DRA

Dielectric resonator antenna is designed for the desired SDARS frequency range (2320-2345MHz). The designed DRA shows high impedance match both in simulation and measured results, see fig. 1.120 and 1.31. As can be seen that a -19.6dB of return loss is measured for the designed DRA with an overall value of at least -17dB over the whole 25MHz frequency band.

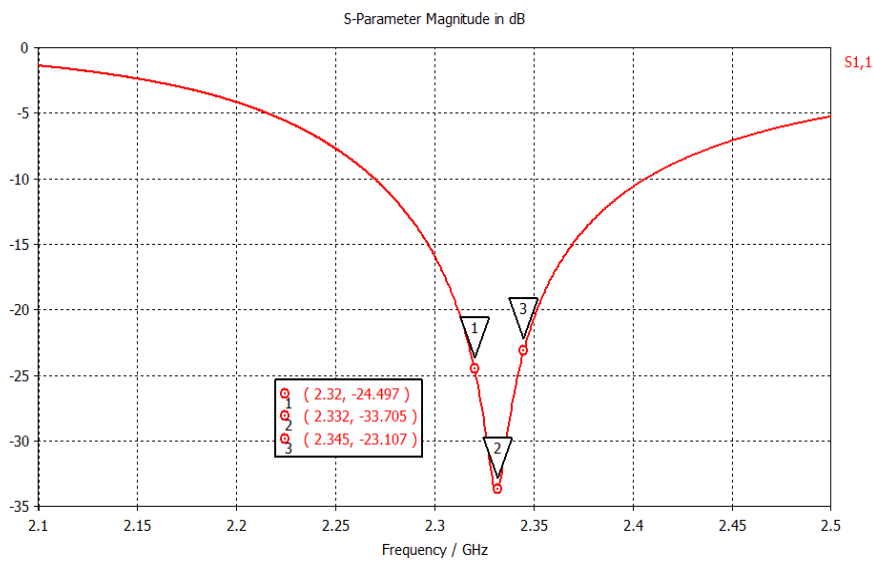


Fig.1.12: Simulated return loss of DRA

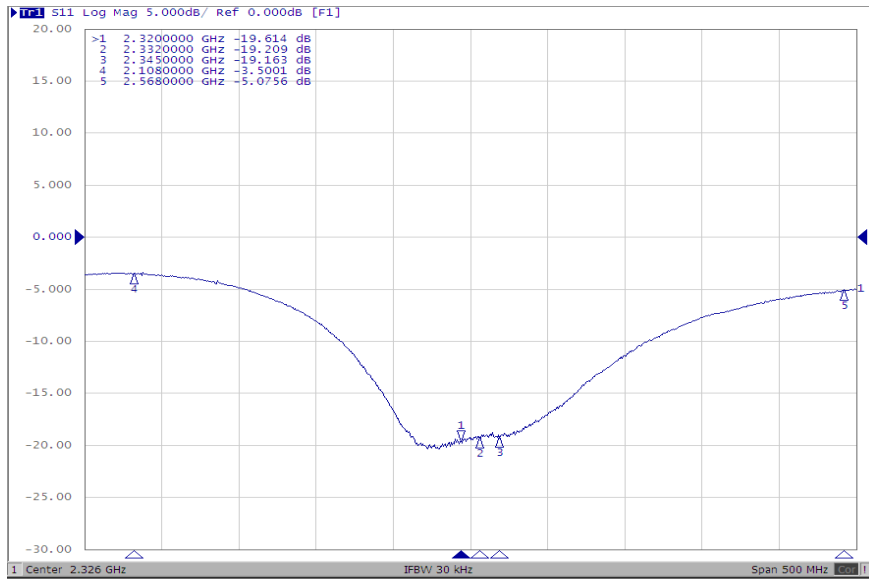


Fig.1.13: Measured return loss of DRA

3.7.2 Axial Ratio of DRA

In all simulated and measured designs about 10dB difference between the cross and co-polarizations is obtained, at the peak gain position. Therefore an axial ratio of less than 3dB is achieved on the peak gain position of the DRA as shown in fig. 1.14 and fig. 1.15. For the measured DRA element, axial ratio is obtained using the eq. 4, by using the measured difference between the cross and co-polarizations of DRA.

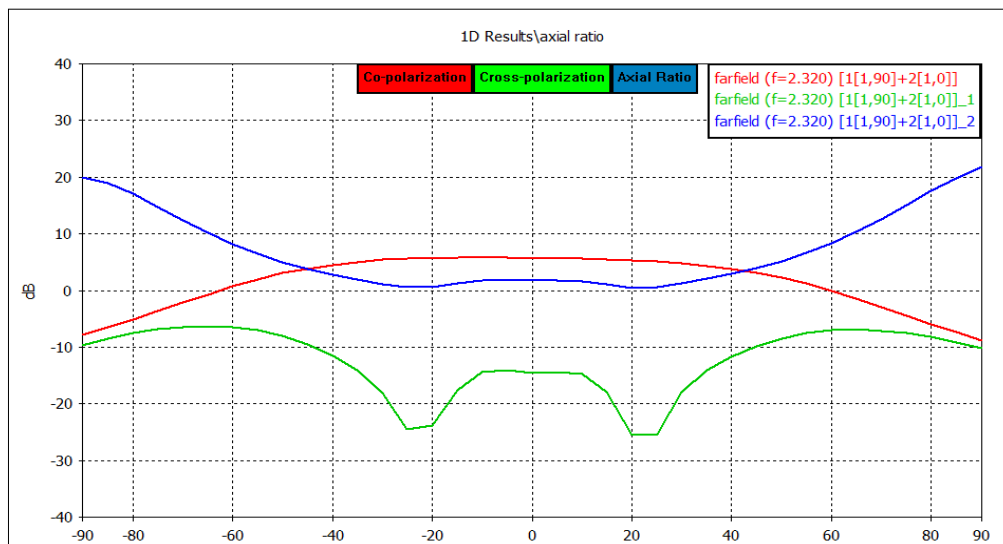


Fig.1.14: Axial ratio of the simulated DRA

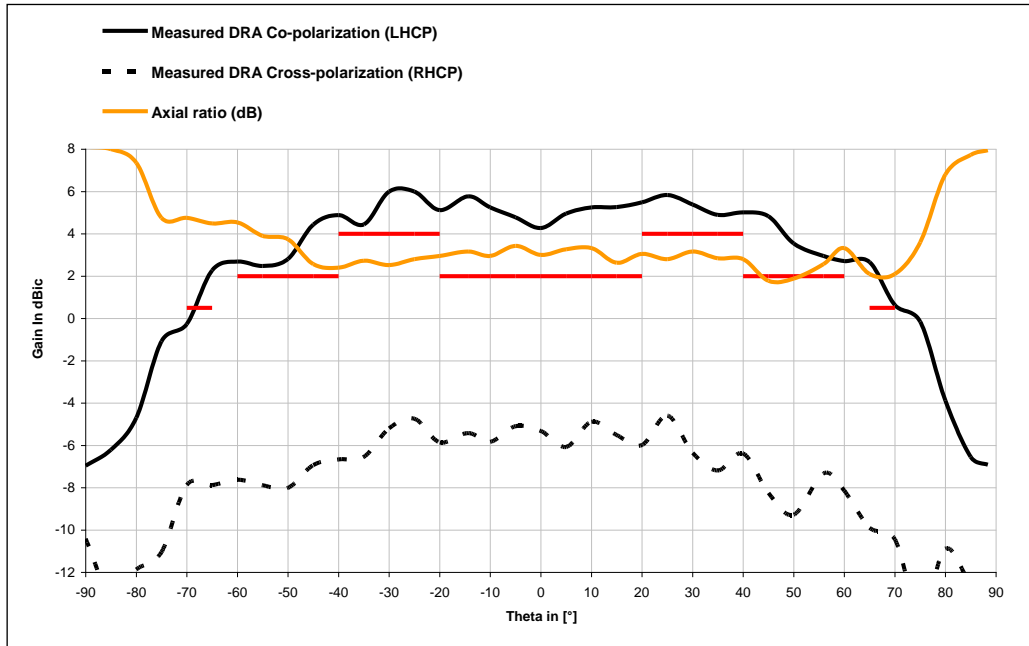


Fig.1.15: Axial ratio of the measured DRA

3.7.3 Effect of Parasitic Element

DRA has very good performance on the 1m ground plane but when the DRA is put into the car cavity it reduces its gain and also axial ratio increases. So to reduce the cavity effects a circular parasitic element above the DRA is placed. There is a significant influence on the DRA performance due to the parasitic element. By changing the size of the p-element it is observed that the resonant frequency of DRA can be adjusted up to 350MHz. It is observed that for 1mm change in the radius of circular p-element the resonant frequency of the DRA shifts by about 25MHz. By changing the thickness of the parasitic element the resonant shifts about 10MHz and the gain of the DRA also changes. If the distance between the DRA and parasitic element is increased the beam broadness and circularity of the antenna is disturbed with a small shift of frequency.

The highest performance with a broad beam, at the operating frequency of 2320MHz, is achieved by placing p-element of diameter 26mm and 0.2mm thickness 1mm above the DRA.

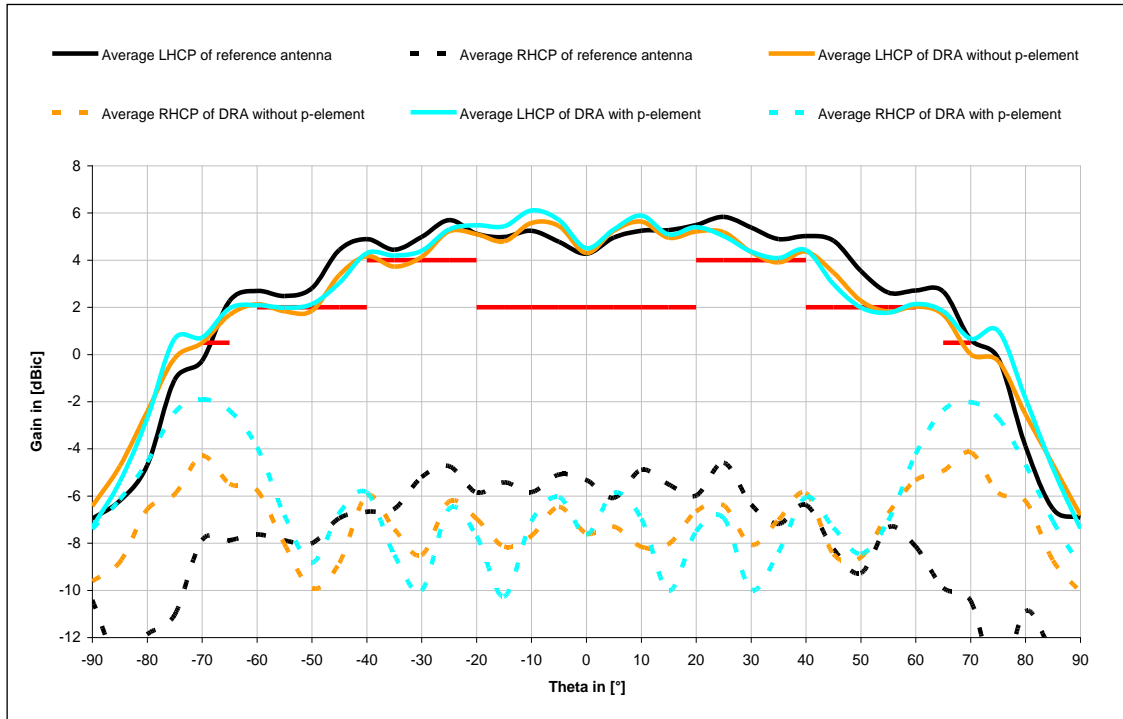


Fig.1.16: Measured effects of *p*-element on the DRA

3.7.4 Optimization of the DRA

The designed DRA element is optimized by changing all possible parameters. As the car cavity is very small so all proposed elements had so much effect of the cavity walls and edges. For the DRA element much less effects are observed and DRA sustained its good performance even in the cavity. It is because of the strong concentrated fields around the DRA element. It is observed that the resonating frequency of the DRA can be adjusted by changing the permittivity, height, diameter and the parasitic element. There is not much effect on frequency due to the two feeding strips.

It is seen the DRA radiation pattern gets broader if the parasitic element is placed parallel to the car cavity hole. Also the circularity of the DRA increases in this case.

The feeding network of the DRA gives the possibility to switch the polarity of the antenna from left hand circular polarization to right hand circular polarization if the order of the phase shift between the ports is changed. It is also observed that the axial ratio goes bad if the phase shift between the ports is more or less than 90 degrees. Width of the feeding strips has minor effects on frequency shift and radiation pattern of the DRA.

The dimensions of DRA have much effect on the gain, radiation pattern, circularity and impedance matching of the developed antenna. It is observed that by increasing the height of the DRA element from 8mm to 12mm, gain and broadness of the beam increases with a shift to lower frequency. Increasing the height of the DRA also affects the circularity of the DRA element. If the radius of the DRA is increased the overall gain of the element increases but due to the cavity wall effects the circularity is not so good.

3.8 DRA Simulation Results

The simulation results for the DRA element obtained using CST microwave studio are presented here. As can be seen radiation pattern is quite broad with an axial ratio of less than 3 dB in the peak gain directions. The DRA element is initially simulated on a 1m ground plane. As the results on the 1m ground plane are very good so the DRA is simulated within the simple car cavity. Results obtained in all three different car positions were simulated which are discussed below.

3.8.1 Roof Top Position

Initially the DRA element is simulated on 1m circular ground plane buried in a cavity with a tilt of 10 degree as shown in fig. 1.17. This is the most suitable position for the DRA with an available space of 50*50*20 and with no edges around the DRA element. In real life top roof position of the car has more than 1m metal roof which serves as the ground plane for the DRA which further improves the DRA performance.

The simulated results show the gain of 5.33dBi is achieved with a wide beam width. The difference between the LHCP and RHCP of the DRA is more than 9 dB which gives an axial ratio of less than 3dB at the peak gain position.

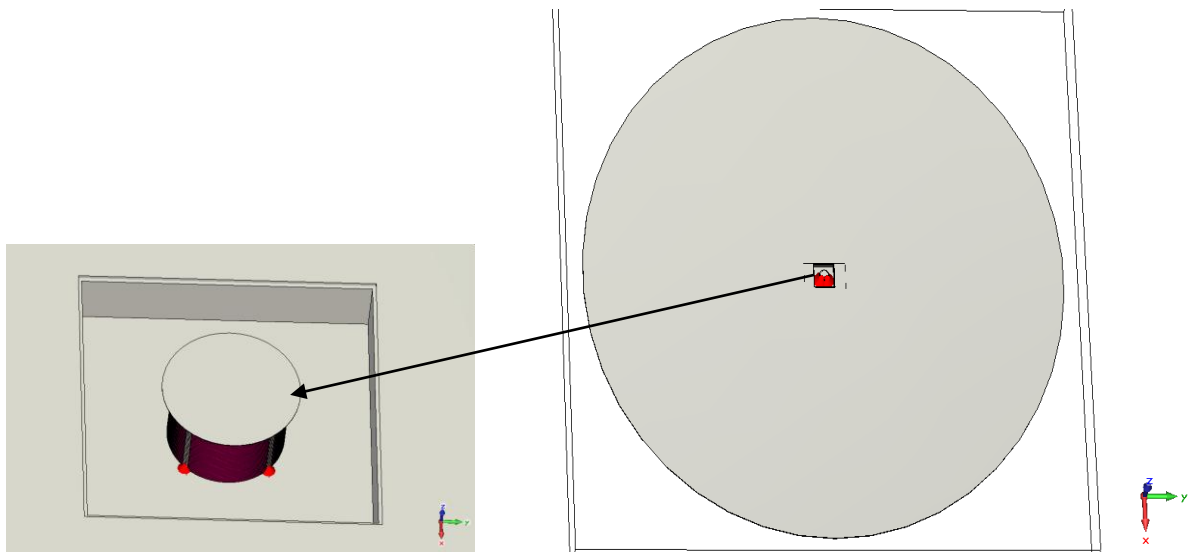


Fig.1.17: Simulated design of the DRA in the top roof position

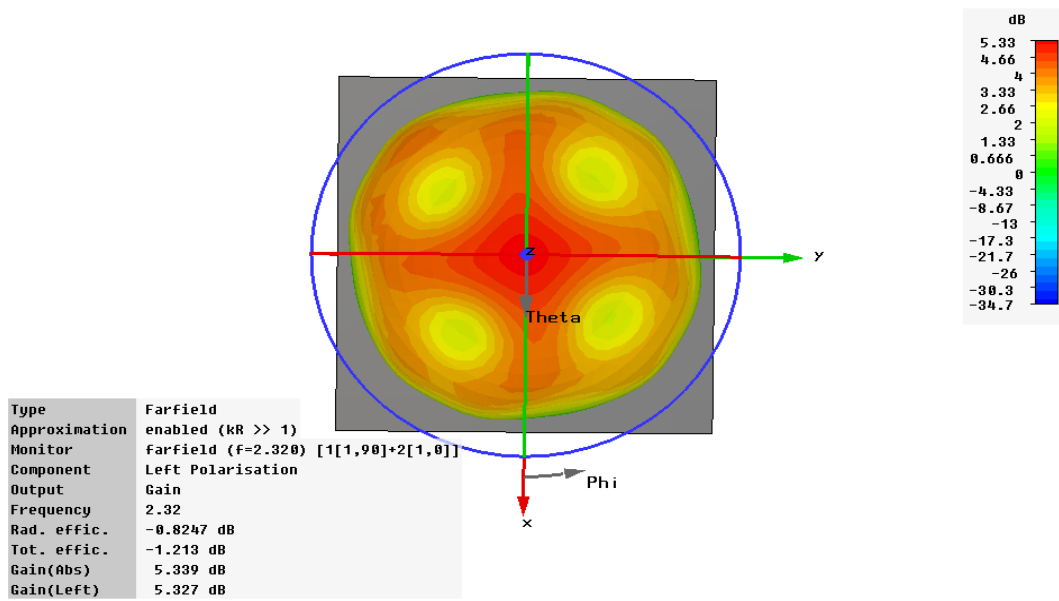


Fig.1.18: Simulated co-polarization of the DRA in the top roof position

3.8.2 Windscreen Position

At the windscreen position the complete DRA element has the available space of 41*42*20 mm³. The designed DRA element is buried in cavity as shown in fig. 1.19. The result obtained from the simulated design is shown in fig. 1.20. Here it is required to hide the antenna within the cavity in such a way that the antenna is not out of the cavity more than 2.5mm. At this position high gain of the antenna is observed but the beam width decreases a little as compare to top roof position. It is due to the near edges and the limited height available out of the cavity at this position. In the radiation pattern cuts at different elevation angles shows the effect of the cavity wall and edges around the DRA element.

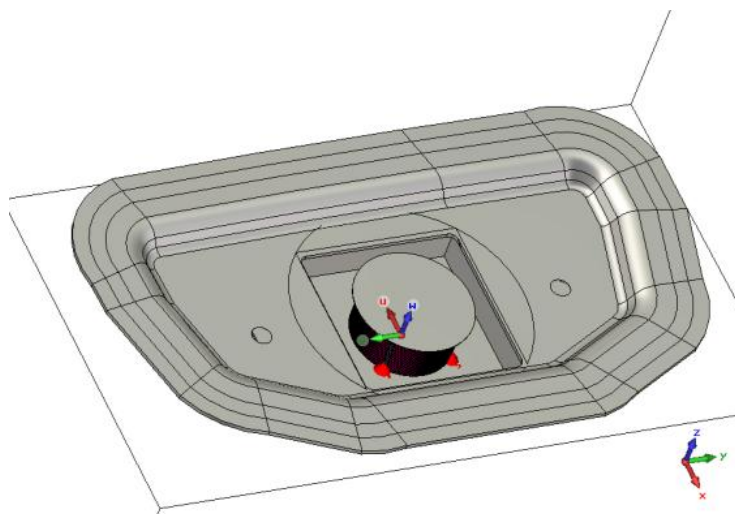


Fig.1.19: Simulated design of the DRA in the windscreen position

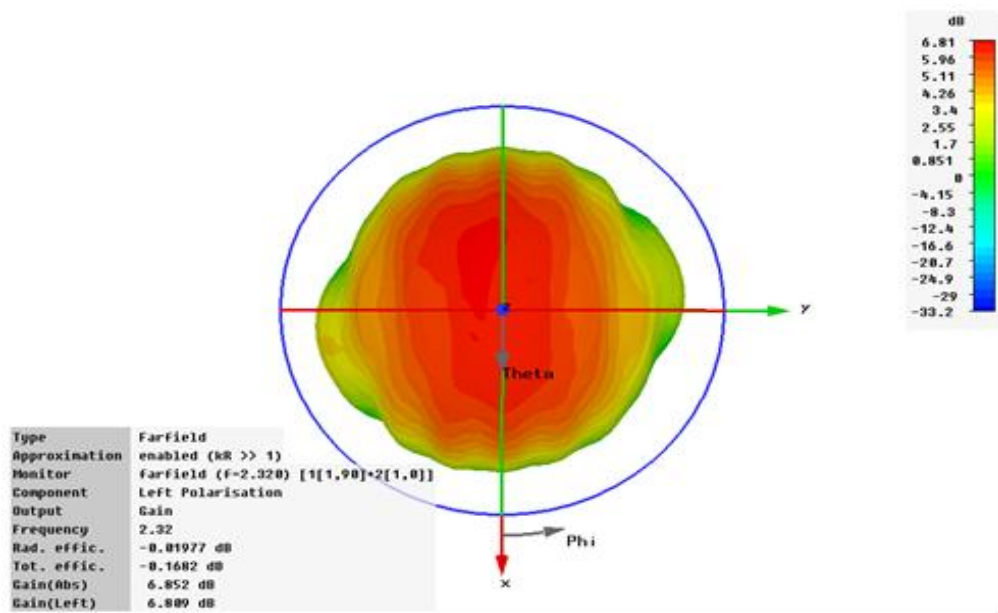


Fig.1.20: Simulated co-polarization of the DRA in the windscreen position

3.8.3 Spoiler Position

At the spoiler position the complete DRA element has the available space of 55*60*20 mm³. The designed DRA element is place in spoiler with high edges of about 8mm around it as shown in fig. 1.21. The result obtained from the simulated design is shown in fig. 1.22. At this position good gain of the antenna is observed but the beam width decreases a little as compare to top roof position. The radiation pattern shows some cuts which are the effects of the side edges in the spoiler position.

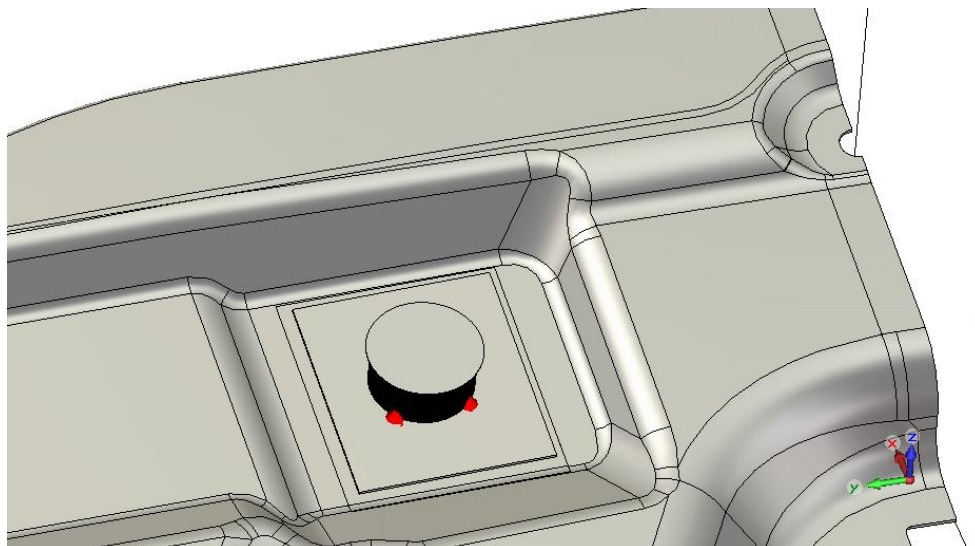


Fig.1.21: Simulated design of the DRA in the spoiler position

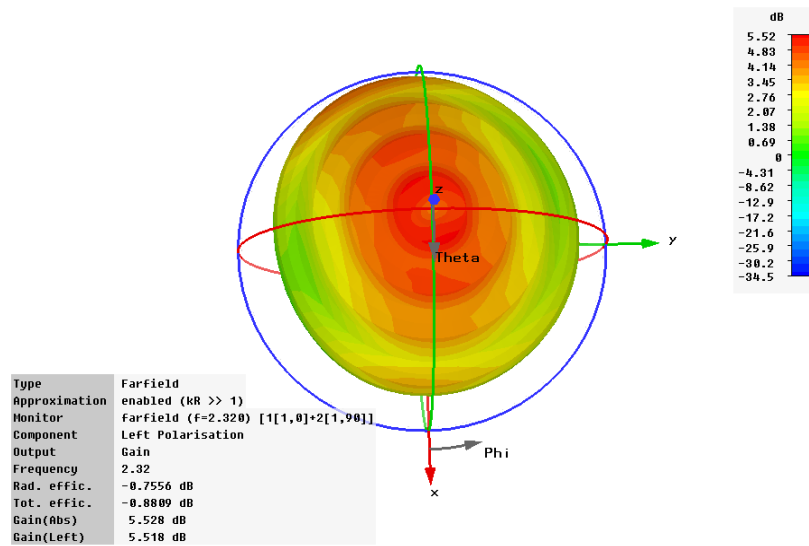


Fig.1.22: Simulated co-polarization of the DRA in the spoiler position

3.9 DRA Measurement Results

After successful simulation results of the DRA element a prototype is measured using vector network analyser and MiDAS 4.1 for the far field radiation pattern measurements. The measured results are similar to the simulated results. The developed SDARS antenna is tested for all three positions.

3.9.1 Roof Top Position

For the realization of the top roof position a circular ground plane of 1m diameter is used as shown in fig. 1.23. The measured DRA element at this position shows very good performance with a high gain at desired elevation angles as shown in fig. 1.24. Both LHCP and RHCP of the DRA are measured in this position. An axial ratio of less than 2dB is observed at this position. It is observed that DRA element has about 1.5 dB higher gain than the reference cross dipole antenna.



Fig.1.23: Measured design of the DRA in the top roof position

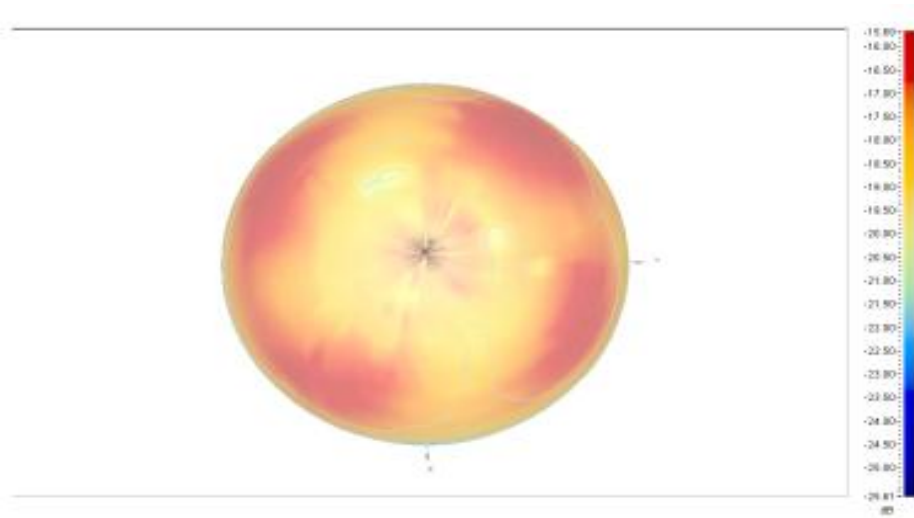


Fig.1.24: Measured co-polarization of the DRA in the top roof position

3.9.2 Windscreen Position

The wind screen position is the most desired position for SDARS antenna from the automotive industry but on the same time this position has huge effects on the performance of the antenna. For the developed DRA element the 3D far field radiation patterns are measured using MiDAS setup. A cavity is used for the measurements to realize the original car mounting position as shown in fig. 1.25. For the DRA LHCP and RHCP are measured at this position. The DRA element has about 0.5 dB more gain than the measured reference antenna, with a little less beam width as shown in fig. 1.26. In the radiation pattern cuts on the different elevation angles are observed similar to the simulated results due to the cavity edges.



Fig.1.25: Measured design of the DRA in the windscreen position

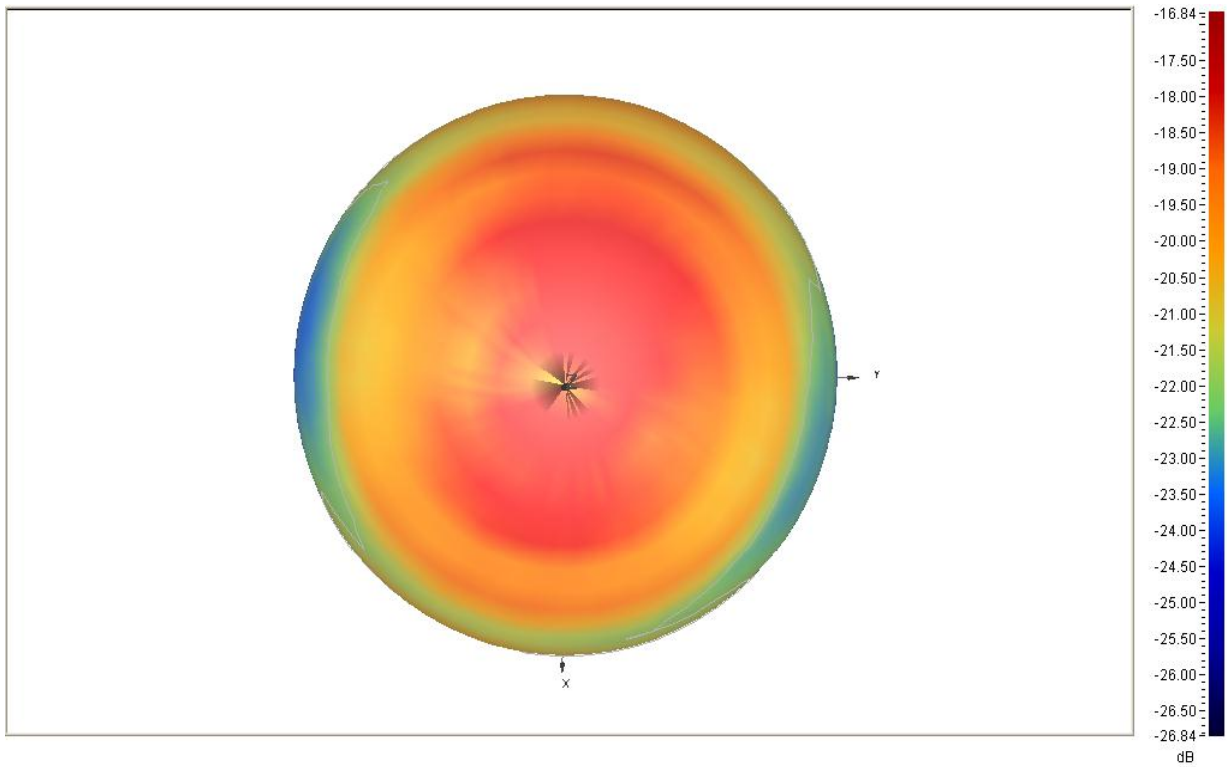


Fig.1.26: Measured co-polarization of the DRA in the windscreen position

3.9.3 Spoiler Position

A spoiler of an old car is used in this measurement for the realization of the spoiler position as shown in fig. 1.27. The measured DRA element at this position has a little less gain than the measured reference antenna element as shown in fig. 1.28.

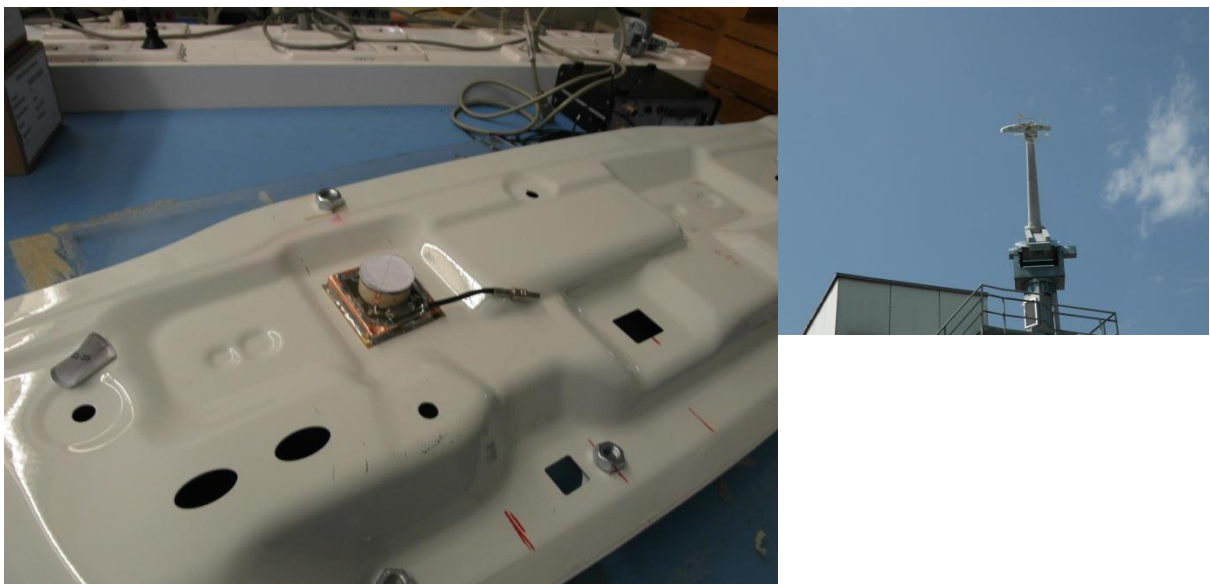


Fig.1.27: Measured design of the DRA in the spoiler position

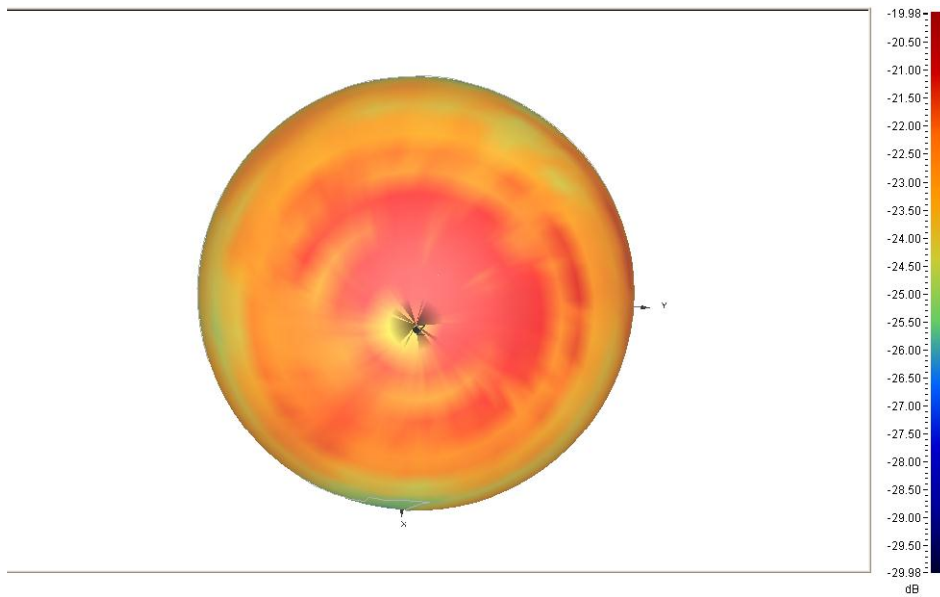


Fig.1.28: Measured co-polarization of the DRA in the spoiler position

Both LHCP and RHCP of the DRA are measured in this position. An axial ratio of less than 3dB is observed at this position. It is observed that DRA element has about 1.5 dB lower gain than the reference cross dipole antenna.

3.10 Discussion

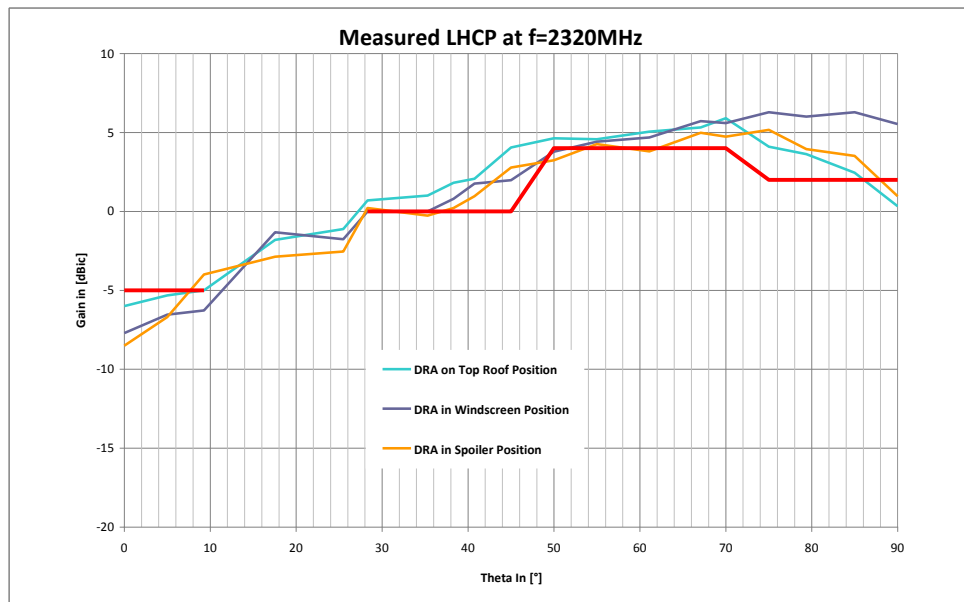


Fig.1.29: Comparison of the measured co-polarizations of the DRA

Different designs were presented for the SDARS applications. All presented antennas show very good performance on the ground plane without cavity. However it is observed that each of the presented antenna elements have strong influence of the different car mounting positions. The presented antenna

elements can be a good solution for the SDARS applications on a big ground plane such as top roof position whereas for the use in the cavity and non-smooth ground planes, the antenna elements should be optimized further. The newly developed DRA element for the SDARS application shows very good performance. All simulated results were well verified by the measured results using MiDAS setup. A high impedance match and less axial ratio is observed. The developed DRA performs best on the 1m ground plane whereas it has some effects of the car cavity on the windscreen and spoiler position. It can be seen that DRA element has high gain at the top roof and windscreen position. A comparison of the DRA gain performance is shown in the fig. 1.29. It can be seen that the DRA element fulfils the SiriusXm gain requirements of 4dBic at the top roof position and the windscreen positions. The DRA performance degrades a little in the spoiler position due to the high edges and bends around the antenna. Each position of the car has its own effects on the gain, operating frequency and circularity of the antenna which needs to be optimized accordingly. Measured DRA is compared with a reference circularly polarized cross dipole antenna. A comparison graph for all three possible positions is shown in Appendix C. It can be seen that the DRA fulfils the SiriusXm gain requirements at the high elevation angles. For the low elevation angles the element has little less gain but for satellite communication gain at the high elevation angles specifically between 50 – 70 degrees must be achieved. For the top roof and windscreen position DRA element has gain more than the reference element.

4 Conclusions and Future Work

This thesis work presents the research and development of the antenna element for the SDARS applications. During the project work different designs were presented and it is observed that each element has a strong influence of the car body on its performance. However the proposed designs can be a good solution for the SDARS applications on a big ground plane such as top roof position whereas for the use on a non-smooth ground planes the antenna elements should be optimized further. Finally the newly developed DRA is presented which has a high gain of more than 6dBi with an axial ratio of less than 3dB at the peak gain position. Return loss, less than -19dB is measured. The DRA element shows best performance on the circular ground plane of 1m diameter. It is observed that the DRA element has broad beam with high gain, if a parasitic element is used above the DRA. The parasitic element helps to tune the resonating frequency of the DRA without changing the dimensions of the DRA.

Rectangular or spherical shaped DRA elements can be optimized for this application resonating at higher modes. It is also observed to have better response by placing the parasitic element directly on the DRA which can be further investigated. All proposed designs can be optimized to improve their performance on the non-smooth ground planes. Circular patch designs should be further optimized with a better feeding network; z-element can be combined with another antenna element to give a better theta element.

References

- [1] A. Petros, I. I. Zafar, S. Licul, "Reviewing SDARS antenna requirements", *Microwaves & RF*, 2003, vol. 42, no9, pp. 51-62.
- [2] C. McCarrick, "A Combination Monopole/Quadrifilar Helix Antenna for S-Band Terrestrial/Satellite Applications", *Microwave Journal*, May 2001.
- [3] H. Lindenmeier, J. Hopf, L. Reiter, "Low profile SDARS-Antenna with diversity Functionality" *IEEE Antennas and Propag. Symp.*, vol. 4, pp. 744–747, 2002.
- [4] D.-C. Chang, J.-H. Cheng, "2.3 GHz Antenna with both LHCP and LP for SDARS," *IEEE Antennas and Propag. Symp.*, vol. 3, pp. 874–877, June 2003.
- [5] International Patent Classification H01Q 21/24, International Publication Number WO 01/80366 A1 - Applicant: Receptec L.L.C.
- [6] A. Petros and S. Licul, "'Folded' Quadrifilar Helix Antenna". 2001 *IEEE Antennas & Propagation Society, International Symposium*, Boston, July 8-13, 2001, 2001 Digest, Volume Four, p. 569
- [7] H.-G. Schuering, G.-H. Hassmann, H.K. Lindenmeier, L.M. Reiter, J.F. Hopf, S.M. Lindenmeier, (Delphi Fuba Reception Syst.). "State of the art of vehicle antennas for satellite radio". *IEEE Antennas and Propagation Society International Symposium*, page(s): 68/71, vol. 1B, 2005.
- [8] H. Man-Hoe; J Joo-Seong. "Microstrip patch antenna for SDARS reception". *Antennas and Propagation Society International Symposium*, 2005, Page(s): 313 - 316 vol. 3B.
- [9] P-S. Kildal and K. Rosengren, "Correlation and capacity of MIMO systems and mutual coupling, radiation efficiency and diversity gain of antennas: simulations and Measurements in reverberation chamber", *IEEE Communications Magazine*, pp. 104-114, Vol.42, No. 12, Dec 2004.
- [10] John D. Kraus, *Antennas*, second edition, McGraw-Hill, Inc. 1988
- [11] David M. Pozar, *Microwave Engineering*, third edition, Jhon Wiley & Sons (Asia) Pte. Ltd., 1989

- [12] Constantine A. Balanis, *Antenna Theory Analysis and Design*, second edition, John Wiley & Sons, Inc
- [13] Computer code Computer Software Technology Microwave Studio, Available at <http://www.cst.de>
- [14] R. H. Rasshofer, M. Spies, and H. Spies, *Advances in Radio Science*, BMW Group Research and Technology, Ingenieurbüro Spies, © Author(s) 2011. CC Attribution 3.0 License.
- [15] K. Fujimoto, "Overview of antenna systems for mobile communications and prospects for the future technology," *IEICE Trans. Commun.*, vol.E74-B, no.10, pp.3191-3201, Oct. 1991.
- [16] K. Nishikawa, "Land vehicle antennas," *IEICE Trans. Commun.*, vol.E86-B, no.3, pp.993-1004, Mar. 2003.
- [17] "MiDAS User Manual", The ultimate in Microwave Measurement Software, by Orbit/FR, 2004.
- [18] Massimo Pannozzo and Luca Salghetti Drioli, "State of the Art Review for Automotive Satellite Antennas" 5th Advanced Satellite Multimedia Systems Conference and the 11th Signal Processing for Space Communications Workshop, 2010.
- [19] "XM Antenna Specification", by XM Satellite Radio, Boca Raton, 2001.
- [20] "Sirius-Antenna Specifications", by Sirius Satellite, Radio, New York, 2001.
- [21] Y.-P. Hong, J.-M. Kim, S.-C. Jeong, D.-H. Kim, and J.-G. Yook, "Low-Profile S-Band Dual Polarized Antenna for SDARS Application" *IEEE Antennas and Wireless Propagation Letters*, Vol. 4, 2005.

Appendix A: Measured reference antennas

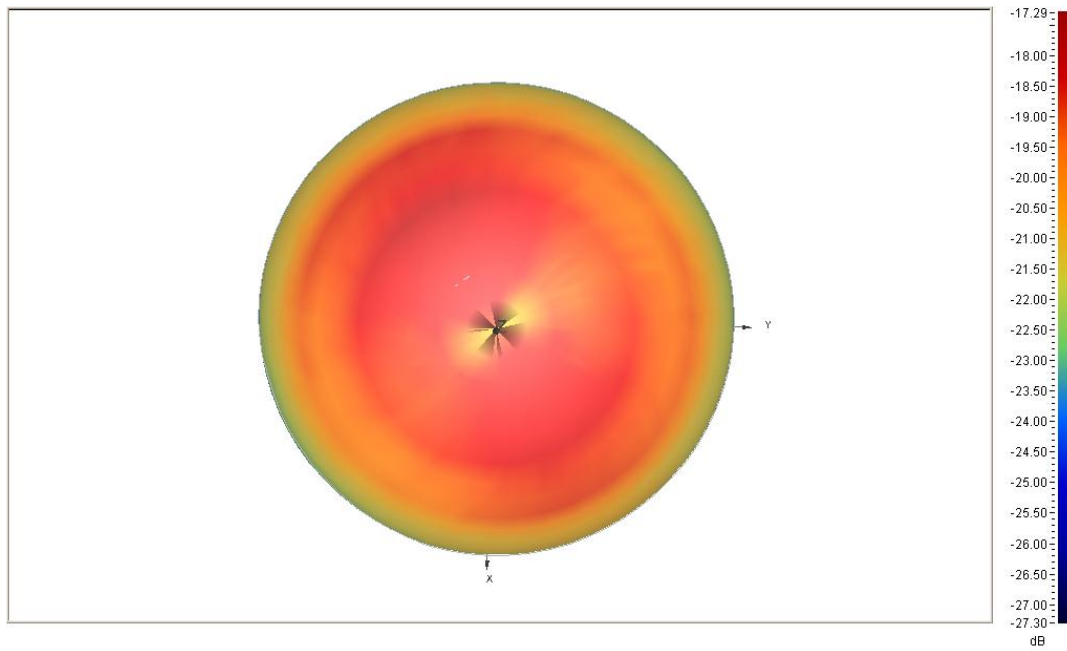


Fig.A.1: Measured LHCP for cross dipole at 2.32GHz

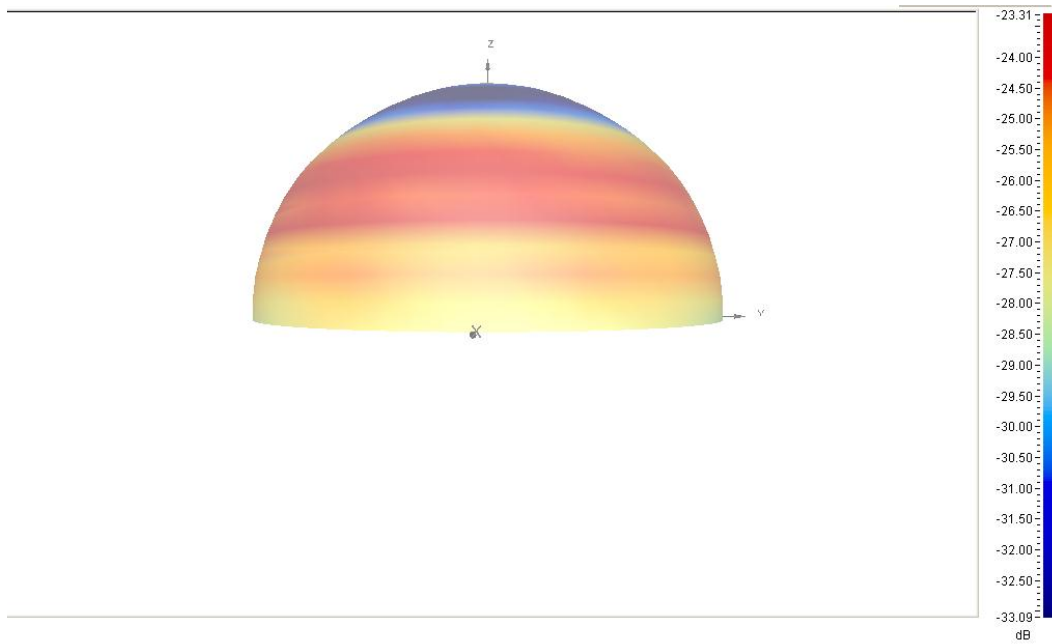


Fig.A.2: Measured vertical component of quarter wave monopole at 2.32GHz

Appendix B: Measured proposed antennas



Fig.B.1: L-shaped patch measured design in windscreen car cavity

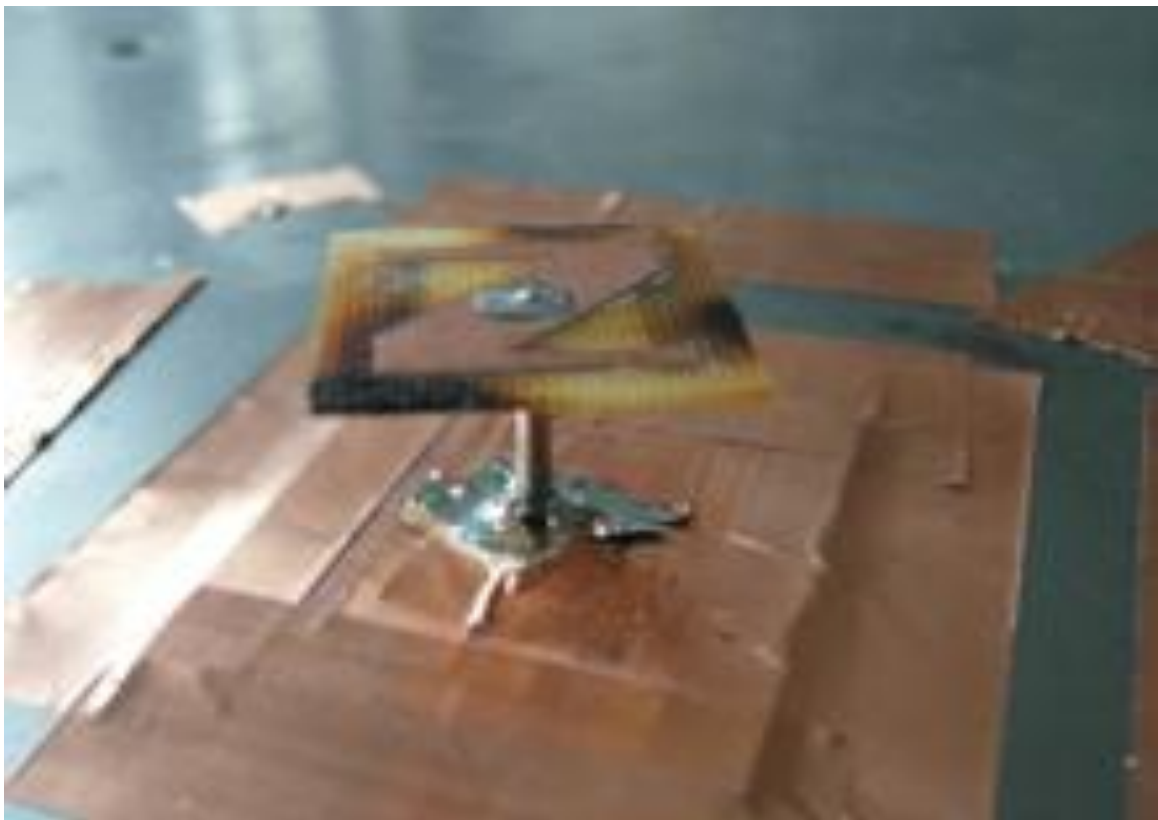


Fig.B.2: Measured Z-element design

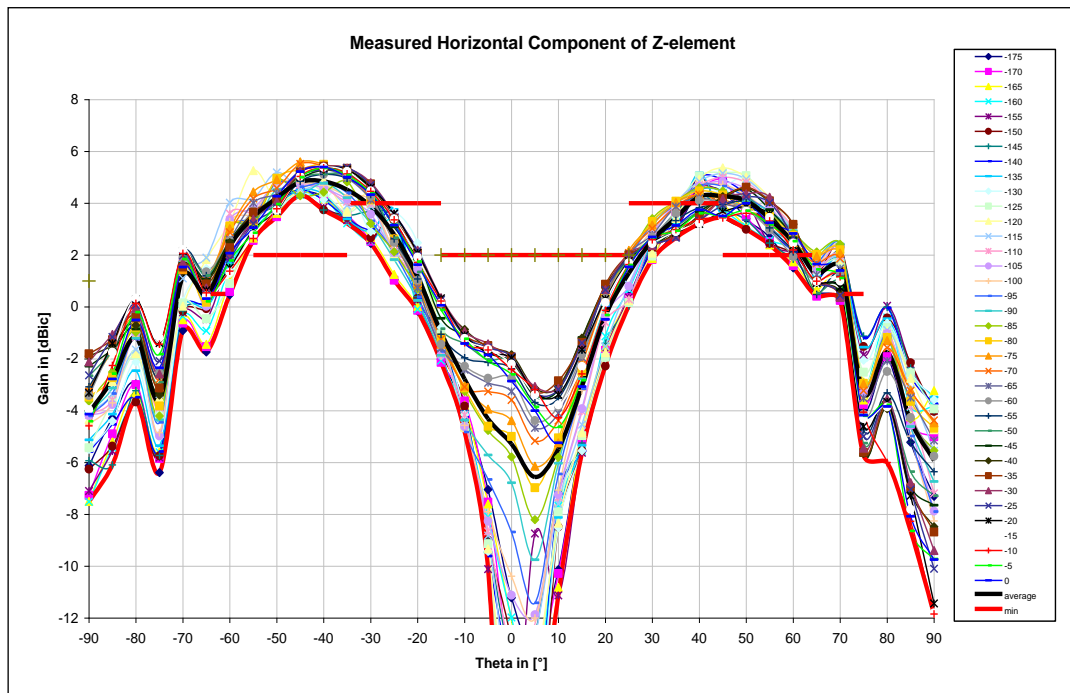


Fig.B.3: Measured horizontal component of Z-element design

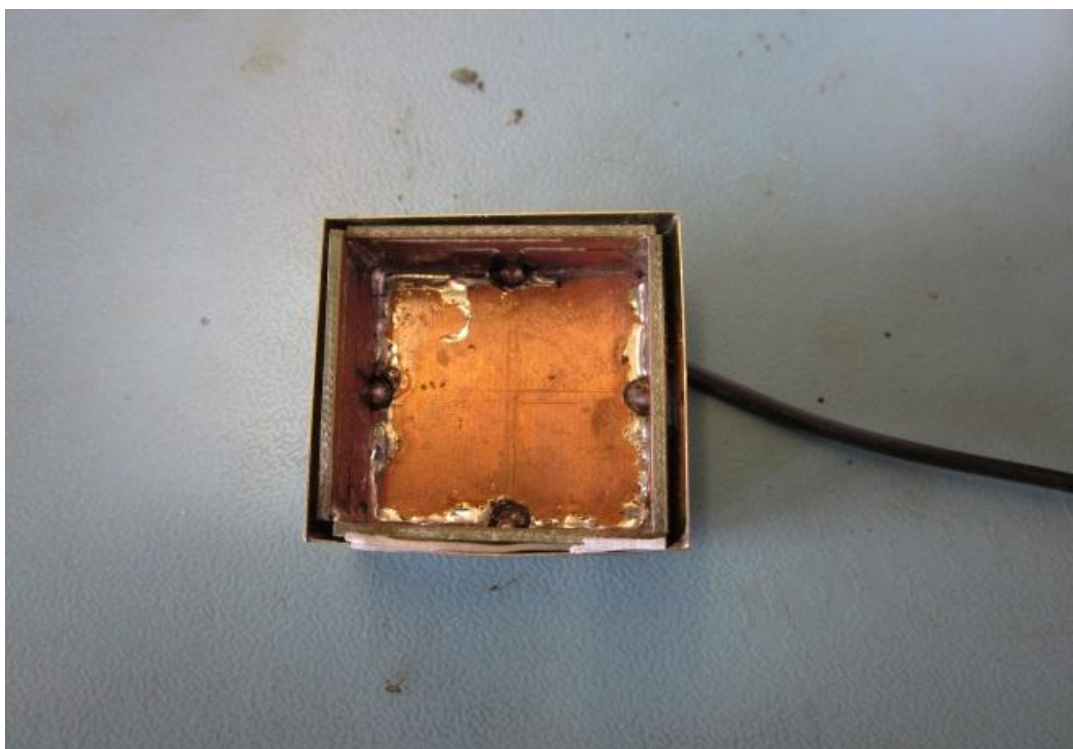


Fig.B.4: Measured T-slot element design

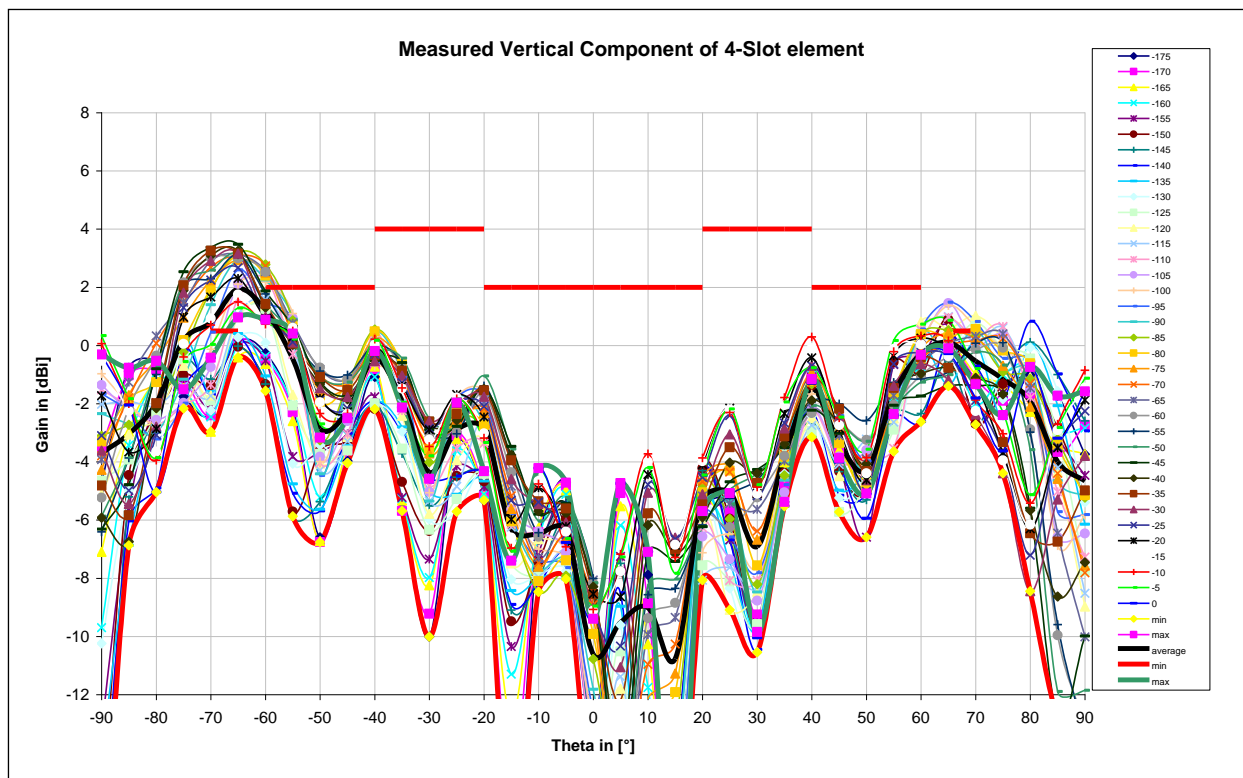


Fig.B.5: Measured vertical component of T-slot element design

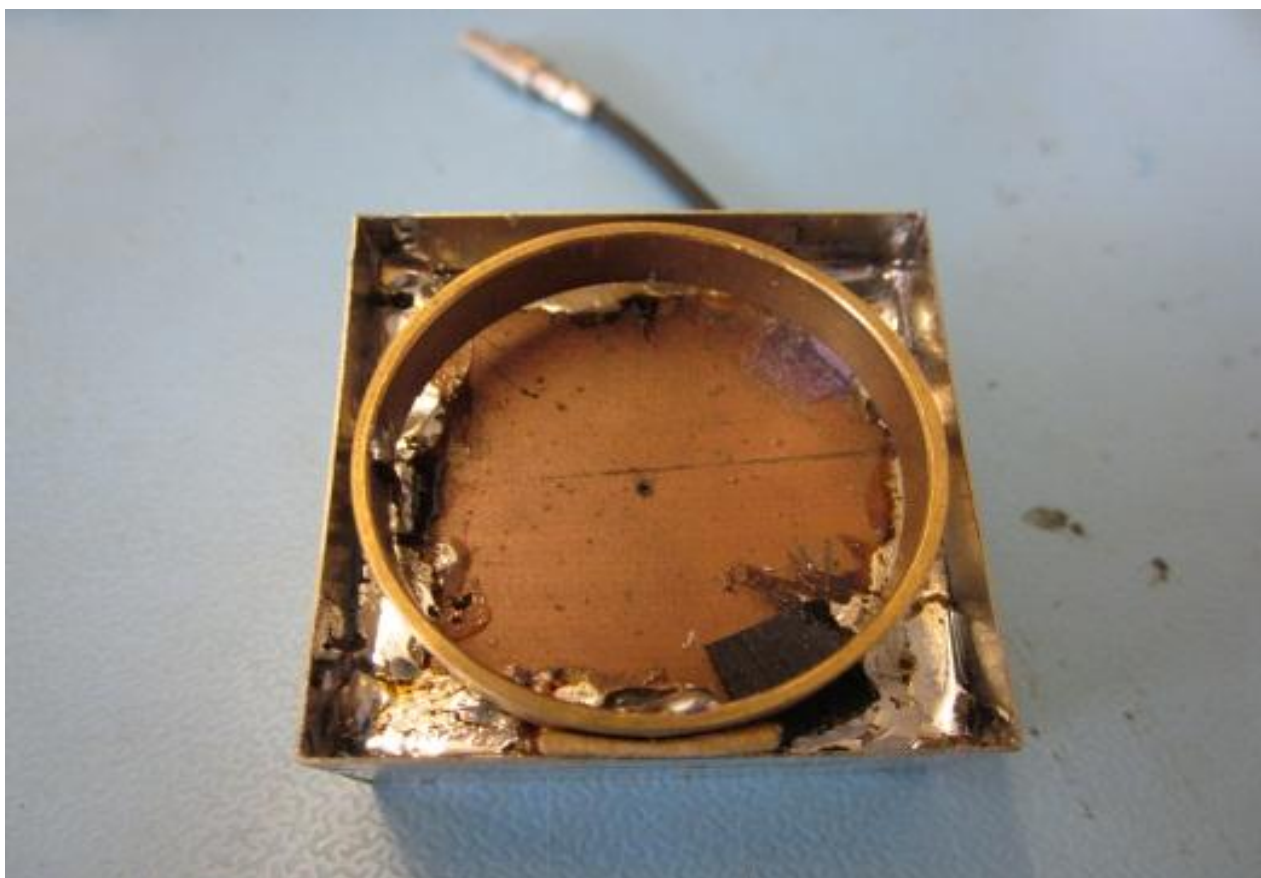


Fig.B.6: Measured ring antenna design

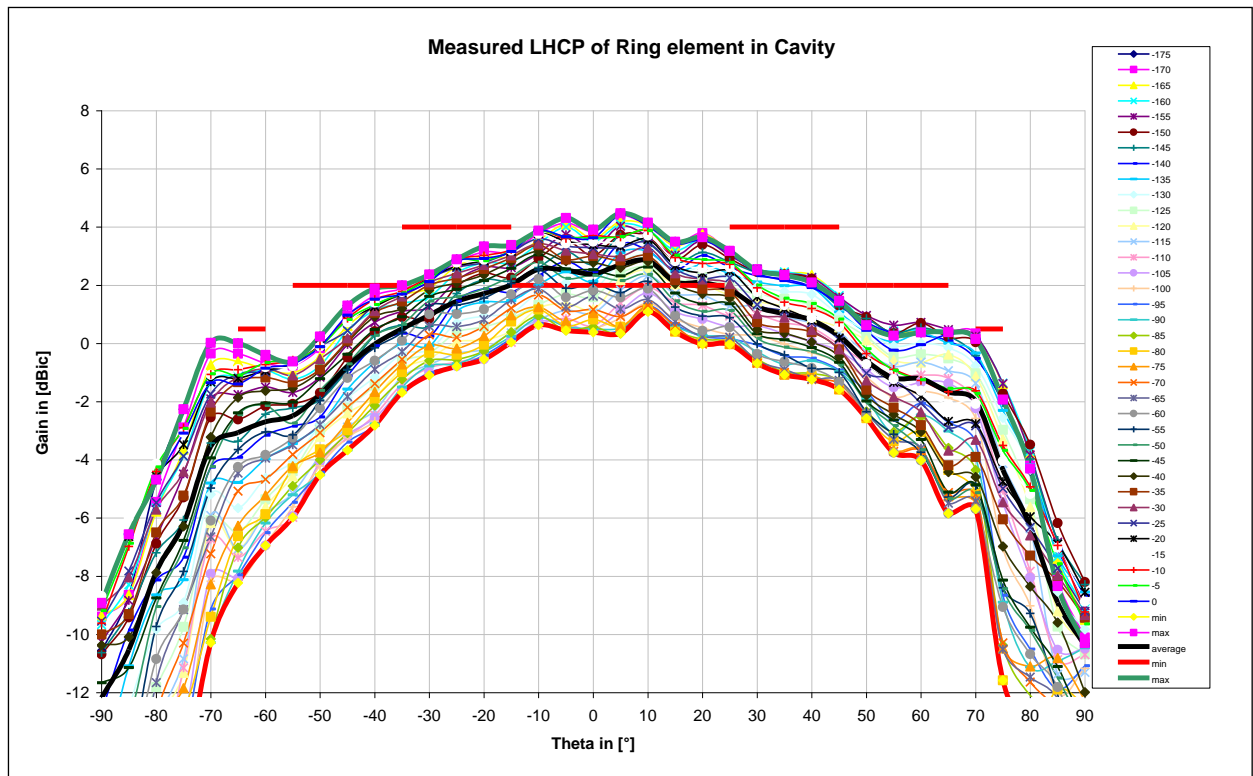


Fig.B.7: Measured co-polarization of the ring antenna at 2320MHz

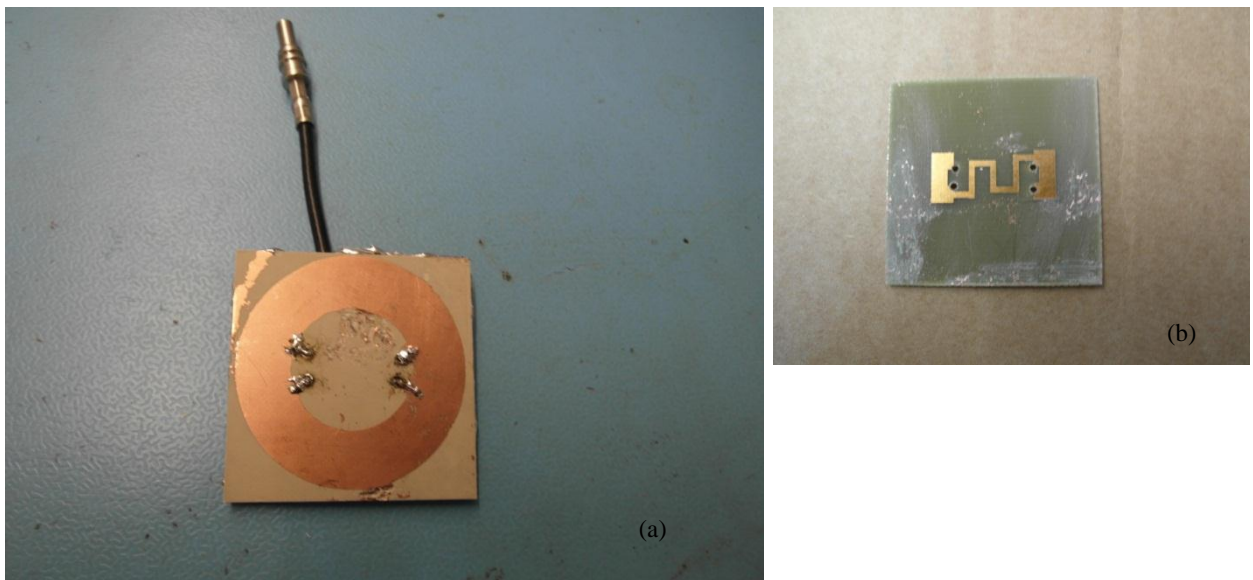
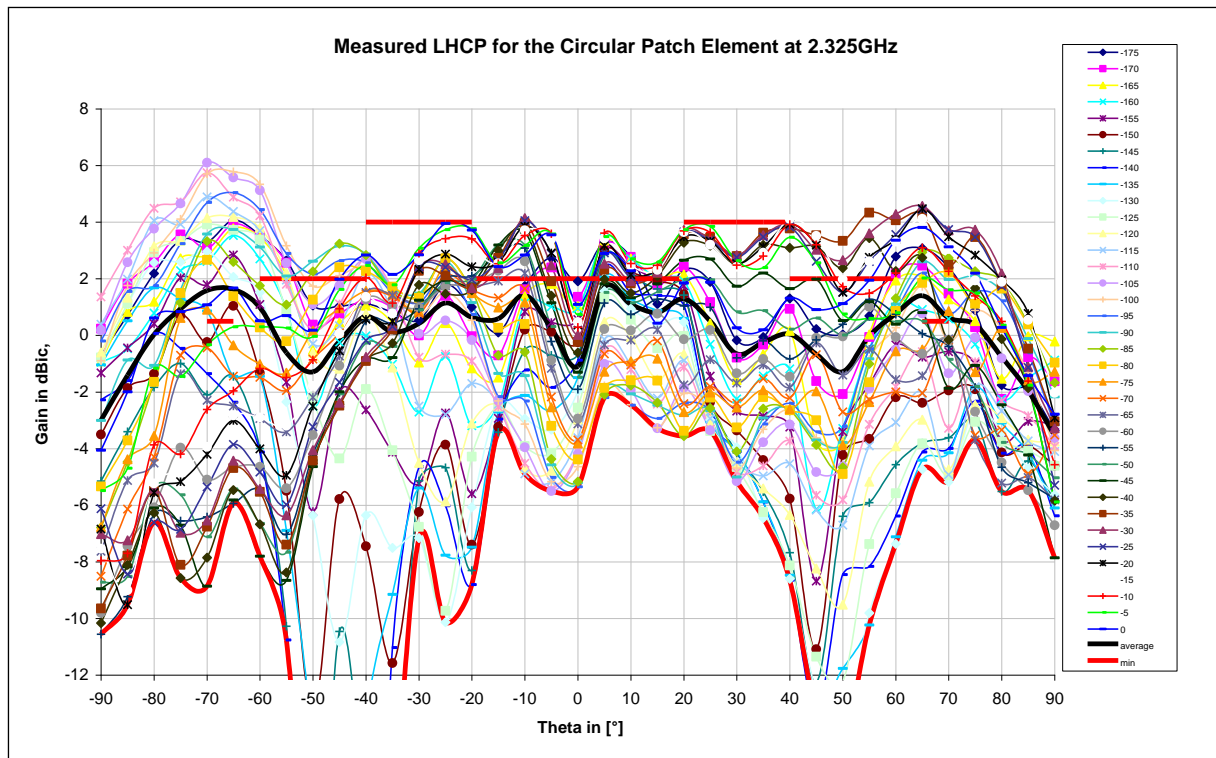


Fig.B.8: Measured circular patch antenna design (a) top view (b) bottom view



FigB.9: Measured co-polarization of the circular patch antenna

Appendix C: Measure DRA in comparison to reference antenna

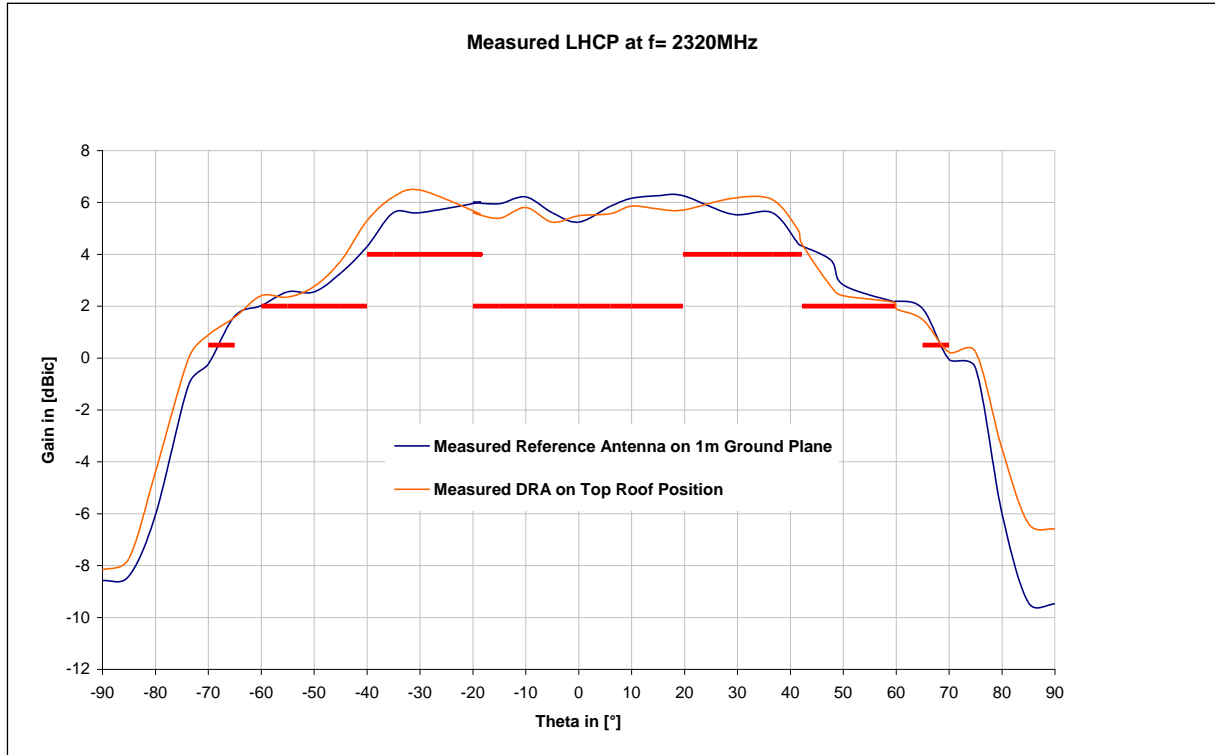


Fig.C.1 Comparison of the measured reference antenna and DRA at Top roof position

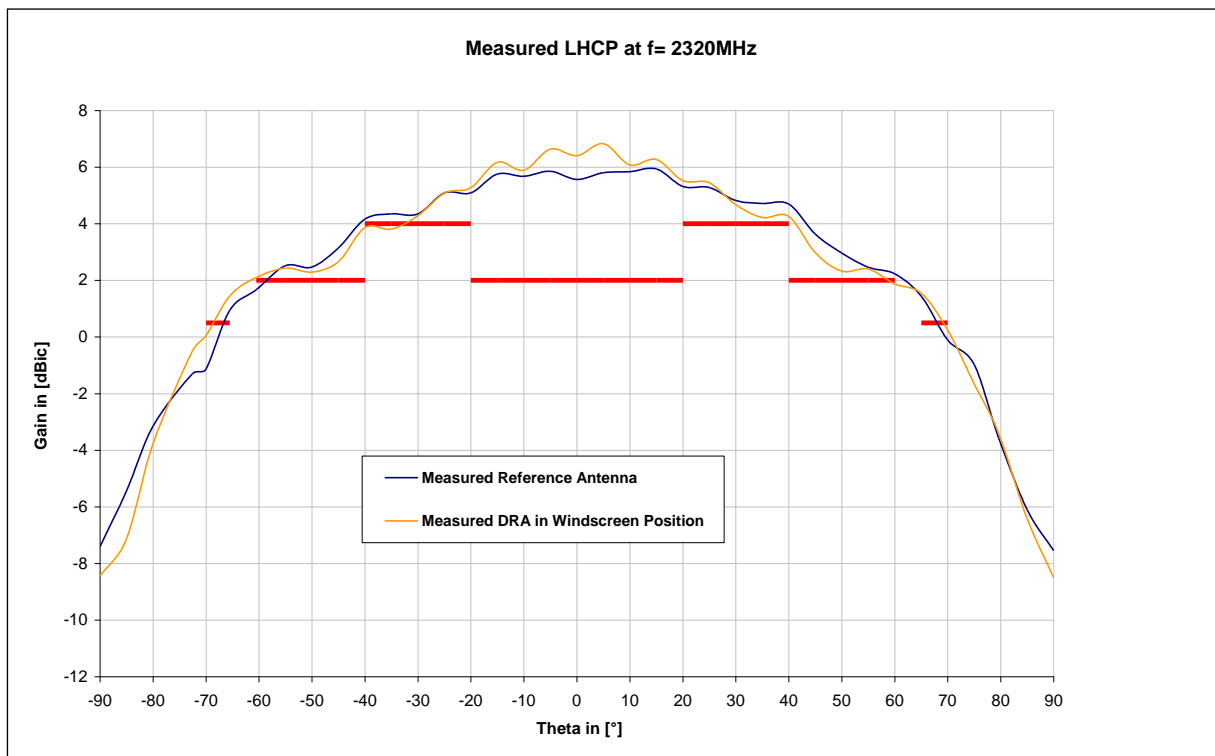


Fig.C.2: Comparison of the measured reference antenna and DRA at windscreen position

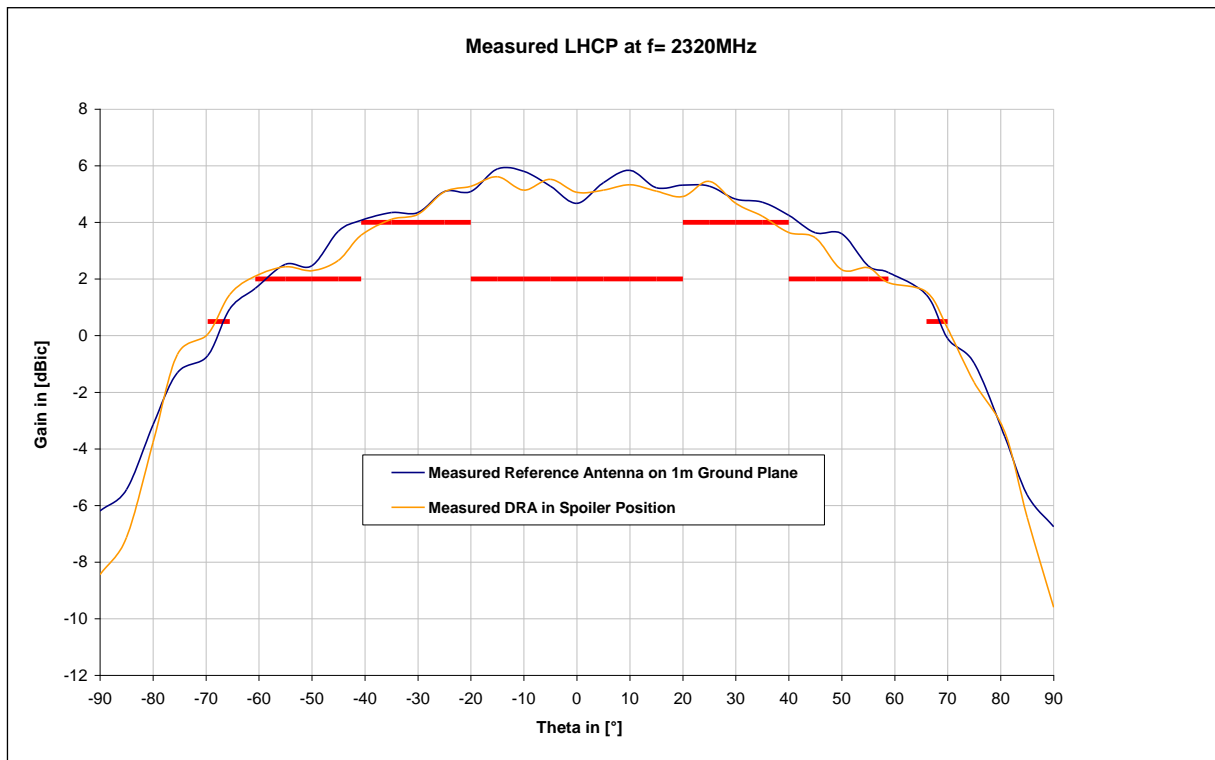


Fig.C.3: Comparison of the measured reference antenna and DRA at spoiler position